

BULLETIN OF THE RESEARCH COUNCIL OF ISRAEL Section C TECHNOLOGY

Bull. Res. Council of Israel. C. Techn.

Page

- 1 Ejector refrigeration from low temperature energy sources
J. Mizrahi, M. Solomiansky, T. Zisner and W. Resnick
- 9 Determination of cold-work energy in copper by means of electro-chemical potential measurements
Asher Peres
- 13 A new indirect tensile test for concrete. Theoretical analysis and preliminary experiments
S. Rosenhaupt, A. C. van Riel and L. Wijler
- 29 New reagent for microscopic strain analysis in steel
A. Taub
- 33 Units in traffic engineering
M. Peleg
- 43 Composition of bitter oranges grown in Israel. II
A. Ephraim and J. J. Monselise
- 47 Rheological properties of concentrated orange juice
A. Ephraim and J. J. Monselise
- 53 Proteolytic and starch liquefying properties of mould cultures
J. Pomeranz
- 59 Milling and baking characteristics of bug infested wheat
J. Pomeranz and L. Adler

LETTERS TO THE EDITOR

- 67 The interaction rubber-sulphur-brass
Z. Rigbi
- 69 Preferential removal of bromides from brines by solvent extraction
H. Aharon, A. Baniel and R. Blumberg
- 71 On three layers in turbulent flow
S. Irmay
- 72 The pantothenic acid content of mouldy wheat and flour
J. Pomeranz
- 73 Determination of magnesium oxide in silicates
W. Bodenheimer
- 74 The titration of calcium with E.D.T.A. in the presence of limited amounts of fluoride
J. Mashal and L. Geyer

PROCEEDINGS

- 77 Second Electronics Convention in Israel
- 85 Israel Association for Theoretical and Applied Mechanics

BOOK REVIEWS

CONTENTS

- 1 Ejector refrigeration from low temperature energy sources
J. Mizrahi, M. Solomiansky, T. Zisner and W. Resnick
- 9 Determination of cold-work energy in copper by means of electrochemical potential measurements
Asher Peres
- 13 A new indirect tensile test for concrete. Theoretical analysis and preliminary experiments
S. Rosenhaupt, A. C. van Riel and L. Wijler
- 29 New reagent for microscopic strain analysis in steel
A. Taub
- 33 Units in traffic engineering
M. Peleg
- 43 Composition of bitter oranges grown in Israel. II
A. Ephraim and J. J. Monselise
- 47 Rheological properties of concentrated orange juice
A. Ephraim and J. J. Monselise
- 53 Proteolytic and starch liquefying properties of mould cultures
J. Pomeranz
- 59 Milling and baking characteristics of bug infested wheat
J. Pomeranz and L. Adler

LETTERS TO THE EDITOR

- 67 The interaction rubber-sulphur-brass
Z. Rigbi
- 69 Preferential removal of bromides from brines by solvent extraction
H. Aharon, A. Baniel and R. Blumberg
- 71 On three layers in turbulent flow
S. Irmay
- 72 The pantothenic acid content of mouldy wheat and flour
J. Pomeranz
- 73 Determination of magnesium oxide in silicates
W. Bodenheimer
- 74 The titration of calcium with E.D.T.A. in the presence of limited amounts of fluoride
J. Mashall and L. Geyer

PROCEEDINGS

- 77 Second Electronics Convention in Israel
- 85 Israel Association for Theoretical and Applied Mechanics

BOOK REVIEWS

EJECTOR REFRIGERATION FROM LOW TEMPERATURE ENERGY SOURCES

JOSEPH MIZRAHI, MORDECAI SOLOMIANSKY, TUVIA ZISNER AND WILLIAM RESNICK

Division of Chemical Engineering, Technion—Israel Institute of Technology, Haifa

ABSTRACT

Calculations have been carried out to determine the feasibility of operating an ejector refrigeration system with a low temperature energy source such as that available from simple solar collectors, or exhaust steam. The calculations were based on data previously reported for a commercial ejector. With an evaporator temperature of 5°F, a condenser temperature of 86°F, and a heat source at 140°F, the refrigerants, propane, Freon-22 and Freon-12 had performance factors of the order of 0.2. Curves are presented to show the effect of changes in operating temperatures on the performance factor. The calculations indicate that an ejector refrigeration system would appear to be a feasible method for producing refrigeration from low temperature energy sources.

NOTATION

A = dimensionless grouping, $\frac{w}{W} \left(\frac{P_b}{P_c} \right)^n$	n = exponent
C = dimensionless grouping, $\frac{P_e - P_o}{P_c - P_o}$	P = pressure, pounds per square inch abs.
H = enthalpy, BTU per pound	Q = heat transferred, BTU per hour
	t = temperature, °F
	T = temperature, °R
	w = entrained fluid, pounds per hour
	W = motive fluid, pounds per hour

Subscripts

b = boiler condition	e = evaporator condition
c = condenser condition	o = suction condition at zero entrainment

One of the many fields in which ejectors have found extensive application is the field of refrigeration. Refrigeration is accomplished in an ejector refrigeration cycle by the evaporation of a liquid at a low pressure which is maintained by the action of the ejector. The ejector serves the same purpose as a compressor in a mechanical refrigeration system, namely, the compression of vapour from the evaporator from a low pressure to a sufficiently high pressure to permit its condensation at the temperature of the available heat sink. An ejector refrigeration system has various advantages over a mechanical system including simplicity, cheapness and the lack

of moving parts. In present practice, steam is used, almost exclusively, as the motive fluid and water as the evaporating fluid. As a result, the usual ejector refrigeration cycle is incapable of producing temperatures below the freezing point of water. The ejector refrigeration system has been limited in practice, therefore, to those fields of application in which refrigeration to a minimum of 35°F is sufficient, such as comfort cooling and the provision of chilled process water.

As part of a research programme on the utilization of solar energy for the production of refrigeration, a series of calculations were made to determine the feasibility of utilizing an ejector refrigeration system for the production of below-freezing temperatures. The results of these calculations are presented in this paper. A schematic diagram of an ejector refrigeration system is presented in Figure 1. The motive

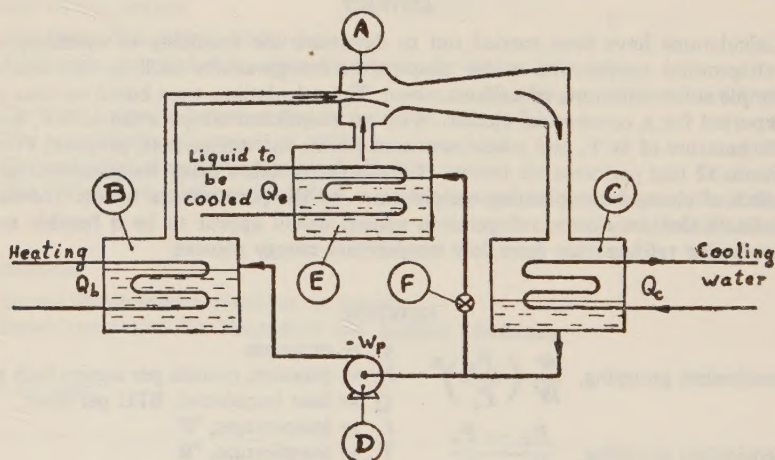


Figure 1

Flowsheet of an ejector refrigeration system

fluid is vaporized at an elevated pressure P_b , in the boiler B, and vapour passes to the ejector A, where low pressure vapour, P_a , is entrained from the evaporator E. The vapour leaves A at an intermediate pressure P_c , and is condensed in the condenser C. Part of the liquid leaving the condenser is returned to the boiler by pump D, and the remainder passes through the expansion valve F, to the evaporator E, where it produces refrigeration during its vaporization.

CALCULATIONS

Work and Haedrich¹ and Work and Miller² reported and correlated performance characteristics for two commercially available ejectors operating on a self-entrainment

cycle. Self-entrainment refers to the case in which the motive material and the entrained material are the same fluid. All the calculations which are reported herein were based on the relationships found by Work et al., for their large ejector.

Work and Miller² found that for a jet ejector a plot of

$$C = \frac{P_c - P_e}{P_c - P_a} \text{ versus } A = \frac{w}{W} \left(\frac{P_b}{P_e} \right)^n$$

yielded a straight line which passed through the point $A = 0$, $C = 1$. For each ejector the line obtained was independent of the fluid used. The ratio w/W , which is the pounds of low pressure vapour entrained per pound of motive fluid, is called the entrainment ratio. For the larger ejector it was shown experimentally that

$$\frac{P_c - P_e}{P_c - P_o} = 1 - 0.313 \frac{w}{W} \left(\frac{P_b}{P_e} \right)^{0.85} \quad (1)$$

Previous work¹ has shown that the ratio P_c/P_o is independent of the fluid and that for the large ejector P_c/P_o is equal to 7.3.

After substitution of this value into equation (1) and algebraic manipulation, it can be rewritten as

$$\frac{w}{W} = \left(3.7 \frac{P_e}{P_c} - 0.507 \right) \left(\frac{P_e}{P_b} \right)^{0.85} \quad (2)$$

Equation (2) permits the calculation of the weight of entrained vapour per weight of motive fluid expended. The amount of cooling obtained per unit of heat expended can then be calculated by

$$\frac{Q_e}{Q_b} = \frac{w \Delta H_e}{W \Delta H_b} \quad (3)$$

The coefficient of performance for a compression refrigeration system is defined as the ratio of the heat removed in the evaporator to the work expended for compression. In order to calculate a coefficient of performance for a no-work cycle, Q_e , the refrigeration obtained is divided by the amount of work which could be obtained if the heat expended in the boiler, Q_b , had been converted into mechanical energy by a Carnot cycle operating between T_b and T_c .

$$\text{C.O.P.} = \frac{Q_e}{Q_b \frac{(T_b - T_c)}{T_c}} = \frac{w \Delta H_e}{W \Delta H_b} \frac{T_b}{T_b - T_c} \quad (4)$$

The conditions chosen for the calculations are as follows:

- (1) Evaporating temperature, 5°F (−15.0°C)
- (2) Condensing temperature, 86°F (30.0°C)
- (3) Boiler temperature, 140°F (60.0°C)

The boiler temperature of 140°F was chosen since this temperature is available with relative ease from simple solar collectors. The evaporator and condensing temperatures chosen are identical with the A.S.R.E. standard cycle temperatures, although actual local condensing temperatures would probably be greater.

In order to determine ΔH_e and ΔH_b it was assumed that liquid leaving the condenser was saturated and that the vapours leaving the boiler and evaporator were saturated vapours at their respective pressures. The pump work required to return the liquid to the boiler was neglected in the calculation, since it amounted to less than 1% of the energy added in the boiler.

RESULTS

Calculations were carried out on eleven refrigerants in order to determine their behaviour in an ejector refrigeration cycle. The results are presented in Table I

TABLE I
Comparison of refrigerants in ejector refrigeration system

Refrigerant	P_e psia	P_c psia	P_b psia	ΔH_e BTU/lb	ΔH_b BTU/lb	w/W	Q_e/Q_b	C.O.P.
Propane	41.9	155.7	305	121.5	149.0	0.275	0.224	2.49
Freon-22	43.02	174.5	352.7	69.28	77.53	0.223	0.199	2.21
Freon-12	26.51	107.9	220.2	51.07	63.52	0.219	0.176	1.95
Methyl chloride	21.15	94.7	199.6	150.2	162.9	0.168	0.155	1.72
Isobutane	13.1	59.5	126.8	187.3	210.7	0.162	0.144	1.60
Ammonia	34.27	169.2	387	474.4	495.2	0.120	0.115	1.28
<i>n</i> -Butane	8.2	41.7	92.6	128.5	169.8	0.111	0.084	0.93
Sulphur dioxide	11.81	66.45	158.61	141.4	137.8	0.072	0.074	0.82
Freon-119	6.772	36.69	84.79	43.1	61.65	0.086	0.060	0.67
Freon-21	5.24	31.23	75.72	89.4	105.1	0.053	0.045	0.50
Freon-11	2.931	18.28	45.5	67.54	83.53	0.040	0.032	0.36

which lists the operating pressures, the refrigerating effect and heat requirement per pound of refrigerant, the entrainment ratio w/W , the performance factor Q_e/Q_b , and the coefficient of performance. The materials are listed in the order of decreasing efficiency. It will be noted that entrainment ratios larger than 0.2 are obtained with propane, Freon-22 and Freon-12 and that performance factors are smaller but of the same order. The theoretical value for the performance factor based on the Carnot efficiency would be 0.52. In order to provide a further basis for comparison, the performance factor was calculated for a normal ammonia absorption system cycle operating at 5°F evaporator temperature and 86°F absorber temperature. An ammonia absorption system cannot operate if it receives heat at 140°F due to the high concentration of the ammonia in the solution leaving the rectifier at this temperature. It was necessary therefore to choose a higher temperature of 200°F for the calculation. On this basis the performance factor for the ammonia absorption cycle was 0.394.

In order to determine the effect of changes in operating temperatures on the performance factor, a further series of calculations were carried out on Freon-12. The results are presented in Figures 2, 3 and 4. Figure 2 shows the variation in

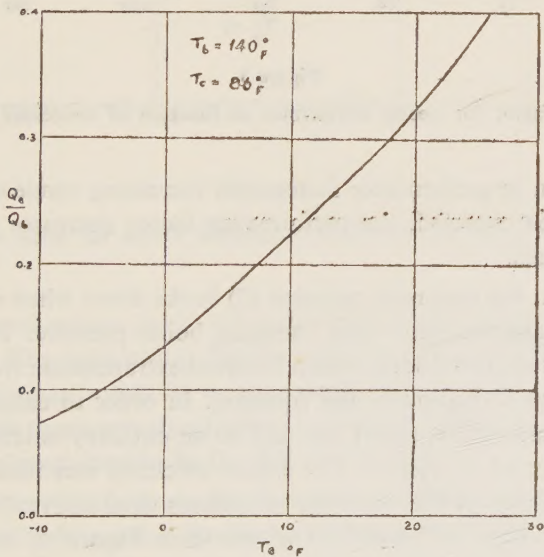


Figure 2

Performance factor for ejector refrigerator as function of evaporator temperature

performance factor with increasing evaporator temperature, the boiler and condenser temperatures being maintained at 140°F and 86°F respectively. As would be expected, the performance factor increases with increasing evaporator temperature. Figure 3

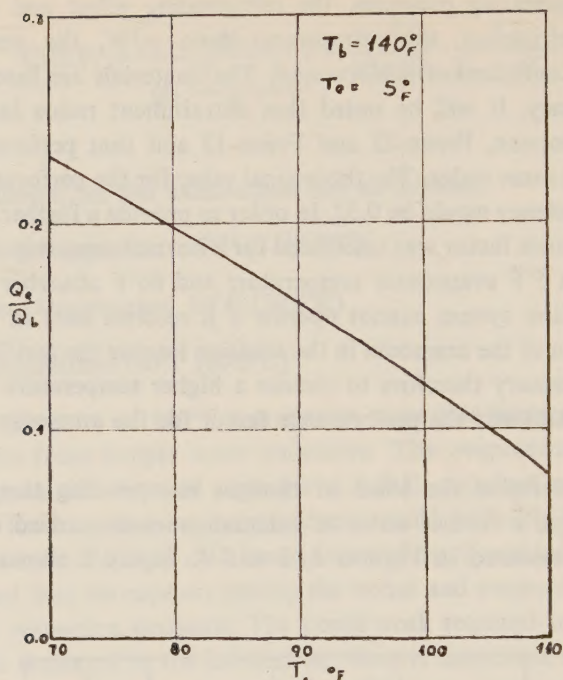


Figure 3

Performance factor for ejector refrigerator as function of condenser temperature

shows the variation in performance factor with increasing condensing temperature. Again, as would be expected, the performance factor decreases as the condenser temperature increases.

It was found that the empirical equation (2) broke down when used to determine the change in entrainment ratio with changing boiler pressure. This was evidently due to the fact that the conditions chosen involved extrapolation from the conditions obtained during the derivation of the equation. In order to calculate the effect of changing boiler temperature, resort was had to an enthalpy balance based on ideal isentropic behaviour of the ejector. The ejector efficiency was then calculated based on the results obtained for the operating conditions cited above. The overall ejector efficiency was calculated to be 42%. On this basis Figure 4, which presents the variation in performance factor with changing boiler temperature, was calculated. As would be expected, the performance factor rises, at first rather sharply, with increasing boiler temperature.

CONCLUSIONS

The use of an ejector refrigeration cycle for the production of refrigeration from low temperature energy sources appears to be quite feasible. Performance factors

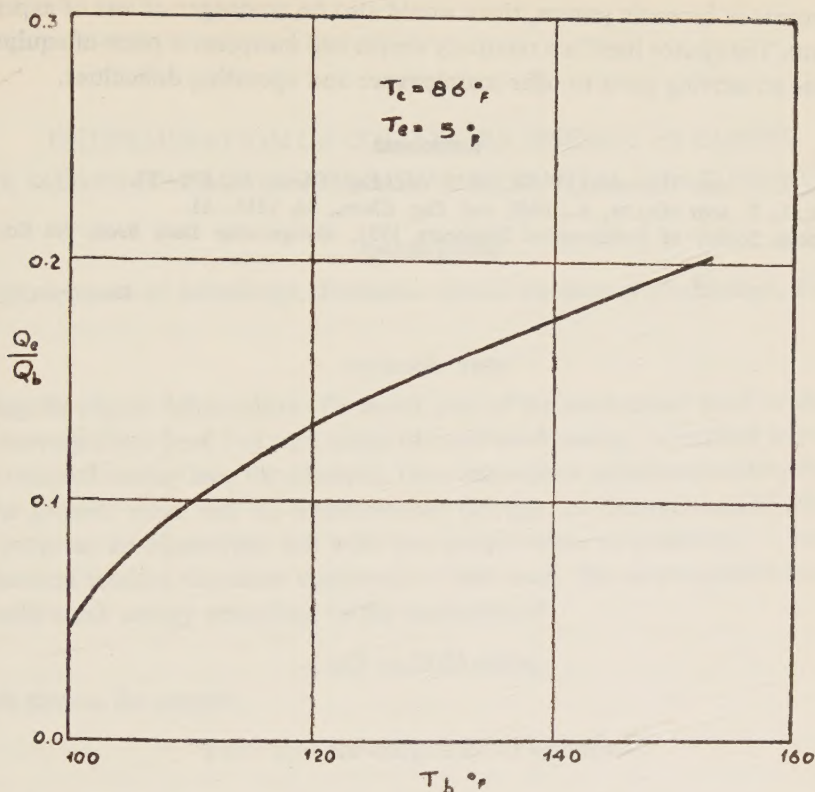


Figure 4

Performance factor for ejector refrigerator as function of boiler temperature

of the order of 0.2 and greater can be expected from propane, Freon-22 and Freon-12 as the refrigerant. The calculations for entrainment ratio and performance factor were based on performance data for a commercial ejector as reported by Work et al^{2,3}. It is reasonable to assume that higher performance factors could be expected from an ejector designed specifically for this type of duty.

The operating conditions chosen for the study were identical with those of the American Society of Refrigeration Engineers. Although the evaporating temperature is reasonable for local conditions, the condensing temperature of the A.S.R.E. standard cycle, 30°C, might be somewhat low for local conditions. A satisfactory local condensing temperature of 35°C would lower the calculated performance factor slightly.

An ejector refrigeration cycle would appear to be a completely feasible method for utilizing low temperature energy for the production of refrigeration. The system is essentially simple in design and should offer no operating difficulties. With recent

developments in hermetic pumps, there would also be no danger of loss of expensive refrigerant. The ejector itself is a relatively simple and inexpensive piece of equipment which has no moving parts to offer maintenance and operating difficulties.

REFERENCES

1. WORK, L. T. AND HAEDRICH, V. W., 1939, *Ind. Eng. Chem.*, **31**, 464—77.
2. WORK, L. T. AND MILLER, A., 1940, *Ind. Eng. Chem.*, **32**, 1241—43.
3. American Society of Refrigeration Engineers, 1953, *Refrigerating Data Book*, 8th Ed., New York.

DETERMINATION OF COLD-WORK ENERGY IN COPPER BY MEANS OF ELECTROCHEMICAL POTENTIAL MEASUREMENTS

ASHER PERES

Department of Metallurgy, Technion—Israel Institute of Technology, Haifa

INTRODUCTION

During the plastic deformation of a metal, part of the mechanical work is dissipated and converted into heat, but part, called the cold-work energy, is retained in the metal. This retained energy has, for example, been determined calorimetrically¹; the object of the present work was its measurement through its electrochemical effect. For this purpose, an electrolytic cell with two copper wires as electrodes — one under mechanical tension, the other unstressed — was used. The electromotive force gives the cold-work energy according to the equivalence⁵

$$1 \text{ mV} \equiv 23.05 \text{ cal/eq.}$$

which means, for copper:

$$1 \text{ mV} \equiv 0.726 \text{ cal/g} \equiv 277.5 \text{ kgcm/cm}^3.$$

EXPERIMENTAL PROCEDURE

The test-piece* (anode) was a carefully annealed copper wire, stretched between the grips of a horizontal tension machine and passing through a container filled with an acid solution of copper sulphate; the walls of the container through which the wire passed were made of soft rubber. The cathode was a short copper wire subjected to prolonged electrolytic coating under very low current (in order to obtain as stress-free a surface as possible), and placed so as to leave a 1 mm gap between it and the anode. A stirrer, actuated by an electric vibrator, was suspended opposite it.

This simple apparatus was inadequate, as a rapid decay of the emf was observed which would only be slowed down by stirring the electrolyte, but not arrested. This is presumably due to the microscopic inhomogeneity of cold-work². When cold-worked metal is dipped into a solution of one of its salts, higher-strained areas of its surface will become anodes and dissolve, while the lower-strained ones will become cathodes and grow. These microcircuits polarize the surface of the test-piece,

* Similar test-pieces, subjected to an ordinary tensile test, showed a tensile strength of 23 kg/mm² and elongation of about 50%. The present experiment lasted about four hours, and it is obvious that the electrolytic bath weakened the test-piece.

and their dominant influence is seen in the fact that opening or short-circuiting of the external circuit has little effect on the rate of decay. In fact, it was observed that after a few minutes, the emf dropped to zero, and even reversed sign.

As the measurement of the initial emf was very difficult (it was found impossible to follow the emf rise as function of the strain) the only means of securing good reproducibility was to electropolish the test-piece and remove the subsequent polarization by application of an alternating current. For this purpose a third electrode was introduced in the form of a grid enclosing both anode and cathode. This grid served as cathode in the electropolishing process, in order not to polarize the original cathode. After the electropolishing, the alternating current was applied between this auxiliary electrode and the anode.

Although this method proved successful in removing the polarization caused by the electropolishing, it introduced a new disturbance, due to the fact that for copper in an acid solution of copper sulphate, the anode efficiency is slightly higher than that of the cathode³. Application of an alternating current will therefore cause a slow reduction of the electrode's volume, with the simultaneous appearance of colloidal copper, positively ionized at first, but tending to capture hydroxyl ions² and eventually assuming a negative charge. The effect is indicated by a shift of the apparent emf. This shift was shown to depend on the density of the alternating current, the relative position of the electrodes and the stirrer, the rate of stirring and the composition of the electrolyte. (The influence of temperature and frequency was not studied). In the course of each measurement, all these factors were maintained rigorously constant.

In this experiment, the current density was such that during each cycle, about one-half of the surface atoms were removed, and then redeposited on the anode. Its surface underwent a severe ionic bombardment, which presumably resulted in rapid levelling of the energy, and in a few minutes reached a practically stress-free state. In fact, it was observed that the emf was fairly stable for one or two seconds. This was followed by a steep drop for 10 to 20 seconds and then by a more gradual drop, finally tending to an asymptotic limit. These intervals were shorter for small strains and longer for larger ones, as can be expected in view of the fact that the more the test-wire is strained, the longer it takes to level its surface energy.

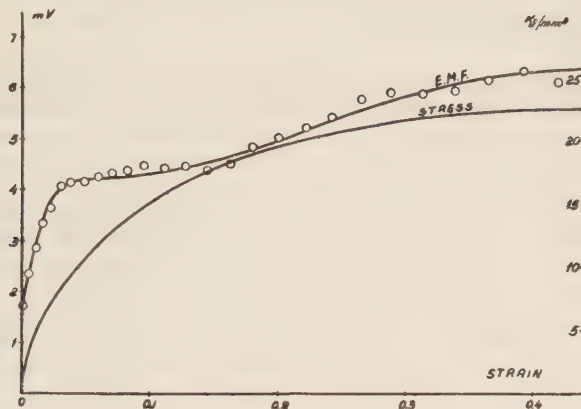
The experimental procedure was as follows:

After each stage of traction, the anode was electropolished by a direct current of about $3\text{mA}/\text{cm}^2$ for 30 seconds — the time found necessary to ensure reproducible results — with the potentiometer set tentatively at the same time for the subsequent measurement of the emf. Next, alternating current was applied and the galvanometer circuit closed simultaneously; a zero reading indicated that the potentiometer had been set at the correct emf value. Failing this, the potentiometer was adjusted and the whole process repeated until the correct position was found. Four more measurements were taken at fixed time intervals, and the value of the emf after an infinite time was determined by extrapolation. Assuming that the shift of the emf caused

by the alternating current remained constant during each measurement, the difference between the initial and asymptotic values represents the cold-work energy.

DISCUSSION OF RESULTS

The results are shown in the following diagram.



Stress (referred to initial section) and the difference between the initial and final emf as functions of strain.

It can be seen that even before the application of any external force, the energy level of annealed copper is higher than that of the electrodeposited, presumably stress-free, material. As soon as an external force is applied, the energy rises very rapidly, at a much higher rate than the imparted work averaged over the test-piece. It is therefore necessary to suppose that the measured emf represents, not an average, but the highest-strained parts of the cold-worked metal. This can be made plausible by noting that the microcircuits on the surface of the anode, due to its inhomogeneity, have a much lower resistance than the external circuit encompassing the whole of the electrolyte and the emf measurement apparatus. The lower-strained parts of the anode will go on growing only at the expense of the higher-strained ones, and no ionic exchange will occur between them and the cathode.

If it is assumed that the whole of this energy is due to micro stresses, these results show that even after annealing there remain residual stresses exceeding 300 kg/mm^2 (presumably due to dislocations, imperfect fits at grain boundaries, etc.). With the onset of strain, they increase very rapidly up to 500 kg/mm^2 . It should be noted that their initial rate of increase is equal to Young's modulus, within the limits of experimental error. For higher strains, increase of the higher microstresses is much slower, with a maximum exceeding 600 kg/mm^2 . The values thus obtained are of the same order of magnitude as those determined by X-ray analysis².

ACKNOWLEDGMENT

The author is indebted to Mr. A. Taub for many helpful suggestions during the course of this investigation, and to Prof. D. Rosenthal for clarifying discussions on the results.

REFERENCES

1. TAYLOR, G. I. AND QUINNEY, H., 1934, *Proc. Roy. Soc.*, **143**, 307; 1937, **163**, 157.
2. WARREN, B. E. AND AVERBACH, B. L., 1952, *Imperfections in Nearly Perfect Crystals*, Wiley, New York, pp. 152—172.
3. BLUM, W. AND HOGABOOM, G. B., 1949, *Electroplating and Electroforming*, McGraw-Hill, New York, p. 291.
4. GLASSTONE, S., 1940, *Physical Chemistry*, Van Nostrand, New York, p. 1217.
5. WAGNER, C., 1952, *Thermodynamics of Alloys*, Addison-Wesley, Cambridge, Mass., p. 12.

A NEW INDIRECT TENSILE TEST FOR CONCRETE THEORETICAL ANALYSIS AND PRELIMINARY EXPERIMENTS*

S. ROSENHAUPT**, A. C. VAN RIEL AND L. WIJLER**

T.N.O. Structural Research Laboratory, Delft, Holland

ABSTRACT

The test consists in applying a compressive load along the middle of two opposite faces of a concrete cube. Tensile stresses result in rupture along the plane containing the load.

The plane-strain problem was studied by the method of differences, with the system of equations solved by matrix inversion. The tensile stress along the middle plane is fairly uniformly distributed, its value being $\sigma = 0.648 P/ah$ (σ = tensile stress in kg/cm², P = force in kg, a, h = dimensions of failure section in cm).

Photoelastic analysis (using a square slab of "catalin") gave values of the stresses σ_x , σ_y , τ_{xy} and trajectories in agreement with the theoretical results, and tests at 28 days, on cubes and cylinders under indirect tensile load and on prisms, provided additional corroboration.

The main advantage of the suggested method is the possibility of using the same moulds and loading apparatus as in the ordinary compression test.

An indirect tensile test, based on the application of a line-load to two opposite generatrices of a cylinder (Figure 1) was developed in Brazil¹ and experimental investigations with regard to it were carried out in England² and at the T.N.O. laboratory (Holland)^{3,4}.

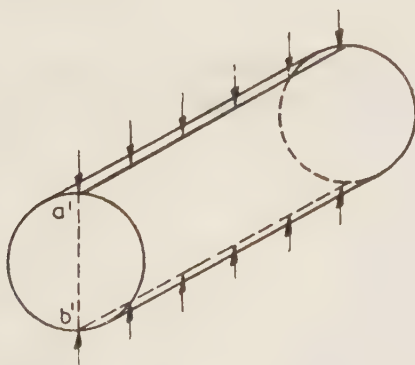


Figure 1
Brazilian indirect tensile test.

* The results were preliminarily summarized in Report No. BI-56-6, I.B.C.-T.N.O. A paper was presented at the Fourth Meeting of the Israel Association for Theoretical and Applied Mechanics on April 14, 1956 at Haifa (*Bull. Res. Council of Israel*, 1956, 5C, 254).

** Present address: Technion—Israel Institute of Technology, Haifa.

As in Holland compression tests are carried out on cubes, it was considered desirable to use the same moulds for indirect tensile tests as well (Figure 2), thus gaining obvious practical advantages.

THE INVESTIGATION

The problem was studied in three steps:

1. Theoretically, by solving the plane-strain problem of a square acted upon by two equal and opposite forces (Figure 3).

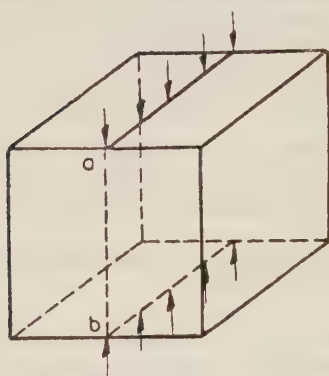


Figure 2
Proposed indirect tensile test.

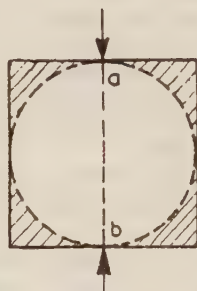


Figure 3
The shaded areas are expected to be of little influence on stress distribution along a b

2. By photoelastic testing of two identically loaded slabs, one square and one circular (Figures 4 and 5) and comparing the isochromatic and isoclinic lines thus obtained.

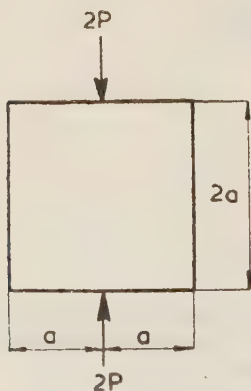


Figure 4
Slabs used in the photoelastic tests



Figure 5
Slabs used in the photoelastic tests

3. By testing concrete specimens (cubes and cylinders) in indirect tension and unreinforced beams in bending, and comparing the results.

A. THEORETICAL SOLUTION

Plane strain is governed by the following equilibrium equations:

$$\frac{\partial \sigma_x}{\partial x} + \frac{\partial \tau_{xy}}{\partial y} = 0 \text{ and } \frac{\partial_y}{\partial y} + \frac{\partial \tau_{xy}}{\partial x} = 0 \tag{1}$$

and the compatibility equation:

$$\frac{\partial^2(\sigma_x + \sigma_y)}{\partial x^2} + \frac{\partial^2(\sigma_x + \sigma_y)}{\partial y^2} = 0 \tag{2}$$

Equations (1) are identically satisfied by

$$\sigma_x = \frac{\partial^2 \Phi}{\partial y^2}, \sigma_y = \frac{\partial^2 \Phi}{\partial x^2} \text{ and } \tau_{xy} = -\frac{\partial^2 \Phi}{\partial x \partial y} \tag{3}$$

where Φ is the Airy function. By (2), this function has to satisfy:

$$\Delta \Delta \Phi = \frac{\partial^4 \Phi}{\partial x^4} + 2 \frac{\partial^4 \Phi}{\partial^2 x \partial^2 y} + \frac{\partial^4 \Phi}{\partial y^4} = 0 \tag{4}$$

The boundary conditions for Φ and $\partial \Phi / \partial x$ are given in Figure 6 and 7. $\partial \Phi / \partial y = 0$ along the boundaries.

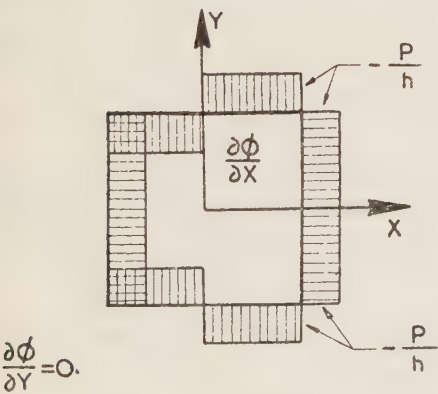


Figure 6
Boundary conditions for $\partial \Phi / \partial n$ and $\partial \Phi / \partial y$.

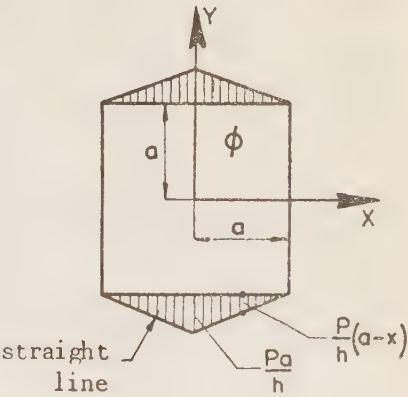


Figure 7
Boundary conditions for Φ .

Φ was found by solving the equations of finite differences at points 1--16 (Figure 8). Using $Pa/h = 10,000$, the values of Φ are as given in Figure 9.

The values of the stresses at each point were obtained from the Φ values, using (3), and are given in Figures 10, 11, 12.

The principal directions were calculated and the trajectories are as given in Figure 13.

The conclusions from the theoretical analysis were:

1. The values of the stresses and their distribution, as well as the trajectories, are very much like those of a circular disc (Figure 14). The stresses in the corners (shaded area in Figure 3) are very low.

2. The tension along the centre line ab is fairly uniformly distributed (Figure 10) and can be taken as:

$$\sigma_{average} = \frac{0.65184 + 0.64720 + \frac{1}{2} \cdot 0.64192}{2.5} \cdot \frac{P}{ah} = 0.648 \frac{P}{ah} \quad (5)$$

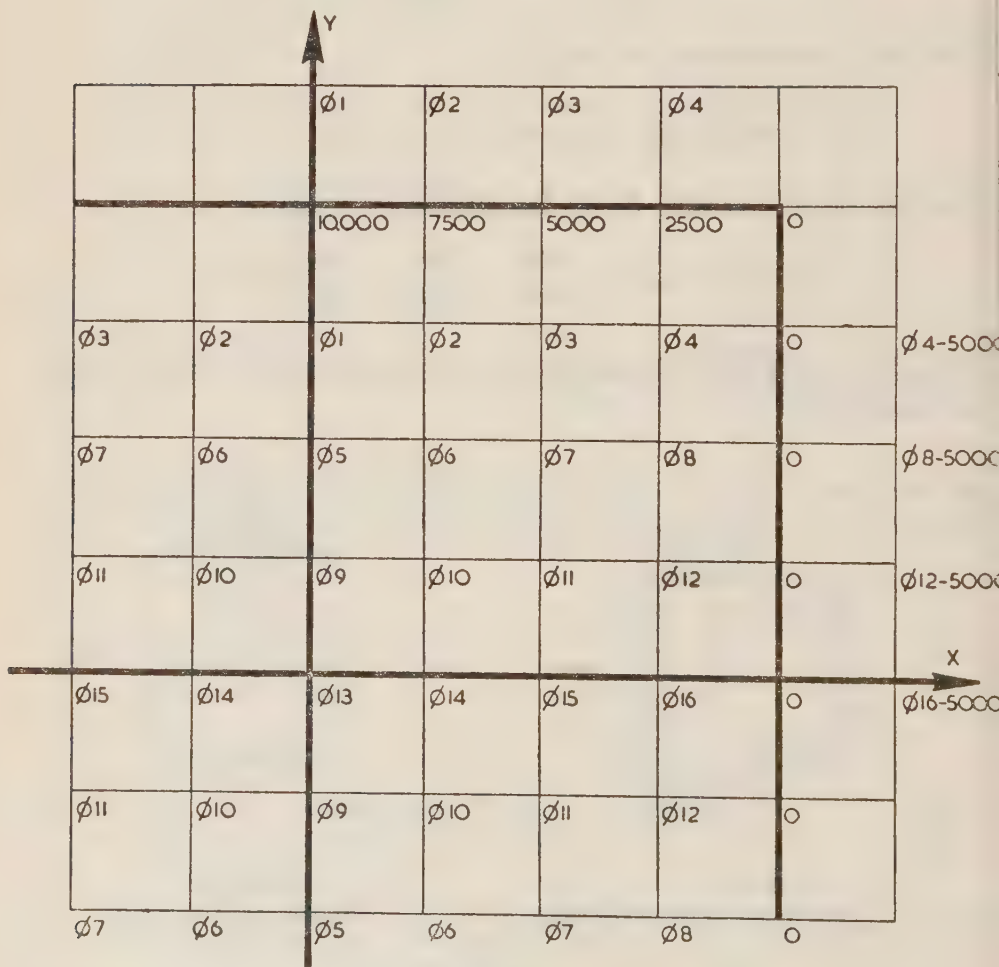


Figure 8

Square grid used for writing the finite differences equation.

In the case of the inscribed circle:

$$\sigma = \frac{2}{\pi} \cdot \frac{P}{ah} = 0.637 \frac{P}{ah} \quad (6)$$

The difference being about 1.5%.

B. PHOTOELASTIC ANALYSIS

The object of this test was:

1. To verify the theoretical solution for the square slab.
2. To compare the stresses with those of the circular slab.

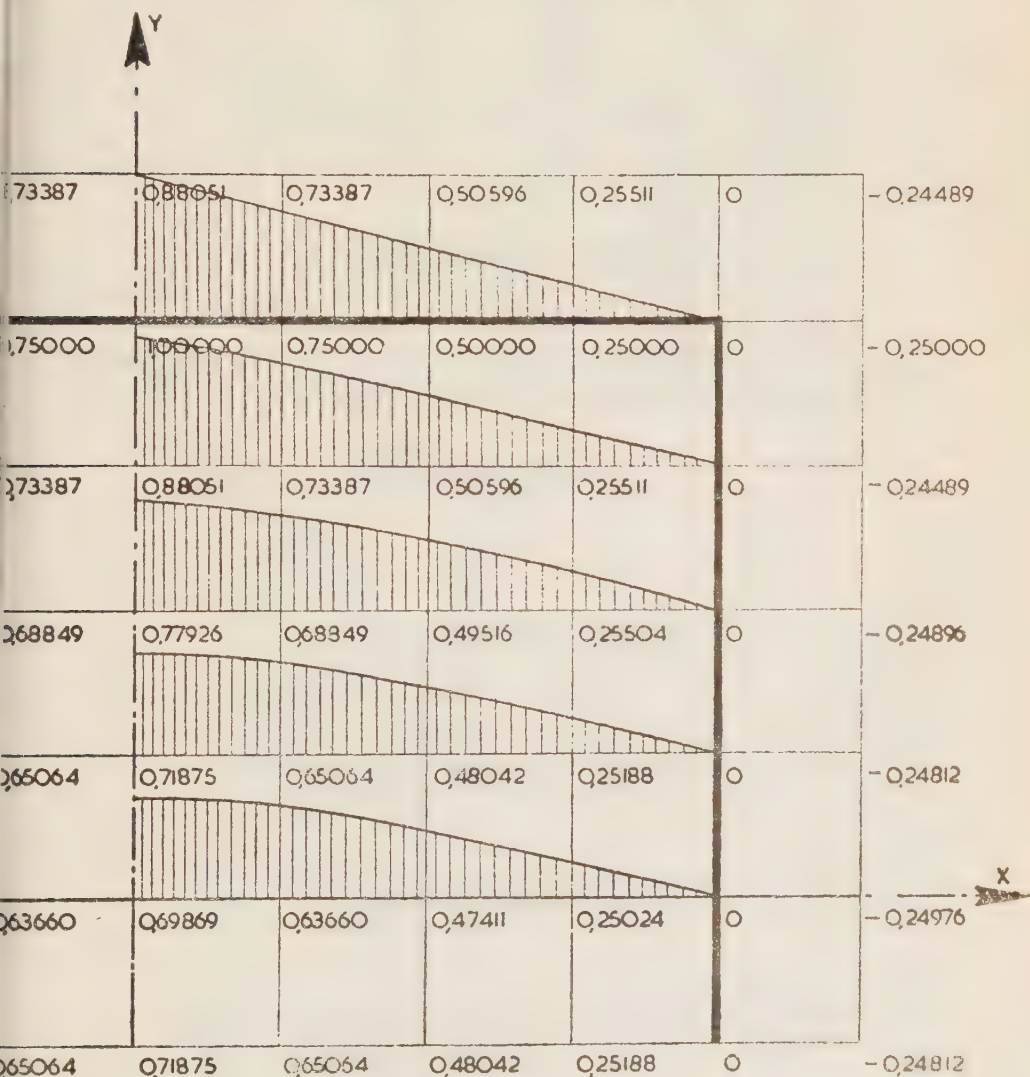


Figure 9
Values of Φ (Airy function = $\Phi \cdot Pa/h$).

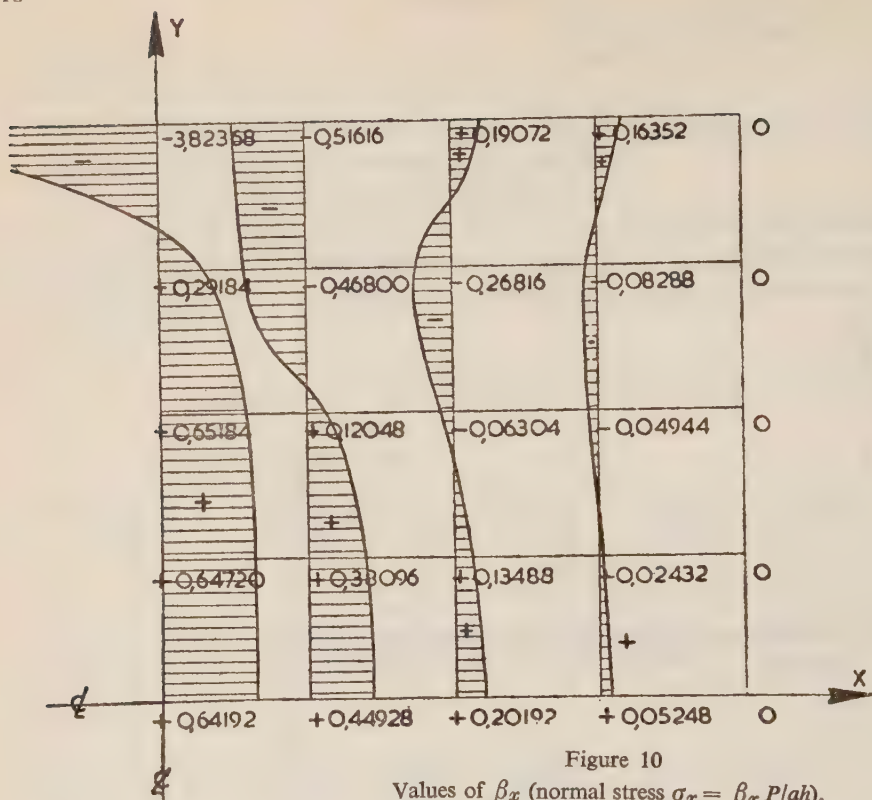


Figure 10
Values of β_x (normal stress $\sigma_x = \beta_x P/ah$).

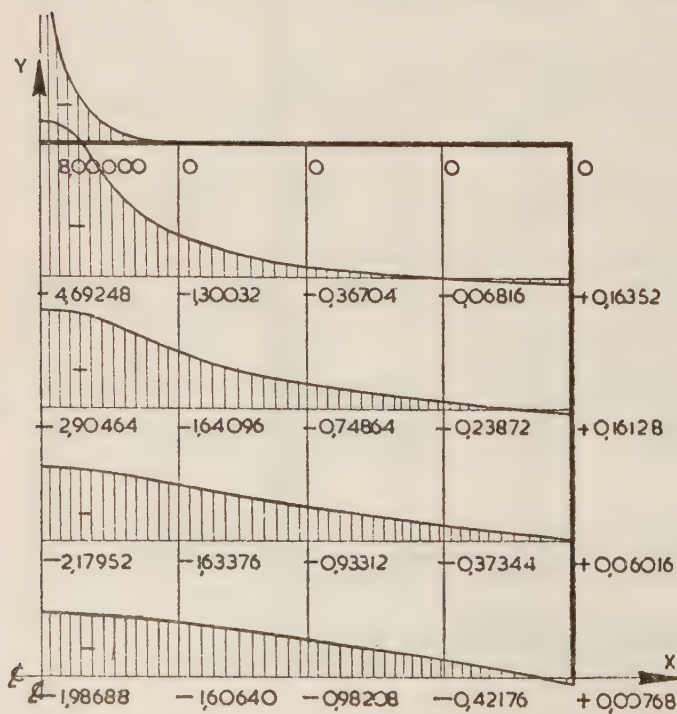


Figure 11
Values of β_y (normal stress $\sigma_y = \beta_y P/ah$).

The isochromatic fringes (i.e. loci of constant difference between the principal stresses) are given in Figures 15 and 16, the isoclines (loci of constant direction of the principal stresses) in Figures 17 and 18.

The calibration of specimens was carried out with the aid of the equilibrium equation along the diameter perpendicular to the direction of the forces. The sum of the principal stresses was found with the aid of the equation of compatibility:

$$\left(\frac{\partial^2}{\partial x^2} + \frac{\partial^2}{\partial y^2}\right)(\sigma_x + \sigma_y) = 0 \quad (7)$$

Equation (7) was solved by the method of differences.

The theoretical and photoelastic results were in close agreement (discrepancies of 0—0.5%).

From Figures 15, 16, 17 and 18, it can be seen that the stress distributions in the circular and square slabs show a high degree of similarity.

C. TESTS ON CONCRETE SPECIMENS

The specimens prepared were as follows:

9 prisms $10 \times 10 \times 30$ cm — tested in bending (Figure 19).

9 cylinders $2a = 15$ cm, $h = 32$ cm — tested in indirect tension (Figure 20).

11 cubes $20 \times 20 \times 20$ cm — tested in indirect tension (Figure 21).

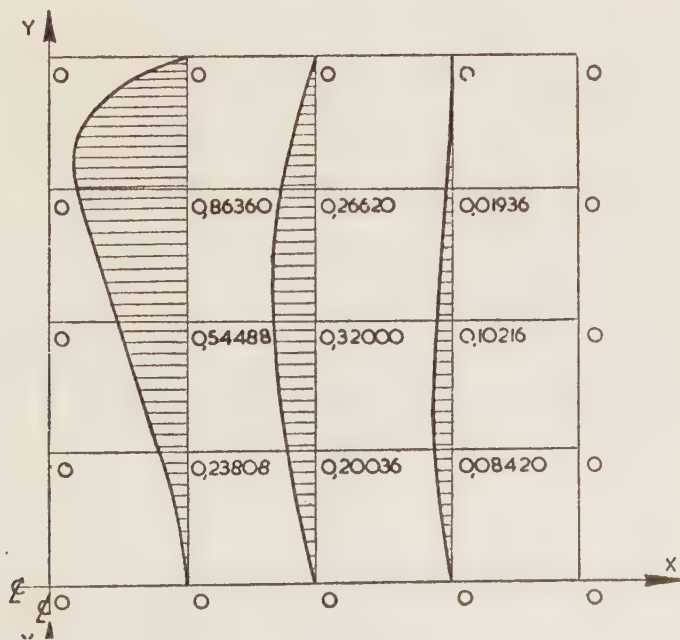


Figure 12

Values of β_{xy} (shear stress $\tau_{xy} = \beta_{xy} P/ah$).

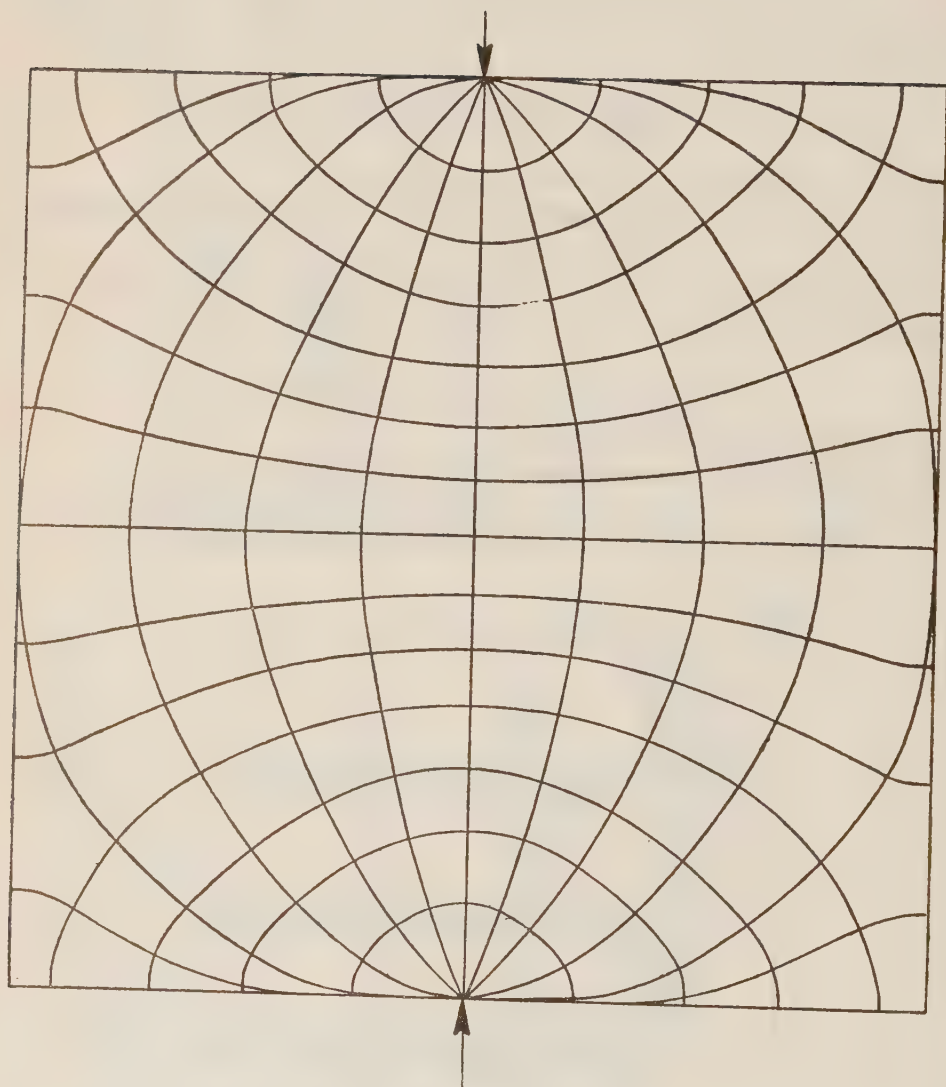


Figure 13
Stress trajectories in the square slab.

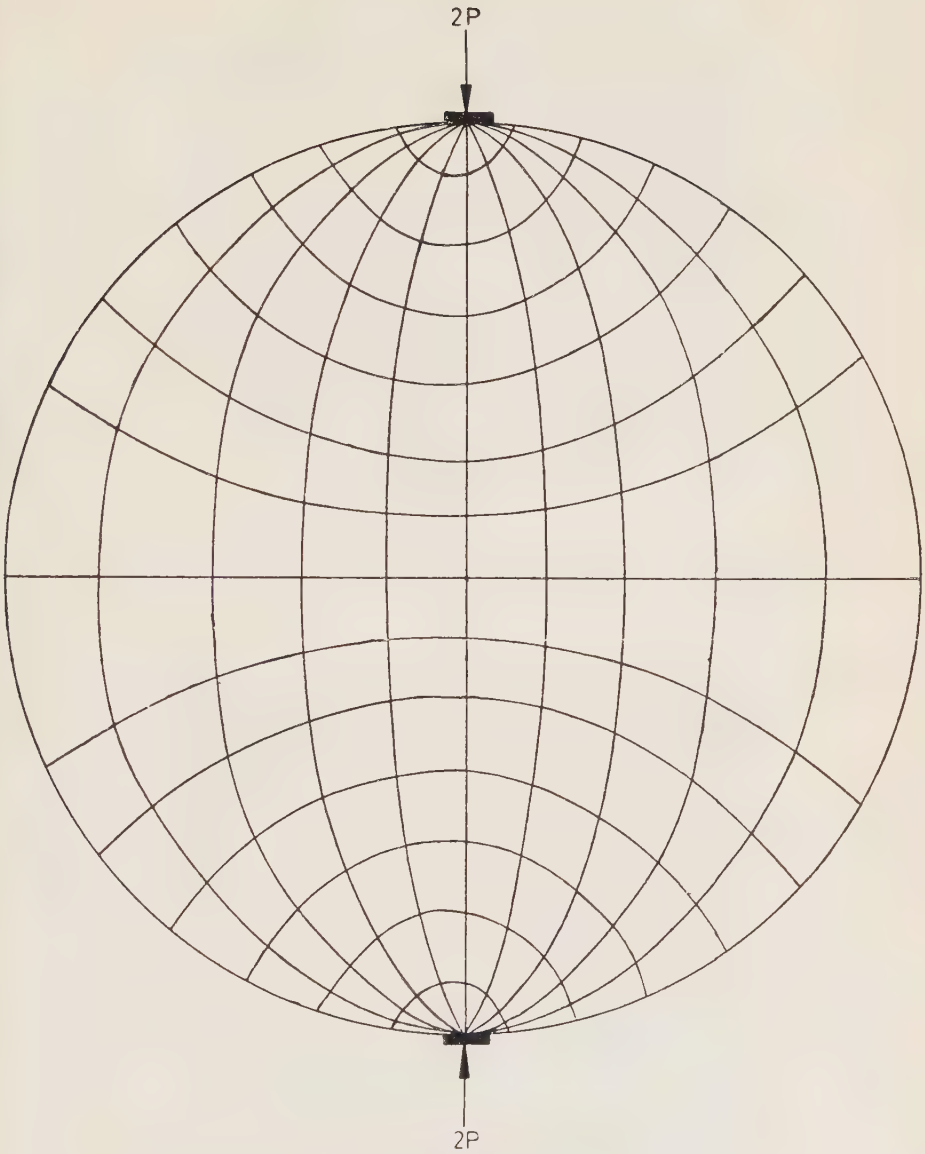


Figure 14
Stress trajectories in the circular slab



Figure 15
Isochromatic fringes in the circular slab



Figure 16
Isochromatic fringes in the square slab

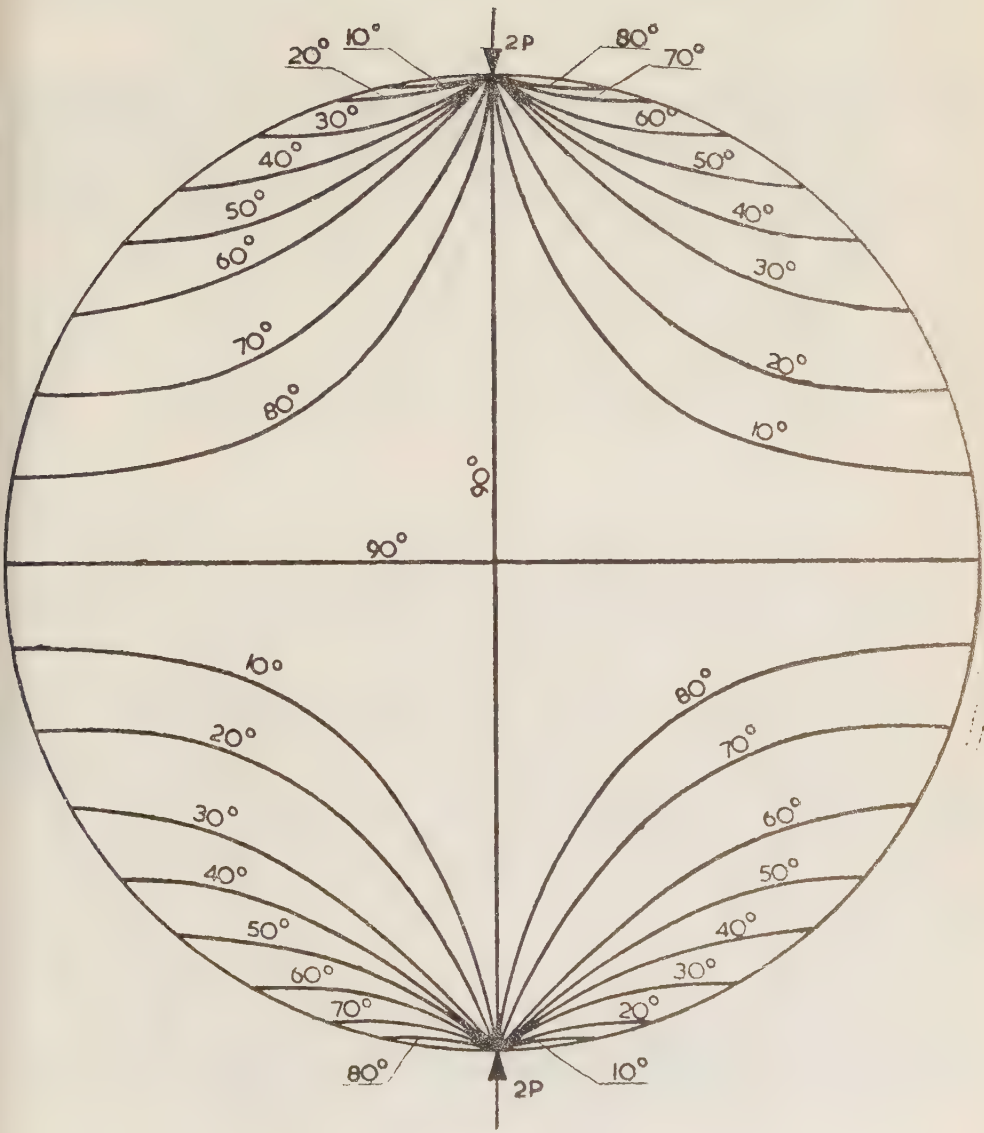


Figure 17
Isoclines in the circular slabs.

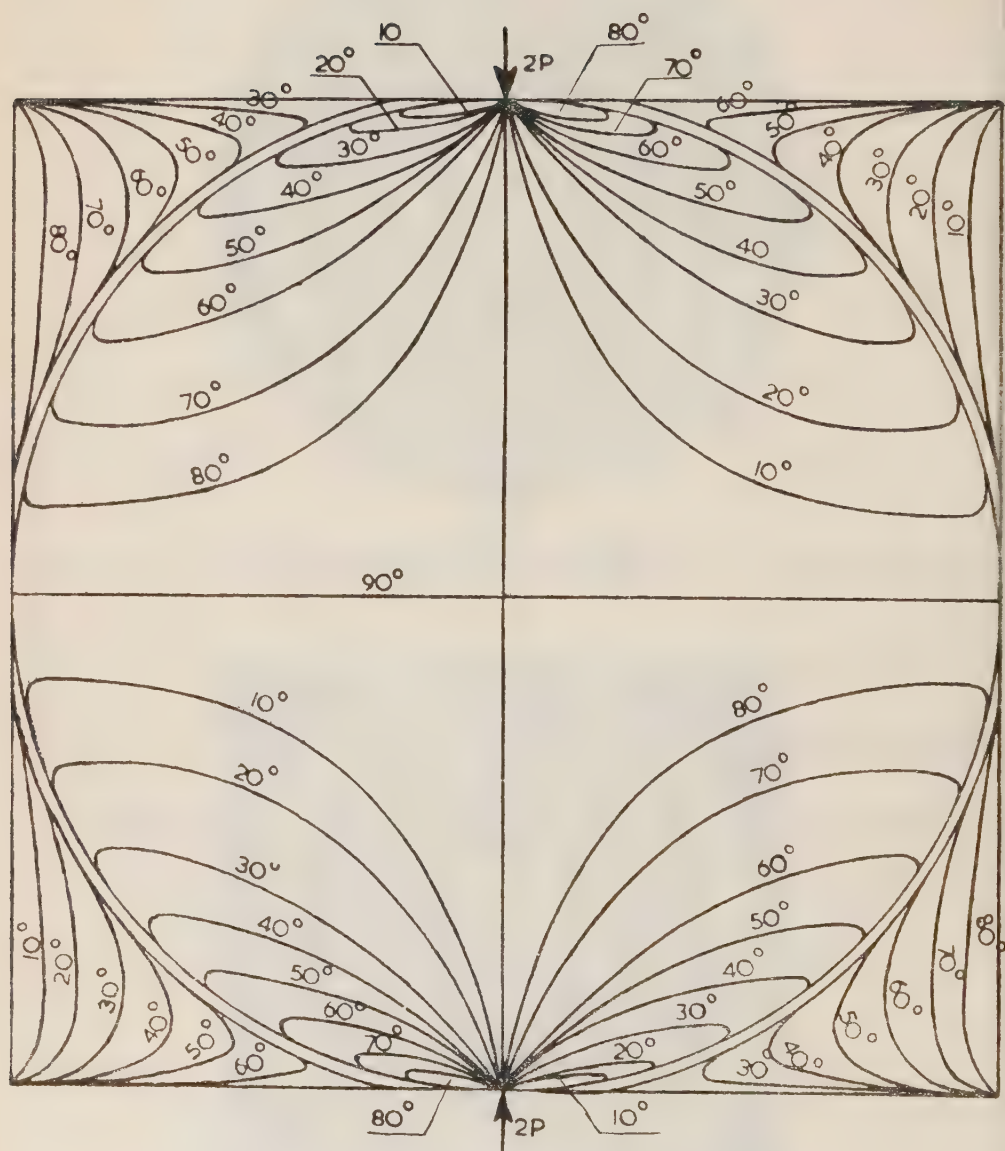


Figure 18
Isoclines in the square slab.

All specimens were tested at 28 days. The results are summarised in Table I.

TABLE I

Specimens		Prisms <i>T</i>	Cylinders <i>T</i>	Cubes <i>T</i>	Cubes (compression) <i>C</i>
Mean strength	kg/cm ²	47.3	26.4	26.1	330*
Standard deviation	kg/cm ²	2.7	2.1	1.4	—
Coefficient of variation	%	4.7	8.1	5.3	—

* only 2 tests made.

Definition:

mean strength $\bar{x} = \frac{\sum x_i}{n}$

standard deviation $s = \sqrt{\frac{\sum (x_i - \bar{x})^2}{n - 1}}$

coefficient of variation $v = \frac{s}{\bar{x}} \times 100$

Nation x_4 = result of test , n = number of tests.

The following observations were made during the tests:

1. In all tests the cubes failed along a diametrical plane containing the load, thus confirming the theoretical calculations which assign the maximum tensile stress to this plane (Figure 22).
2. The tensile strength as determined by the theoretical calculation was in very close agreement with that obtained from the photoelastic test and the concrete specimens.
3. The tensile strength as determined on prisms was about 80 % higher than that determined on cubes and cylinders. An important cause seems to be the fact that the stress distribution is not linear, as assumed in the stress calculation.

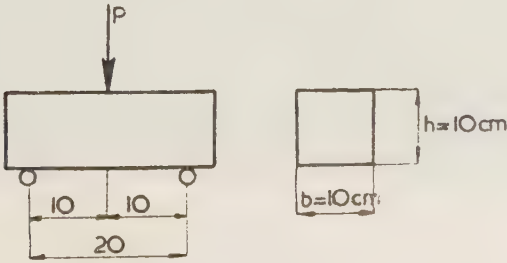


Figure 19
Bending test on prisms.

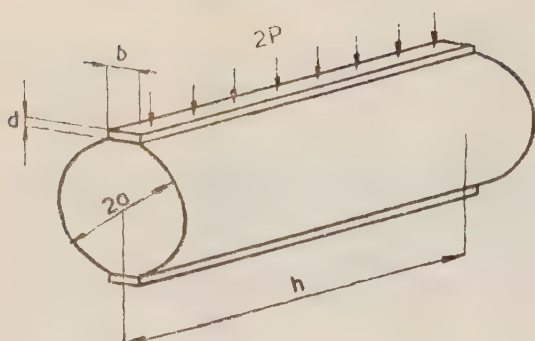


Figure 20

Indirect tensile test on cylinders.

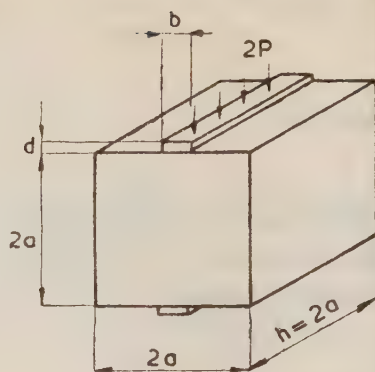


Figure 21

Indirect tensile test of cubes.

CONCLUSIONS

1. The new tensile test has proved reliable.
2. It has the advantage of permitting the use of the same moulds and loading apparatus as the ordinary compression test.

ACKNOWLEDGMENT

The authors wish to express their indebtedness to Ir. J. G. Hageman, Head of the T.N.O. Structural Research Laboratory, for his kind permission to publish the Laboratory Report in this Bulletin.

REFERENCES

1. CARNEIRO, F. L. L. AND BARCELLIS, A., 1953, Tensile strength of concretes, *RILEM, Bull.*, No. 13.
2. WRIGHT, P. J. F., 1955, Comments on an indirect tensile test on concrete cylinders, *Mag. Concr. Res.*, 7.
3. ROSENHAUPT, S. AND VAN RIEL, A. C., 1955, Indirect tensile test on concrete cylinders — Preliminary investigations, *Report No. BI-55-19, T.N.O. Rijswijk, Holland.*
4. VAN RIEL, A. C., ROSENHAUPT, S. AND WYLER, L., 1956, A new indirect tension test for concrete, *Report BI-56-6 T.N.O. Rijswijk, Holland.*

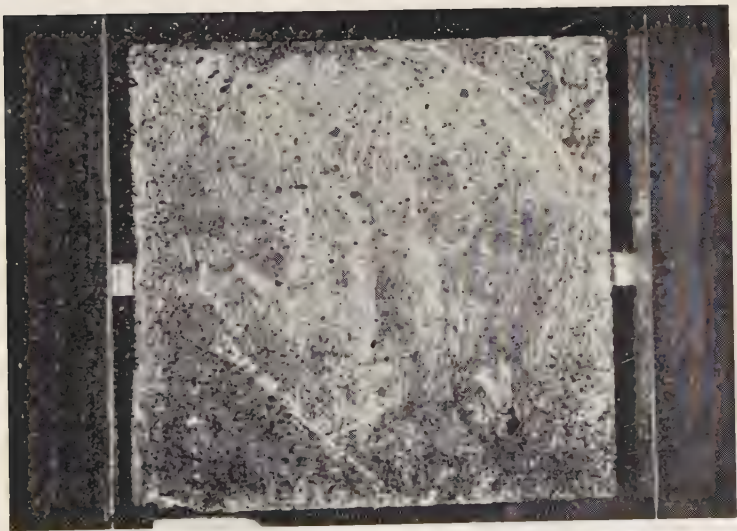
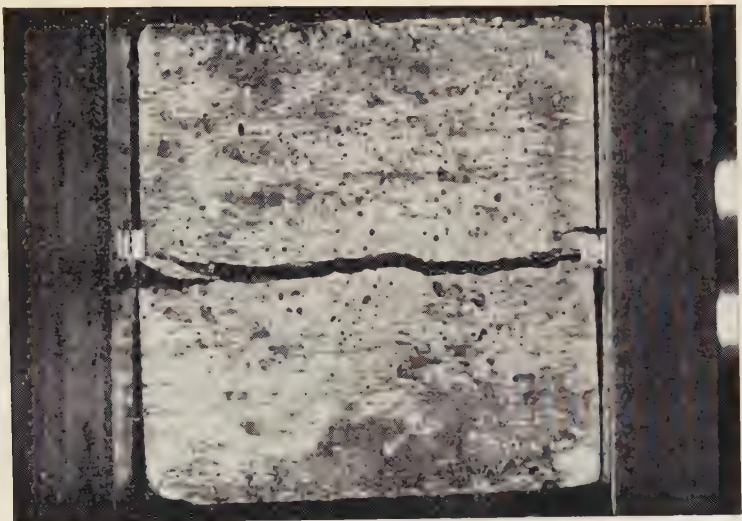


Figure 22
Photographs of the indirect tensile test on cubes

NEW REAGENT FOR MICROSCOPIC STRAIN ANALYSIS IN STEEL

ARIEL TAUB

Department of Metallurgy, Technion—Israel Institute of Technology, Haifa

ABSTRACT

A newly discovered gold reagent permits quantitative microscopic strain analysis of steel specimens.

INTRODUCTION

It has been observed that strained metals, or strained areas in metals, tend to higher chemical reactivity than strain-free metals. This higher reactivity is due to increased internal energy resulting from the distortion of the crystal lattice. The physical effects of this distortion (such as appearance of surface lines, local variation of hardness, increase in catalytic activity and selective tendency to etch-pitting) were studied by Lüder and Hoffman, Jevons^{1,2}, Schwab^{3,4,5} and Smakula and Klein⁶.

A copper-base reagent, by means of which strain lines could be detected in any metallographically polished steel cross-section, was developed by Fry^{7,8} and used by Jevons in his studies referred to above. However, in view of its high rate of reaction Fry's process does not lend itself to control, and application of the reagent results in the formation of a non-uniform deposit of copper—of varying thickness according to the local state of strain—over the entire polished specimen, so that its structure is obscured and quantitative analysis of the strained areas is impossible; the so-called "Fry lines" obtained in the process are merely topographical phenomena of the copper plate.

Unsuccessful attempts were made to modify Fry's reagent so as to slow the reaction down substantially and obtain a thin, nearly transparent and homogeneous copper plate. The transfer of the topography of the copper plate onto the steel specimen was also found impracticable, due to the cathodic protection effect.

PROPOSED TECHNIQUE

The object of this work was to find a suitable reagent for quantitative analysis of strained specimens under a controlled rate of reaction, based on a metal which would not provide cathodic protection to the steel in the final etching process. The metal finally selected was gold, and the proposed technique is based on a reagent of the following composition:

AuCl ₃ (anhydrous)	1 g
HCl (30%)	76 cc
H ₂ O	157 cc

A metallographically prepared steel specimen (Figure 1) is immersed in the gold solution for 15 sec. at room temperature, and a thin layer of gold is deposited on its surface (Figure 2). Next, the specimen is quickly rinsed in running water and transferred to a 4% nital solution where it is allowed to remain for 120 seconds, and then washed under the tap and at the same time lightly rubbed with cotton wool in order to dislodge any loose particles of the metal, leaving only the firmly adhering gold plate. Finally, the specimen is washed in alcohol and dried in a stream of hot air.



Figure 1

Cross section of unetched specimen. The A—A plane represents the surface of the specimen, B its structure, and hatched areas the strained grains.



Figure 2

Specimen after immersion in gold solution, showing gold deposit C.

The thickness of the gold layer ranges from 0.02 to 0.1 millimetre, dependent on the time of contact and the amount of strain. In the nital solution, the plate is attacked uniformly and goes into colloidal solution while the iron goes into ionic solution, so that no electrolytic interference takes place between the two dissolving metals. The gold is removed completely where the coating had been thin, and the nital then attacks the steel surface in the conventional way, revealing the microstructure (Figure 3).

Alternatively, the whole of the gold plate can be dissolved by allowing longer immersion in nital. In this case, the topography of the gold plate is transferred onto the specimen, as the rate of the colloidal dissolution of the gold is slower than that of the attack on the steel (Figure 4). In this way, a clearly visible steel microstructure is developed, and information provided at the same time with regard to the strained areas, which are left projecting upwards in relief over the other parts of the microstructure.

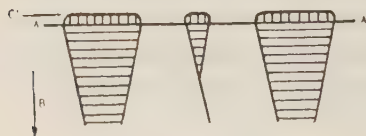


Figure 3

Specimen after immersion in nital long enough to dissolve thinly-plated areas, showing gold plate C on strained areas only.



Figure 4

Specimen after immersion in nital long enough to dissolve all of the gold, showing the transfer of the topography D of the gold plate (C in Figure 2) onto the steel specimen.

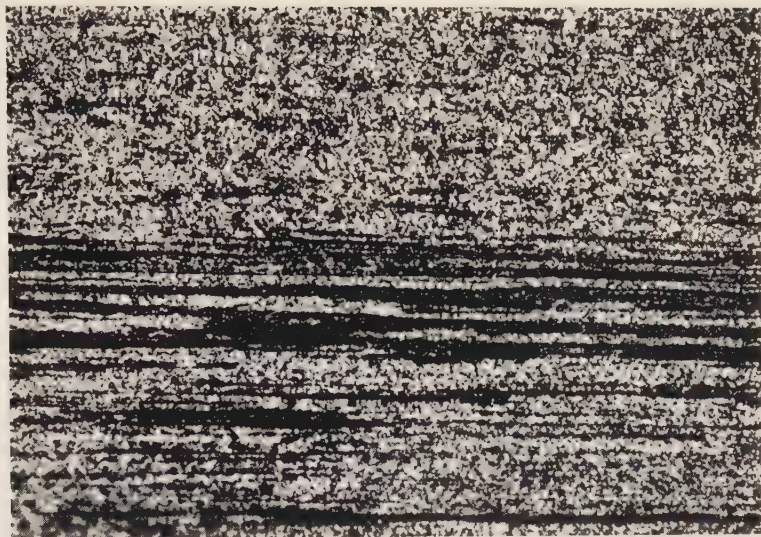


Figure 5

Gold chloride etch followed by 4% nital (magnification $\times 25$). Specimen surface (very low carbon steel) in the state shown in Figure 4. Dark lines — projecting strained areas.

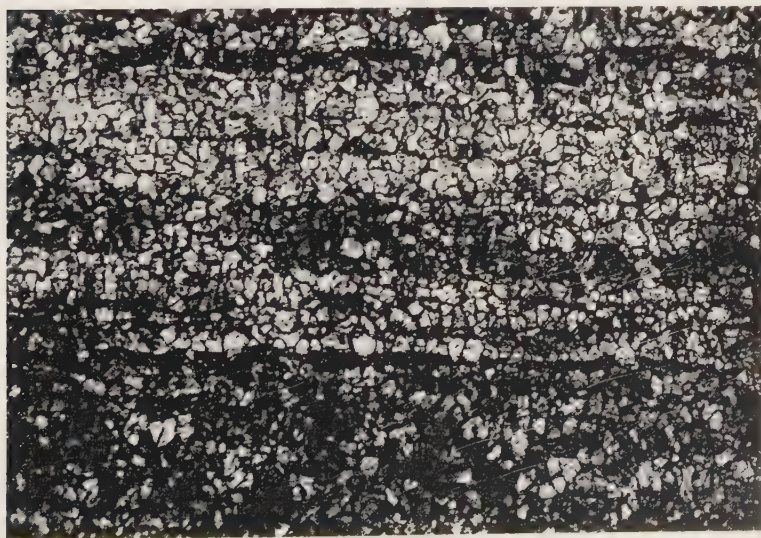


Figure 6

Same specimen at higher magnification ($\times 100$).

ACKNOWLEDGMENT

The author is indebted to Mr. Paul Wynblatt of the Department of Metallurgy for preparing the first draft of this paper.

REFERENCES

1. JEVONS, J.D., 1927, *Engineering, Lond.*, **123**, 155.
2. JEVONS, J.D., 1925, *Engineering, Lond.*, **119**, 585.
3. SCHWAB, G.M. AND PIETCH, E., 1929, *Z. Electrochem.*, **35**, 573.
4. SCHWAB, G.M. AND RUDOLF, L., 1931, *Z. phys. Chem.*, **12**, 427.
5. SCHWAB, G.M. AND PETROUSWOS, G., 1950, *I. Phys. et Colloid Chem.*, **54**, 591.
6. SMAKULA, A. AND KLEIN, M.W., 1953, *J. chem. Phys.*, **21**, 100.
7. FRY, A. AND STRAUSS, B., 1921, *Stahl u. Eisen, Düsseldorf*, **41**, 1133.
8. FRY, A., 1921, *Stahl u. Eisen, Düsseldorf*, **41**, 1093.

MEASUREMENT UNITS IN TRAFFIC ENGINEERING

M. PELEG (POLONSKY)

Technion—Israel Institute of Technology, Haifa

ABSTRACT

The introduction into traffic engineering of a system of units, similar to that used in mechanics and based on the CGS or on the metric system, is suggested. In addition to the unit of traffic capacity already in use, the units of number of vehicles, traffic momentum, traffic force, traffic power and traffic energy are defined and discussed. Examples are given for the use of some of these units for the comparison of the state of traffic on the road under different conditions, and for drawing practical conclusions referring to improvement of the traffic. Finally, a critical comparison of the terms "friction coefficient" and "braking coefficient" is given.

1) The universal CGS system of dimensions covers all fields of the exact and applied sciences. But sometimes units are used which, while based on the CGS system, are different from similar units used in other fields. Thus in mechanics there is the term "force" with dimensions cgs^{-2} ; in electrical engineering the term "electromotive force" is used and its dimensions are $\text{c}^{3/2} \text{g}^{1/2} \text{s}^{-2}$. For this, there are two main reasons: (a) Natural phenomena are not uniform in character, nor specially adapted to the system of dimensions introduced by the scientists for their convenience; (b) the different fields of science and engineering have in the course of their development taken different directions. This has involved the use of different measuring instruments and, consequently, of different units as well.

Once a certain branch of engineering has reached a suitable degree of development, it is desirable to fit the units used in it into a general measurement system such as the CGS system. During the last few years, the branch of traffic engineering has made considerable progress with respect to road construction and improvement of vehicles; its influence is now felt outside the limits of pure traffic problems, and has spread into such fields as town planning and even national planning.

There has always been a close connection between traffic problems and economics, mechanics and dynamics. The time has come to adapt the units and dimensions used in traffic engineering to those used in other fields of engineering science. What follows is an attempt at a beginning on this assignment.

2) The term "traffic capacity" is in common use in traffic engineering. It denotes the number of vehicles that can pass a given point of the road in one hour (the maximum traffic volume of a road carrying traffic of definite composition) and is

used to compare different roads with respect to their traffic qualities. The traffic capacity of a traffic lane is sometimes calculated with the aid of Agg's formula

$$N = \frac{3600v}{l + tv + cv^2}$$

where:

N is the traffic capacity in vehicles per hour

v is the speed of vehicles in metres per second

l is the length of vehicles in metres

t is the braking time in seconds

c is the braking coefficient (determined experimentally).

The braking time is sometimes defined as consisting of two parts, $t = t_1 + t_2$. t_1 is the reaction time required for the driver to decide on applying the brakes; t_2 - the time required for their application. t_1 depends on the individual qualities of the driver; t_2 - on the individual qualities of the driver, design of the vehicle and quality of the road surface. The expression $tv + cv^2$ in the denominator is the "safe distance" between vehicles driving in single file.

3) The traffic capacity calculated according to the above formula cannot be recognized as a satisfactory means of comparison for different roads with respect to their traffic qualities, for the following reasons:

a) It is not a fixed value, but depends on speed. As speed increases the traffic capacity increases too, until it reaches a certain maximum. Further increase in speed results in decrease of the traffic capacity. The rate of variation of the traffic capacity is different for different vehicles.

b) The traffic capacity diagram represents a curved line with a peak value for a certain speed. From this point the curve descends on both sides, both for increasing and decreasing speed. Each value of traffic capacity (except the peak value) has two corresponding values of speed. This certainly does not mean that when vehicles drive on the road at different speeds at some full traffic capacity, the state of traffic is also the same in both cases.

c) It is also desirable to take into consideration the change of value of the braking coefficient when determining the road qualities in respect of traffic. This will permit comparison between different roads, or, for the same road, between its different states. This is most important, as not only the size of vehicles is variable (length and width) but also the braking coefficient of the same road is different in different weather.

4) "Ideal" conditions could be found for which the traffic qualities of the road would be highest; comparing the state of traffic at a certain moment to the "ideal" conditions, it would be possible to know whether the road is used effectively or underexploited, or whether it is overloaded with respect to "safe conditions" and should be widened or otherwise improved in order to comply with traffic requirements.

From 3(c) it follows that the vehicle speed is one of the factors affecting the traffic qualities of the road. The speed factor is included in the following expression, which may be defined as "traffic force":

$$F = \frac{\text{speed} \times \text{number of vehicles}}{\text{hour}} = Nv \frac{\text{car kilometres}}{\text{hour}^2}$$

(*N* denotes traffic capacity in vehicles per hour, *v* — vehicle speed, in kmh⁻¹).

F may be expressed as the product of the number of vehicles passing a certain point of the road in the course of one hour (traffic volume) by their speed; or, as the product of the speed and the number of vehicles in a section of the road of length equal to the speed.

The traffic volume observed is generally less than the calculated traffic capacity, but traffic volumes have also been observed exceeding the calculated capacities, with the spacing of the vehicles less than the "safe distance".

5) If we calculate the "traffic force" of a traffic lane, according to the formula

$$F = Nv = \frac{3600 \, v^2}{l + tv + cv^2} \, ,$$

given *t* = 1 second, *c* = 0.1, *l* = 6.0 m, it can be seen that for different values of *l* the intermediate values of *F* are different; but as the speed increases the value of *F* approaches a certain limit

$$\lim_{v \rightarrow \infty} F = \frac{3600}{c} \text{ car km h}^{-2}.$$

This limit value of *F* may be called the ideal "traffic force" of the road. It is independent of the size of the vehicles or of their speed, and only depends on the braking coefficient of the road with respect to the vehicles; this value is a definite measure of the traffic quality of the road surface.

6) The expression "traffic force" is analogous to "force" in mechanics, owing to the similarity of dimensions: force—cgs⁻² (LMT⁻²); traffic force—km car h⁻²

The difference is that "mass" in the definition of "force" in mechanics is replaced by "number of vehicles" in that of "traffic force". If, instead of this number, we write down their total mass (comprising the mass of the vehicle and load) both expressions become identical.

The analogy can be extended to other expressions in mechanics; a system of units in traffic engineering would result, similar to that of mechanics.

Units in mechanics		Units in traffic engineering		
Term	Dimension	Term	Symbol	Dimension
Mass	<i>M</i>	Number of vehicles	<i>Q</i>	<i>Q</i>
—	—	Traffic capacity	<i>N</i>	<i>Q</i> ⁻¹
Momentum	<i>MLT</i> ⁻¹	Traffic momentum	<i>S</i>	<i>QLT</i> ⁻¹
Force	<i>MLT</i> ⁻²	Traffic force	<i>F</i>	<i>QLT</i> ⁻²
Power	<i>ML²T</i> ⁻³	Traffic power	<i>E</i>	<i>QL²T</i> ⁻³
Work (energy)	<i>ML²T</i> ⁻²	Traffic energy	<i>T</i>	<i>QL²T</i> ⁻²

The meaning of the above expressions in traffic engineering requires some explanation.

7) Q , the number of vehicles, takes the place of mass in mechanics. As, in fact, the load of the vehicles is what matters, the number of passengers or equivalent number of tons of load could be substituted in the expressions for the number of vehicles. For the sake of simplicity, it can be assumed that the number of tons of load is proportional to the length of the vehicle.

There is no unit analogous to "traffic capacity" in mechanics. Traffic capacity has been studied extensively and numerous observations made of its performance.

The product of the number of vehicles and their speed is the traffic momentum S , analogous to momentum in mechanics. Traffic momentum is proportional to speed. The dimensions of traffic momentum are QLT^{-1} .

Traffic momentum per unit time is the value F , called "traffic force" above. Its dimensions are QLT^{-2} . This value is dependent on the structure of the road and the type of traffic.

Diagram (3) shows the relationship between traffic force and speed, and Diagram (4) shows how the braking coefficient c affects the ultimate value of traffic force.

The product of traffic force and the length of the path (or the product speed \times time) is the "traffic work" or "traffic energy" T of the road. Its dimensions are QL^2T^{-2} . Traffic work may be calculated by multiplying the values of traffic force, the speed and the time the traffic force acts:

$$T = F \times v \times t$$

Traffic work per unit time is traffic power

$$E = \frac{T}{t}$$

Traffic power is the product of traffic force and speed. The dimensions of traffic power are QL^2T^{-3} .

8) The terms mentioned above constitute a system of units similar to that used in mechanics. But similarity would not in itself justify setting up a system of units. There should be practical reasons and also a possibility of their utilisation in the study and improvement of traffic.

It was shown in the preceding paragraphs that the "ideal traffic force" can be used as a means of comparison between different roads. This value may also be used for comparing different states of the same road; the braking coefficient of the road may change under the influence of the weather (dry or wet, fog, dust, snow, ice or mud). The state of the road surface also affects the braking conditions of the road and, as a consequence, the traffic force. The actual traffic force may be compared to the ideal traffic force. It is possible to calculate the actual traffic work of the road in the course of 24 hours and to determine to what extent the road is economically used at different times of the day, or throughout the 24 hours.

9) When analysing the changes of the above-mentioned values in relation to basic values in traffic engineering (speed, vehicle length, coefficient of braking), conclusions may be drawn with respect to traffic performance and to the trend of traffic development.

Take, for instance, the expression of traffic capacity (Diagram 1)

$$N = \frac{3600v}{l + tv + cv^2}$$

The maximum and minimum values of this expression can be found by the usual method of equating the first derivative of N with respect to v to zero.

$$N = \frac{3600v}{l + tv + cv^2} = \frac{3600}{\frac{l}{v} + t + cv} ; \quad N' = \frac{3600l - 3600cv^2}{(l + tv + cv^2)^2} = 0$$

$$\text{a) } 3600l - 3600cv^2 = 0 ; \quad v = \sqrt{\frac{l}{c}}$$

Assuming the range of values $c = 0.05 \div 0.5$, $l = 20 \div 5$, and $t = 1$ sec (reaction time of driver) the optimum speeds are within the range

$$v = \sqrt{\frac{20}{0.05}} \div \sqrt{\frac{2}{0.5}} = 20 \div 3.17 \text{ m sec}^{-1} (= 72 \div 11.4 \text{ kmh}^{-1})$$

$$\text{Optimum } v_1 = \sqrt{\frac{5}{0.05}} = 10 \text{ msec}^{-1}; \text{ optimum } v_2 = \sqrt{\frac{20}{0.5}} = 6.3 \text{ msec}^{-1}$$

and

$$\text{Max } N_1 = \frac{3600 \times 10}{5 + 10 + 0.05 \times 10^2} = 1800 \text{ car h}^{-1}$$

$$\text{Max } N_2 = \frac{3600 \times 6.3}{20 + 63 + 0.5 \times 6.3^2} = 263 \text{ car h}^{-1}$$

$$\text{b) } l + tv + cv^2 = \infty ; \quad v = \infty, \quad N = 0.$$

As the speed increases beyond the optimum value, the traffic capacity decreases; it approaches zero as speed approaches infinity.

From the calculations of the optimum range of speed and of the corresponding maximum traffic capacity it is obvious that the maximum traffic capacity lies within a narrow range of speed and it is useless to increase the speed in order to increase the traffic capacity. The optimum speed depends on the length of the vehicle and the braking coefficient

$$\text{Max } N = \frac{3600}{2\sqrt{lc} + t}$$

But as the speed increases, the differences between traffic capacities for different lengths and different values of c became smaller and as it approaches infinity, the traffic capacity in all cases approaches zero.

The optimum value of speed lies between 11–72 kmh⁻¹. But in fact the range is narrower, as there is a certain relationship between the type of the vehicle and its

braking coefficient. Thus it can be assumed that the practical speed range is 10—50 km per hour.

10) The traffic force of the road is (Diagram 3)

$$F = \frac{3600 v^2}{l + tv + cv^2}$$

The maximum value of F can be found as above for N

$$F' = \frac{3600 tv^2 + 1200lv}{(l + tv + cv^2)^2} = 0$$

$$a) 3600 tv^2 + 7200 lv = 0; \quad v = 0, \quad F_0 = 0$$

$$b) (l + tv + cv^2)^2 = \infty; \quad v = \infty$$

$$\text{Max } F = \frac{3600 v^2}{l + tv + cv^2} = \frac{3600}{c}$$

As the speed approaches infinity the traffic force approaches the value

$$\text{Max } F = \frac{3600}{c}$$

The intermediate values of F are different for different vehicle lengths, but the ultimate value is the same, as long as the value of c , the braking coefficient, remains unchanged (Diagram 4). It is obvious that the value of the braking coefficient is very important for the exploitation of a road, and the economical construction of the road affects its exploitation to a large extent. It is desirable to construct roads in such a way that the braking coefficient would not be considerably affected by change of weather and the traffic force would not be reduced.

From Diagram 3 it can be seen that the traffic force reaches 70—90% of its ultimate value at moderate speeds. This means that it is not worthwhile to increase the speed too much in order to reach the ultimate (limit) value of traffic force. It was shown earlier that when the speed increases above the optimum, the traffic capacity decreases. This means that only few vehicles would benefit from the increase of speed.

The construction of roads specially designed for high speeds (autostradas) is very expensive compared with ordinary roads. It is essential to ascertain in each case whether such high expenses, for the benefit of only a small number of vehicles, would be justified. It was pointed out above that the length of the vehicle has little influence on the intermediate values of traffic force and none on its ultimate value. This is true as long as we are dealing with the number of vehicles only. But if we consider the number of passengers or tons of goods transported, the vehicle length assumes great importance.

In paragraph 6, the dimensions of traffic force were given

$$F = QLT^{-2}$$

If Q is assumed to denote not the number of vehicles but that of passengers (for passenger cars) or tons (for lorries), we may write that, approximately,

$Q = al$, where a is the number of passengers (or tons) per metre run of vehicle, and the expression for traffic force will become $F = (al)LT^{-2}$. The result is that the traffic force will be proportional to the vehicle length, which proves the advantage of using longer vehicles or trailers in attempting to improve the exploitation of the road.

11) The expression "traffic work" is derived directly from that of traffic force through multiplication by length (or speed and duration of drive)

$$T = QL^2T^{-2}$$

Traffic work increases with speed and time, and also with the vehicle length if the number of passengers or tons is dealt with. If the road is used for intermittent traffic, or if the number of vehicles varies with time, the traffic work can be calculated for different periods of the day and the results added up. The total actual traffic work may be compared to the traffic work that could be performed on the road under conditions of maximum traffic capacity at the optimum speed, or at a given speed, in the course of 24 hours of the day.

12) A better measure of the exploitation of the road during different periods of the day is the "traffic power" which is the rate of traffic work per unit time. The traffic power can be obtained by multiplication of the traffic force by speed. Its dimensions are

$$E = QL^2T^{-3}$$

The "possible traffic power" is the product of the traffic force and the corresponding speed. Actually, the number of vehicles on the road may be less than the speed allows, and the actual traffic power will be less than the possible traffic power; from this the degree of exploitation of the road under given conditions can be found. When dealing with the number of passengers or tons, power can also be taken as proportional to vehicle length.

13) In the preceding paragraphs mention was made of the braking coefficient, which depends on the character of the road (type of surface, etc.), on the type of vehicle (design, tyres, weight, brakes) and on the qualities of the driver (driving efficiency, reaction time, etc.), i.e. the three factors which determine the performance of traffic on the road, as well as on the formula used, i.e. the method of calculation.

It is known that the braking coefficient is affected by the climate and the weather, and the values used should be determined and tested under local conditions.

The range of values of the braking coefficient, in relation to the coefficient of friction, can be calculated from the following considerations. Suppose the total weight of the vehicle is P , of which one-third is borne by the front axle and two-thirds by the rear axle, the road coefficient of sliding friction is f and that of rolling friction f_1 , the coefficient of braking c and the braking distance L .

Then in the case of perfect braking the energy of motion would be equal to work of friction.

$$\frac{Mv^2}{2} = \left(\frac{2}{3} Pf + \frac{1}{3} Pf_1 \right) L$$

$$\text{Suppose } f_1 = 0.2f \text{ and } M \simeq \frac{P}{10}; \text{ then } \frac{Pv^2}{20} = P \left(\frac{2}{3}f + \frac{0.2}{3}f \right) L$$

$$L = \frac{v^2 \times 3}{20 \times 2.2f} = cv^2$$

$$\text{and } c = \frac{3}{44f} \simeq \frac{1}{15f} \quad (\text{see Diagram 7})$$

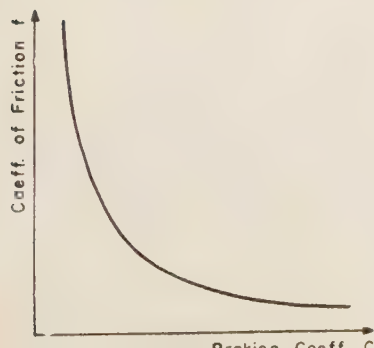
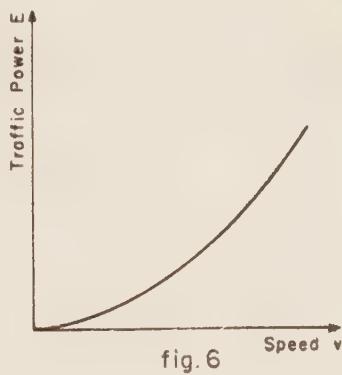
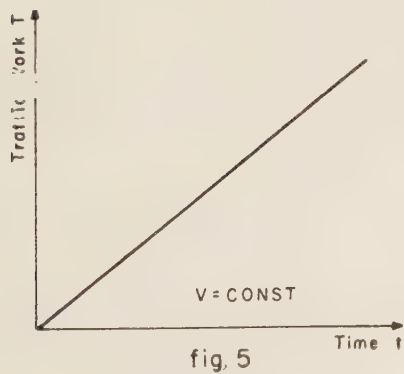
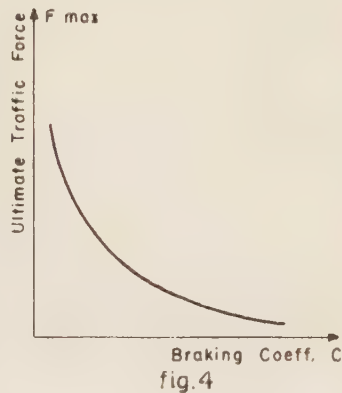
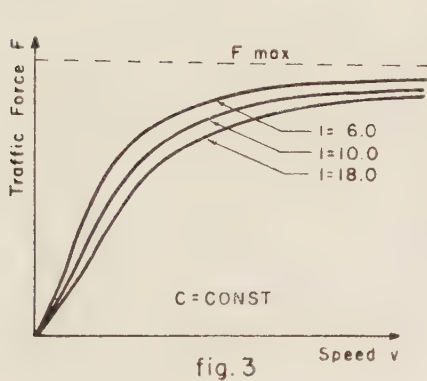
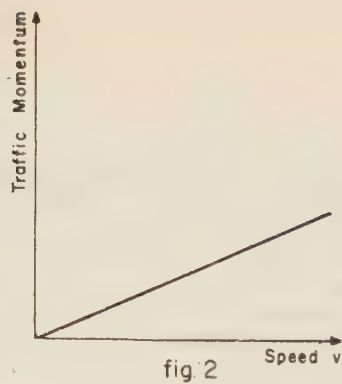
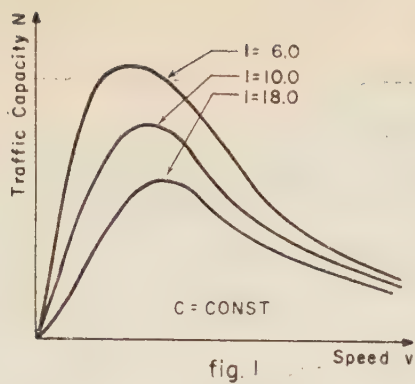
This calculation of the lower limit of c is a very rough one, being based on certain inaccurate assumptions, one of which is that the brakes of the vehicle are applied instantaneously. Generally, this is not the case; the "braking time" in the expression of traffic capacity depends on the design of the brakes and the determination of the braking coefficient must be made experimentally, not by means of theoretical calculations. Nor was it taken into consideration that the value of braking coefficient depends on the formula used for calculation of traffic capacity. (In addition, the kinetic energy of the revolving parts of the motor does not appear in the above calculation of c . This energy is estimated by some writers to amount to 15% of the translatory energy of the vehicle, and certainly depends on the design of the vehicle, speed, load, etc.)

The ratio $c = 1/15f$ is therefore only an approximation which gives an idea of the magnitude of c .

The value of c should be determined by means of tests and observations of different vehicles under different road and weather conditions. This deserves special attention and care as the value of c may involve important conclusions for traffic engineering problems.

14) Some of the units of traffic engineering mentioned above are already in use. The introduction of other units will permit a more convenient analysis of traffic problems and a more effective and useful comparison of the influence of different factors, such as the type and state of the road, type of the vehicle, qualities of the driver, the weather, the values of traffic quantities etc. The other units have been included for the sake of completeness and use could possibly be made of them in the course of future developments in traffic engineering.

The values mentioned above depend on local conditions and should not be automatically applied from one country to another, as not only climatic conditions are different, but also the design of vehicles, roads, and intersections, the number of traffic lanes, and the habits and behaviour of drivers and pedestrians. Research on these problems, including exchange of information, should be carried out with local conditions taken into consideration.



REFERENCES

1. AGG, T. R., 1940, *The Construction of Roads and Pavements*, McGraw—Hill.
2. TRIPP, H. ALKER, 1950, *Road Traffic and its Control*, E. Arnold, London.
3. NIEKRASSOFF, V. K., 1935, *Town Road Coustructions*, Gosizdat (Russian).
4. 1937, *Proceedings A.S.C.E.*, II.
5. PELEG (POLONSKY), M., 1946, Road Capacity at Intersections, *Engineering Forum*, I (Hebrew).
6. PELEG (POLONSKY), M., 1938. The Traffic at Intersections, *J. Assoc. Engnrs & Arch.*, (7); *ibid*, 1950, (3) (Hebrew).
7. PELEG (POLONSKY), M., 1948, Traffic Force, *At the Plant*, (10—12) (Hebrew).

COMPOSITION OF BITTER ORANGES GROWN IN ISRAEL II.¹

A. EPHRAIM AND J. J. MONSELISE
Laboratories of Assis Ltd., Ramat Gan

ABSTRACT

Examination of bitter oranges grown in Israel in the 1956 season yielded the following results:

- 1) Pectin content of juice: 0.020%—0.025%.
- 2) Pectin content of peel: 3.72%—4.25%.
- 3) Ash content of juice: 0.26%—0.31%.
- 3) Ash content of peel: 0.58%—0.75%.
- 5) Alkalinity of ash (juice): 9.60—10.20.
- 6) Alkali number of ash (juice): 2.65—3.14.
- 7) Alkalinity of ash (peel): 15.9—17.7.
- 8) Alkali number of ash (peel): 9.22—12.37.
- 9) Ascorbic acid in juice: 34.2—39.0 mg/100 g.
- 10) Ascorbic acid in flavedo: 190—211 mg/100 g.
- 11) Ascorbic acid in albedo: 85.0—103 mg/100 g.

No substantial differences were observed between bitter oranges of 1955 and 1956 crops.

(I) A drop of the aldehyde content of the oil was noticed and a rise of the total sugars/Invert sugar ratio. The acidity and the ascorbic acid content of the juice were somewhat lower in 1956 than in 1955.

About 70% of the pectin contained in the peels was extracted and its jelly grade strength was found to be 234° by the sag method².

Work carried out on bitter oranges in our laboratory in 1955¹ was resumed during the 1956 season. Further determinations were carried out of some components, and several other components were analysed.

ANALYTICAL METHODS

In addition to the analytical methods referred to in the last paper¹, the following methods have been used:

Ash content of the juice was determined by concentrating the juice on a water bath till dryness and igniting the residue till a white ash was obtained.

Pectin was determined according to Carre and Haynes³.

Alkalinity and alkali number of ash was carried out according to Samisch and Cohen².

RESULTS

The results are reported in the following tables.

It is to be noted from Table I that lower figures were obtained for the aldehyde content in oil in the 1956 crop than in the 1955 crop (0.82 against 1.04). The acidity and the ascorbic acid of the juice too yielded lower figures this year than last year.

Received May 30, 1956.

TABLE II

Juice	Pectin %	Peel
0.025		4.01
0.020		3.72
0.020		3.84
0.023		3.95

TABLE III

Ash %		Alkali number		Alkalinity of ash	
Juice	Peel	Juice	Peel	Juice	Peel
0.31	0.62	3.14	10.97	10.13	17.7
0.28	0.75	2.75	13.37	9.85	16.5
0.34	0.63	3.26	10.14	9.60	16.9
0.26	0.58	2.65	9.22	10.20	15.9

TABLE IV

T.S.S.	Total sugars	Invert sugar	Total sugars Invert sugars	T.S.S.— Total sugars
10.8	7.30	4.25	1.71	3.5
11.0	7.23	4.00	1.80	3.8
11.0	7.20	3.95	1.82	3.8
10.6	7.15	4.00	1.78	3.5

TABLE V

Ascorbic acid mg/100 g		
Juice	Albedo	Flavedo
37.2	85.0	211.0
39.0	103.0	190.0
34.2	95.0	201.0

The total sugars/invert sugar ratio, on the other hand, was lower in 1955 than in 1956. Extraction of pectin was further carried out by treatment of minced peels at pH 1.7 during 30 minutes, at 95°–100°C. This way about 70% of the total pectin

was extracted. The jelly test, carried out according to the sag method² yielded 234° jelly grade strength.

REFERENCES

1. EPHRAIM, A. AND MONSELISE, J. J., 1955, *Bull. Res. Council. of Israel*, **5C**, 60.
2. COX, R. E. AND HIGBY, R. H., 1944, *Food Ind.*, **16**, 441.
3. CARRE, M. H. AND HAYNES, D., 1922, *Biochem. J.*, **16**, 60.
4. SAMISCH, ZDENKA AND COHEN, A., 1949, *Bull. No. 51, Agr. Res. Station, Rehovot*.

RHEOLOGICAL PROPERTIES OF CONCENTRATED ORANGE JUICE

A. EPHRAIM AND J. J. MONSELISE
Laboratories of Assis Ltd., Ramat Gan

ABSTRACT

The rheological properties of concentrated orange juice were investigated. The 65°Bx concentrated orange juice is a non-Newtonian thixotropic fluid. It shows a certain degree of regeneration of original viscosity if left undisturbed after stirring. A synthetic concentrate was prepared and its rheological properties studied after addition of each component. The pectin content of the concentrates is the most important factor influencing viscosity.

Concentrated orange juice* 65°Bx may vary in its viscosity from a free-flowing liquid to a highly viscous almost solid gel. High viscosity is undesirable because it hinders the handling of the finished product and impairs its quality. In order to acquire a systematic knowledge of the mechanical behaviour of the concentrate and to investigate the factors influencing it, a study of its rheological properties was undertaken.

EXPERIMENTAL

All measurements were carried out with a Brookfield synchroelectric viscometer (Multi Speed mod. R.V.F.). The instrument was checked and found accurate to within $\pm 1\%$ of its full scale.

Dependence of apparent viscosity on shear

Viscosities of 65°Bx oranges concentrate were tested at 20°C at different constant r.p.m. and were compared with the viscosities of sucrose solutions of the same Bx° tested in the same way (Figures 1 and 2). The sucrose solutions show, of course, the behaviour of a Newtonian fluid, while the orange concentrate shows distinctly non-Newtonian behaviour. There is a decrease in the viscosity with increase of rate of shear. This is the behaviour of many pseudoplastic materials containing large deformable molecules or clusters of chain molecules¹. The authors tried to apply to

* Average composition: 65°Bx., spec. grav. (20°C) 1.325, acidity % (as anhydrous citric acid) 5.50, ascorbic acid (mg per 100 g) 210, ash % 2.16.

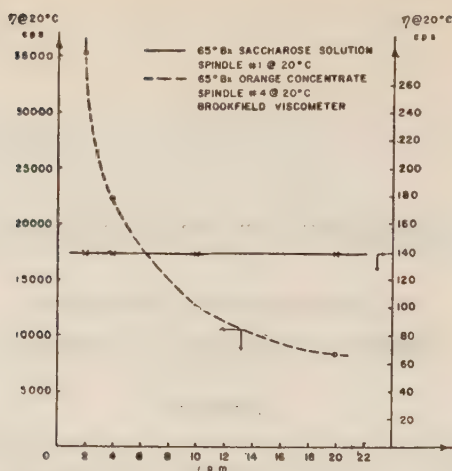


Figure 1

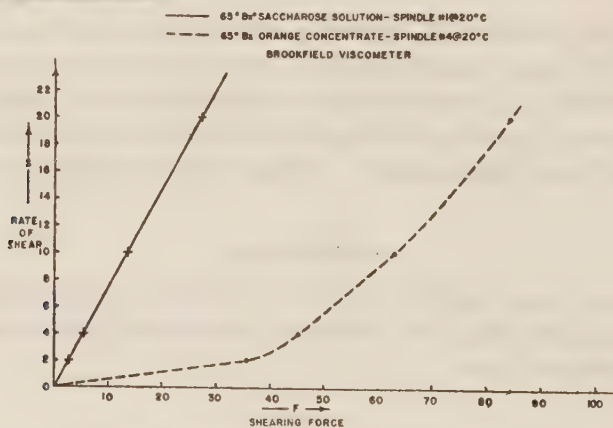


Figure 2

the results of viscosity determination of the investigated orange concentrate the formula:

$$D = \frac{T^n}{\eta}$$

where D = rate of shear

T = stress

η = viscosity

n = the capacity of the particles to be deformed and/or oriented².

In the case of our concentrate the above formula cannot be applied, because n is not constant but decreases and approaches 1 with increasing rate of shear. This may be explained by the orientation and deformation of clusters of chain molecules with increase of rate of shear. The clusters of chain molecules originate from the pectinic acids, which form a rigid structure pectin-sugar-acid-water gel, predominantly through hydrogen bonding³.

Dependence of apparent viscosity on deformation

The viscosity of the concentrate constantly stirred and kept at constant temperature drops gradually (Figure 3) according to the characteristic behaviour of a thixotropic substance.

The concentrate was left undisturbed for 48 hours and then a second time—viscosity curve was plotted. A curve was obtained resembling the first one and showing a certain degree of regeneration, i.e. a certain time after the applied deformation was removed and the same operating conditions maintained, the concentrate partially regained the original viscosity. These observations are confirmed by a third curve (Figure 3).

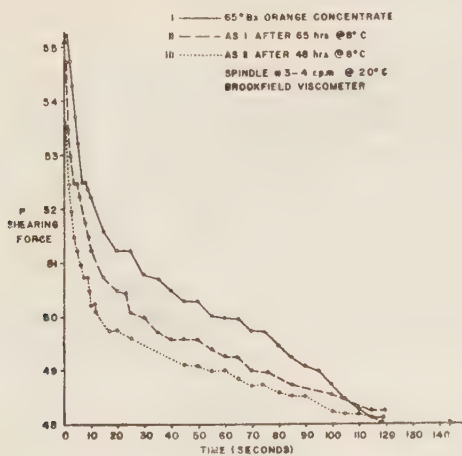


Figure 3

Dependence of apparent viscosity on temperature

Temperature—viscosity relation of the concentrate was investigated (Figure 4). The effect of temperature on viscosity is much stronger in the range of 15°–40°C and smaller at higher temperatures.

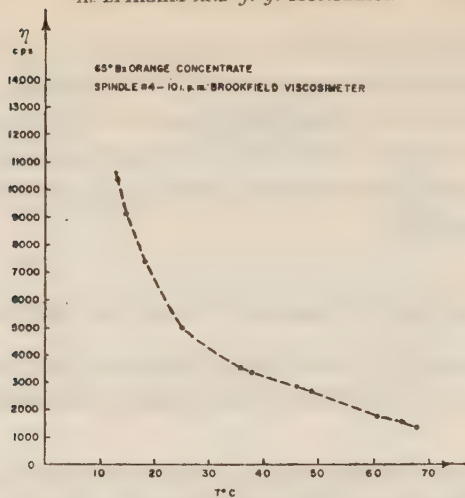


Figure 4

Dependence of apparent viscosity on concentration of orange juice

The effects of concentration on viscosity were studied. In sucrose solutions a simple linear relation exists between the log of the viscosity and the concentration of soluble solids, while the orange concentrate curve shows a clear deviation from the linear behaviour of the sucrose solution (Figure 5).

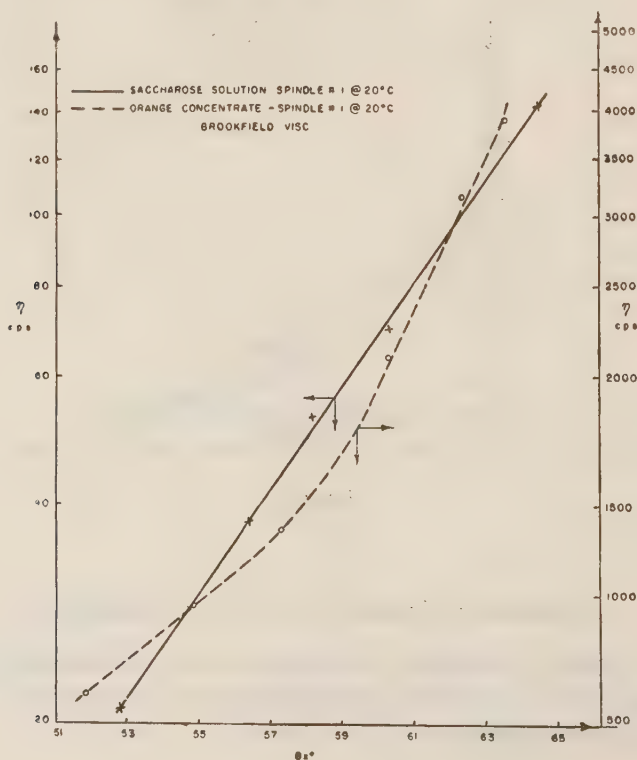


Figure 5

Dependence of apparent viscosity on chemical components

The influence of the different chemical components of the orange concentrate on viscosity was studied. Synthetic 65°Bx concentrate was prepared from sucrose solutions to which the other chief components of the concentrate were added one after the other in amounts corresponding to those found in the real concentrate^{4,5}. The viscosity was checked after the addition of each component (see Table I). The

TABLE I

	Saccharose solution 64.4°Bx	6.26% citric acid pH 1.55	0.9% Na ₂ CO ₃ pH 2.25	0.18% pectin
Spindle No. r.p.m.	1	1	1	3
2	140.0	175.0	170.0	4800.0
4	140.0	171.2	167.5	4125.0
10	139.0	172.5	170.0	3750.0
20	141.5	175.0	172.0	3500.0

sucrose solution, at different rates of shear, showed the same viscosity, i.e. it behaved as a Newtonian fluid. Then citric acid was added and the solution was left undisturbed for 24 hours. Because of the inversion of the sucrose, the viscosity was found to increase but the solution remained Newtonian. Further, Na₂CO₃ was added⁴ in the same proportion as the alkalinity found in the ash of the concentrate. A slight increase in viscosity was noticed, but the solution remained Newtonian. Pectin ("Genu" apple pectin 200° rapid set) was then added⁵. After 24 hours a haze was observed indicating the incipient formation of a gel structure. A considerable rise in viscosity appeared, and the solution clearly showed non-Newtonian behaviour (see Table I).

CONCLUSIONS

65°Bx orange concentrate is a non-Newtonian thixotropic fluid. It shows a certain degree of regeneration of initial viscosity when left undisturbed after stirring. The effect of temperature on viscosity is much more pronounced in the range 15°–40°C than at higher temperatures. Different batches of 65°Bx orange concentrate show different viscosities, but are always non-Newtonian in character. The differences in viscosity are due to factors which affect the pectin-sugar-acid-water gel structure. The most important factors are the pectin content⁶, the quality of the fruit processed, and mainly the method of juice extraction and its subsequent handling (screening, enzymes inactivation, concentration and storage temperatures).

REFERENCES

1. HOEKSTRA, AND FRITZIUS, C. P., *Rheology of Adhesives*, Cap. 3, Pag. 35. Edited by N. A. Bruyne and R. Houwink, Philips Res. Lab. Eindhoven, Netherlands.
2. HOUWINK, R., 1937, *Elasticity, Plasticity and Structure of Matter*, London, p. 11.
3. KERTESZ, Z. I., *The Pectic Substances*, 1951, p. 193.
4. SAMISCH, ZDENKA AND COHEN, Z., 1949, *Composition of Oranges in Israel*, Agric. Res. Station Fruit Prod. Lab., Rehovot. p. 27.
5. HINTON, C. L., *Fruit Pectins*, 1940, Food Investigation Special Rep. No. 48 of Dept. of Sc. and Ind. Res. London.
6. INGRAM, M., 1948, *The Viscosity of Concentrated Orange Juice*, Board of Sc. and Ind. Res. Jerusalem, p. 22.

PROTEOLYTIC AND STARCH LIQUEFYING PROPERTIES OF MOULD CULTURES

Y. POMERANZ

Ministry of Trade and Industry, Food Testing Laboratory, Haifa

ABSTRACT

The proteolytic and starch liquefying properties of enzymes elaborated by fungi, as related to bread quality, were studied. *Aspergillus ochraceus* and *A. flavus* were characterized both by pronounced starch liquefying and by proteolytic properties. *Penicillium chrysogenum* was found to show a high alpha amylase activity. *Aspergillus niger* and *Alternaria tenuis* showed a low ratio of proteinase to alpha amylase. *A. caudatus* and *A. amstelodami* showed properties similar to *A. ochraceus* and *A. flavus*.

INTRODUCTION

In an investigation of effects of moulds predominating on wheat, changes produced in flour properties and bread quality were described (Pomeranz, Halton and Peers 1956)¹. *Aspergillus candidus* and *A. amstelodami* were found to have deleterious effects, but not such pronounced ones as those of *A. flavus* and *A. ochraceus*. *Alt. tenuis* and *A. niger* showed improving action. The effect of *P. chrysogenum* was negligible. The present study was undertaken to secure additional information on the influence of enzymes elaborated by the various fungi on bread quality.

MATERIAL AND METHODS

The flour used in this investigation was a commercially milled bakers' straight untreated composite of Hard Red Winter and Soft Red Winter Wheat. The flour had a water absorption of 63% and dough development time of 3.5 minutes. Both latter factors were determined on the Farinograph*. The flour and the wheat starch

* The Farinograph is used to determine optimum absorption i.e. the quantity of water required by a flour to yield a dough of predetermined consistency.

The dough is prepared in a jacketed mixing bowl and the power required for the kneading is transferred to a balance system. The latter is connected to a device which records the power consumed on a chart paper in form of a Farinogram curve. Any changes in power consumption during mixing of the dough cause the curve to mount or to drop.

Dough development time is the interval (in minutes) from the addition of water to the point of maximum consistency in the curve.

The drop consistency—measured in Brabender Units—is the difference between 500 B.U. and consistency (in B.U.) recorded on mixing after the dough has rested for a fixed time.

used showed the following analytical characteristics (expressed on a 14% moisture basis):

	Ash (%)	Protein (%)
Flour	0.65	11.3
Wheat starch	0.28	0.4

The fungal cultures used in this study were originally carried on the following media:

<i>A. niger</i>	potato-dextrose-agar
<i>A. flavus</i>	potato-dextrose-agar
<i>A. ochraceus</i>	potato-dextrose-agar
<i>A. candidus</i>	maize
<i>A. amstelodami</i>	malt extract containing 20% sucrose
<i>P. chrysogenum</i>	potato-dextrose-agar
<i>Alt. tenuis</i>	potato-dextrose-agar

The various fungi were inoculated into a bran mash prepared by autoclaving 50 g aliquots of commercial bran with 200 ml distilled water, contained in 500 ml Erlenmeyer flasks, for 30 min. at 20 lbs pressure. These cultures were incubated for 4 weeks at 30°C. Extracts of the bran cultures were prepared by the method of Dirks and Miller (1948) i.e. 5 g (based on dry matter weight) were extracted with 100 ml of 0.2% calcium chloride solution at 35°C for 1 hr with stirring. The cultures were filtered through Whatman No. 2 filter paper following extraction. This method of extraction was established so that the proteinase and alpha amylase activity would not be appreciably influenced. (Kneen, Sandstedt and Hollenbeck 1943)².

The filtrates from the fungal extractions were added at a level of 5 ml/50 g of flour for the Farinograph determinations and as a part of the aqueous phase (25 ml out of the total volume of 450 ml) in the preparation of suspensions for the Amylograph* determinations.

Changes in dough mobility were followed with a Farinograph at a predetermined consistency (500 B.U.) at the mixing stage, employing the small bowl. The rest period curves were obtained on two minutes' mixing during the mixing stage after the curve was centered around the 500 unit line, and after one and two hours' rest period. The starch liquefying properties of alpha amylase were determined with the

* The Amylograph measures and records paste viscosity of flour suspensions either at a selected fixed temperature or under uniformly rising temperature conditions. The increase in viscosity, which takes place during gelatinization of the starch, is opposed by the liquefying properties of amylase present. The height of the curve at maximum viscosity is an index of amylase activity.

Amylograph by the technique described by Anker and Geddes (1944)³. In order to enable a preliminary swelling of the starch granules, the suspensions were heated in a normal way in the Amylograph bowl and held at a constant temperature of 50°C for 30 minutes. This digestion was found necessary in view of the heat lability of fungal amylases which have been found to be markedly inhibited by continuous heating.

RESULTS

The influence of fungal extracts on dough consistency changes are given in Table I.

TABLE I
Effect of bran cultures' extracts on dough consistency

	Consistency drop (Brabender Units)	
	After 1 hr rest	After 2 hrs rest
Control	10	20
Sterilized bran extract	10	20
<i>A. niger</i>	20	80
<i>A. flavus</i>	80	170
<i>A. ochraceus</i>	100	180
<i>A. candidus</i>	70	160
<i>A. amstelodami</i>	70	160
<i>P. chrysogenum</i>	80	170
<i>Alt. tenuis</i>	40	110

The effects produced by the moulds used in this study are summarized in Table II.

TABLE II
Summary of effects produced by mould culture extracts

	Bread volume (as compared with control)	Crumb texture*	Consistency drop (B.U.)	Starch liquefying power
Control	100	7	—	—
<i>A. niger</i>	115	9-soft	+	++
<i>A. flavus</i>	85	2-coarse	+++	+++
<i>A. ochraceus</i>	90	2-coarse	+++	+++
<i>A. candidus</i>	105	4-open	++	+
<i>A. amstelodami</i>	105	5-open	++	++
<i>P. chrysogenum</i>	100	6-open	+++	+++
<i>Alt. tenuis</i>	110	8-soft	+	++

* Texture score 1—10.

The influence of the various extract additions on the course and maximum gelatinization temperature of flour suspensions (registered in form of a viscosity time curve at the described temperature increase) is given in Figure 1.

In order to study the effect of fungal amylases on diastatic starch degradation and eliminate possible effect of components other than starch on the gelatinization curve character, a series of experiments was undertaken in which pure wheat starch (in form of a 10% suspension) was used as substrate. These data are graphically represented in Figure 2.

DISCUSSION OF RESULTS

When comparing the data summarized in Table II, it must be stressed that the information obtained from Farinograms must be used within certain limitations. Dough properties e.g. plasticity, mobility and consistency, change during prolonged mixing, fermentation etc. Consistency determined on the Farinograph—even after rest period—is not the desirable consistency at the end of fermentation. This is best exemplified by the fact that while the water—flour dough containing addition of extracts from *P. chrysogenum* preparation showed an appreciable consistency drop, only minor changes in dough mobility—as compared with the control flour—were found in fermented doughs. Whereas results of baking tests represent a summation of several factors operating during the whole process of bread making, the methods employed for determination of changes in dough consistency and starch liquefying power measure only some specific properties.

Notwithstanding these limitations, the data given in Table II enable to correlate findings based on bread baking experiments with results of consistency drop and starch liquefying power determinations.

The detrimental effect of fungal preparations of *A. ochraceus* and *A. flavus* on dough handling properties and bread characteristics was accompanied by a pronounced proteolytic and alpha amylase activity of these fungi. Additions of *A. amstelodami* and *A. candidus* culture extracts showed a mild deleterious effect on bread baking quality and excessive ratio of consistency drop to alpha amylase.

P. chrysogenum was found to have a high amylolytic activity but addition of extracts of this mould caused little deterioration in baking quality. The negligible effect of *P. chrysogenum* on bread quality in spite of a pronounced consistency drop needs additional clarification.

The improving effect of preparations from *A. niger* and *Alt. tenuis* on bread characteristics can be explained by the desirable balance of proteinase and alpha amylase elaborated during the growth of the fungus on the medium employed.

REFERENCES

1. POMERANZ, Y., HALTON, P. AND PEERS, F. G., 1956, *Cereal Chem.*, **33**, 157.
2. KNEEN, E., SANDSTEDT, R. M. AND HOLLENBECK, C. M., 1943, *Cereal Chem.*, **20**, 399.
3. ANKER, C. A. AND GEDDES, W. F., 1944, *Cereal Chem.*, **21**, 335.
4. DIRKS, B. M. AND MILLER, B. S., 1948, *Cereal Chem.*, **26**, 98.

MILLING AND BAKING CHARACTERISTICS OF BUG INFESTED WHEAT

Y. POMERANZ AND L. ADLER

Ministry of Trade and Industry, Food Testing Laboratory, Haifa

ABSTRACT

Experiments reported in this paper were undertaken to determine the milling and baking characteristics of bug infested wheat. A method for detection and estimation of the percentage of flour milled from bug-infested wheat in a composite flour is given. Procedures necessary to eliminate the deleterious effect of flour milled from bug infested wheat in Israeli type bread are described.

INTRODUCTION

The term bug infested wheat covers grains attacked by several types of insects belonging mainly to the two genera: *Aelia* and *Eurygaster*. It is generally accepted that during their feeding act the insects puncture the kernels causing harm due to the introduction of a potent proteolytic enzyme which causes damage due to changes in the composition of the gluten. If the attack occurs during the ripening stage the grains shrivel up, whereas in case mature wheat is attacked, no shrivelling occurs. Damaged grain can sometimes be recognized by characteristic shrivelling and mainly by a yellowish patch surrounding the small black puncture made by the attacking bug. Generally only 0.5 to 5.0% of the kernels are injured, but percentages as high as 87% have been reported¹.

Wheat-bug has a most harmful effect on the baking quality of flour. Though it is considered that as little as 2—3% of damaged wheat causes considerable injury, Kent-Jones and Amos² found that except in long fermentation systems even 2% were hard to detect. The extent of damage depends upon the baking strength of the undamaged flour to which flour milled from bug infested wheat has been admixed—the harmful effect is much greater in weak than in strong flours.

Kretovitch³ studied the biochemistry of the damage to grain by the wheat-bug. Bug infested wheat shows changes in protein content and composition, possesses higher titratable acidity, higher amylase and proteolytic activity. Proteinases of the damaged wheat are most active in neutral or faintly alkaline solution, their activity is greatly reduced by moderate acidification.

Methods for detection of damaged grains include visual inspection, changes in cohesion of gluten, characteristic disintegration of the doughball in the Pelschenke test and determination of tyrosine.

Bug attacked wheat is said to be improved by heat treatment. As the deleterious effect was confined to the outer zone of the grain, Jones and Simpson⁴ suggested

Received April 3, 1956.

to inactivate bug damage by plunging the grain into nearly boiling water or subjecting it to live steam for a short period — so as to cause no damage to the bulk endosperm.

MATERIALS AND METHODS

(Throughout this report bug infested wheat will be referred to as damaged wheat and flour milled from such wheat as damaged flour).

Four lots of imported soft wheat (from Turkey) were tested; two of them were damaged and contained (on visual inspection) three percent punctured kernels. The lots were moistened, cold tempered—for 18 hours—and milled at 15.5% moisture on a laboratory experimental (Bühler) mill, so as to obtain white flour. Flour of 85% extraction was obtained from the damaged wheat in a commercial mill.

In part of the experiments white flour was admixed to the damaged high extraction flour. The sound flour was a commercially milled bakers' straight, untreated, milled from Hard Red Winter wheat.

The characteristics of the commercially milled flours are given in Table I.

TABLE I
Characteristics of commercially milled flour

	Damaged flour (85% extraction)	Sound flour (75% extraction)
Ash (%)	0.84*	0.71
Protein (%)	11.4	11.1
Water absorption (%)	62.5	63.5
Dough development time (min.)	1.0	4.0

* All figures expressed on 14% moisture basis

Moisture, ash, fat, crude fibre, protein and pH determinations were made according to A.A.C.C. methods. The test weight was determined on the Avery balance giving readings in pounds per bushel (Imperial). Porosity determinations in bread were made by the method of Liman and Zvilov⁵. Changes in dough mobility were followed with a Farinograph at a predetermined consistency (500 B.U.) at the mixing stage, employing the small bowl. Farinograms, water absorption capacity and dough development time were determined on ten minutes' mixing; rest period curves were obtained on two minutes' mixing — during the mixing stage and after one and two hours' rest period (64 r. p. m. drive).

The starch liquefying properties were determined with the Amylograph by the method of Anker and Geddes⁶.

Bread was both of hearth type and pan loaves. The straight dough method was employed in the baking tests and doughs were of such size as to yield commercial loaves of 900, 750 and 500 g. The formula for the basic control loaf included flour, water, 3% compressed yeast and 1–2% salt (the higher percentage in series of experiments containing addition of sour). The loaves were moulded by hand and

optimal absorption was determined by the feel of the dough. Bulk fermentation and proofing time were chosen so as to secure optimum conditions as judged by the operator.

Composition of wheat

Table II shows the composition of damaged kernels (selected visually) as compared with sounds ones.

TABLE II
Composition of wheat kernels

	Damaged wheat	Sound wheat
Thousand kernel weight (g)	23.2	29.3
Moisture (%)	11.0	11.2
Ash (%)	1.4	1.3
Crude fibre (%)	2.6	2.5
Proteine (%) (N \times 5.7)	12.6	11.4
Oil (%)	3.4	2.9
Carbohydrates (by difference) (%)	69.0	70.7

The test weight of the damaged wheat containing 3% punctured kernels was slightly lower than that of the sound wheat (61.85 and 62.00 lb/bushel resp.).

Milling characteristics

When milled on an experimental mill, the wheat containing 3% punctured kernels gave, under equal milling conditions (moisture of tempered wheat, rate of feed, setting of rolls), a lower total extraction and higher release of break flour.

TABLE III
Milling characteristics of tested wheat

		Total extraction (%)*	Break flour (%)*
Damaged wheat	No. 1	63.0	16.9
	No. 2	63.1	16.8
Sound wheat	No. 1	64.4	14.8
	No. 2	63.9	15.8

* Percentage of the whole wheat

Proteolytic activity

The flour from damaged wheat, when tested on the Farinograph, showed invariably inferior characteristics than flour milled from sound wheat. The water absorption capacity, at the mixing stage, of the experimentally milled damaged flour was 60.7% as compared with 61.0% in the sound flour. The Farinograms showed a pronounced

breakdown in the damaged flour. Rest period curves show a considerable consistency drop in the case of flour milled from damaged wheat.

TABLE IV
Consistency drop of dough (B.U.)

	After 1 hr	After 2 hrs
Damaged flour	170	210
Sound flour	90	130

Diastatic activity

Damaged flour was characterized by pronounced starch liquefying properties. Amylograms of experimentally milled flours—damaged and sound—showed considerable differences in gelatinization characteristics.

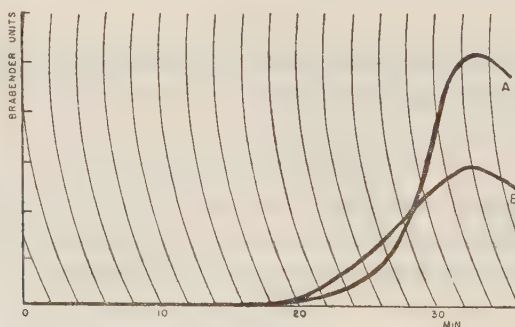


Figure 1
Gelatinization curves of flour experimentally milled:
A—sound flour B—damaged flour

These results show that the production of inferior bread (moist, sticky crumb) from damaged flour should be attributed not only to proteolytic activity but also to excessive enzymatic degradation of starch—thereby lowering its ability to bind water liberated by the proteins during baking.

The addition of various amounts of commercial damaged flour to sound wheat flour showed a gradual change in height of the curve at maximum viscosity and transition temperature of the Amylograms (Figure 2).

The essentially linear decrease of maximum paste viscosity could be used as a measure of the amount of damaged flour contained in flour milled from mixed grist—provided the thermal gelatinization curve characteristics of the individual flours were known.

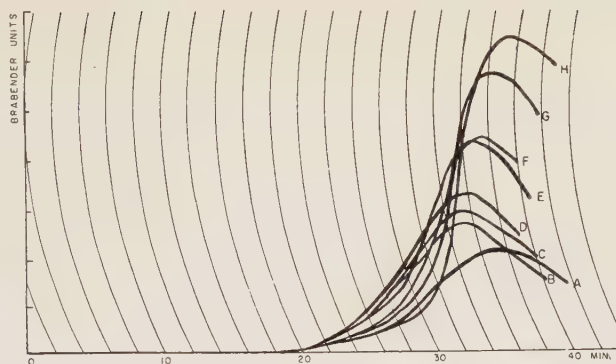


Figure 2

gelatinization curves of flour mixtures (sound and damaged) Percentage of damaged flour: A-100; B-75; C-66; D-50; E-33; F-25; G-10; H-0.

Baking Characteristics

Means to improve the undesirable baking characteristics of damaged flour (handling of dough, critical fermentation and proofing time—the basic loaf required practically no proofing—and inferior quality of bread) have been established by baking tests. These tests were made regarding the maximum percentage of damaged flour to be used, dough consistency, influence of oxidizing improvers and of sour fermentation.

The results of baking tests from blends containing different amounts of damaged flour and 30 g of potassium bromate per ton are shown in Table V.

TABLE V

Baking characteristics of flour blends

Damaged flour (%)*	Bread porosity (%)	Proofing time (minutes)
100	63	5
30	74	20
15	74	25
0	75	40

* The balance being sound Hard Red Winter Wheat flour.

Data in Table V show that an addition of damaged flour up to 30% had no influence on the porosity of the bread, whilst bread from 100% damaged flour showed a pronounced decrease in volume. Notwithstanding the fact that the quality of the baked loaf remained fairly constant (up to 30% damaged flour) at the given oxidation level, dough handling properties deteriorated gradually with increased percentage of damaged flour. Results given in Table V refer to flour milled two days

before baking; repetition of tests on flour aged naturally for 4 weeks resulted in marked improvement of the dough handling properties in all tests.

Variation of dough consistency showed stiffer doughs being advantageous with regard to dough handling as well as to bread quality. Consequently a decrease of about 2% in bread yield was found in tests made on flour containing an addition of 25–30% of damaged flour.

Addition of an oxidizing improver brought about a remarkable improvement. Tests were carried out with additions of 0, 20, 30, 40 and 60 g of potassium bromate per ton of flour. Whilst dough handling properties showed a response in accordance with the quantities of potassium bromate employed, the optimum bread was obtained by adding 40 g of potassium bromate per ton of flour—about twice the quantity usually employed (Figure 3).

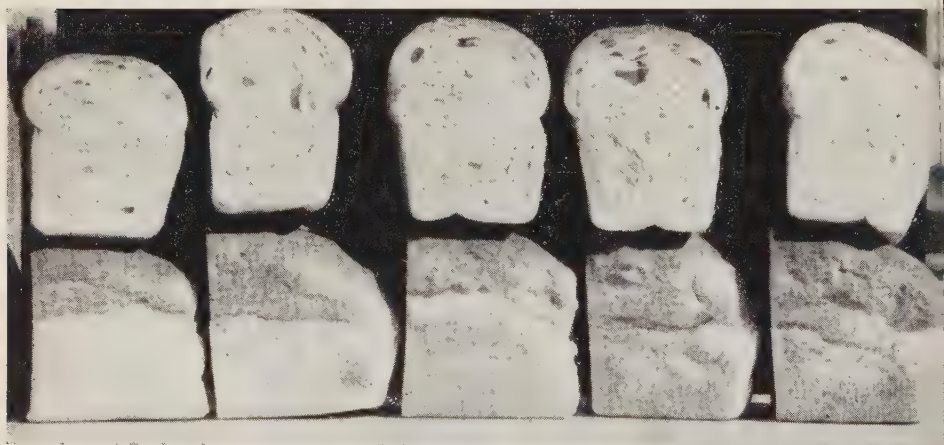


Figure 3

Influence of potassium bromate on bread baked from 100% damaged flour
Left to right: addition of 0, 20, 30, 40, 60 g per ton of flour

Overall improvement was obtained on addition of sour. Though newly prepared sour was used successfully for the first tests, systematic tests have been carried out with dry sour as a matter of convenience. This preparation ("Protosauer" of the Diamalt A.G.) had no leavening power of its own and was added to the basic formula containing 3% compressed yeast.

From two series of tests with additions of dry sour—varying from 0 to 6%—one without potassium bromate, the second containing potassium bromate at optimum level, application of 4% dry sour showed the best results in both cases, the series containing potassium bromate being superior to that without.

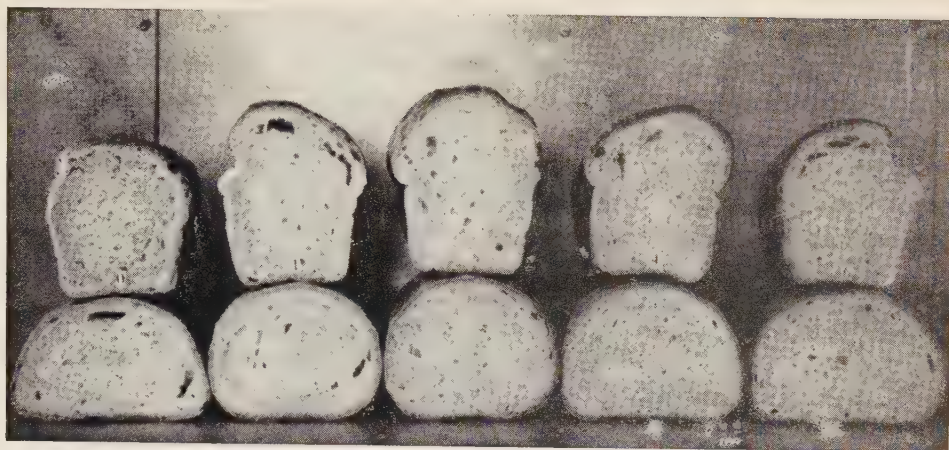


Figure 4

Influence of dry sour on bread baked from 100% damaged flour (containing 40 g potassium bromate per ton of flour)

Left to right: addition of 0, 1, 2, 4 and 6% dry sour

In Table VI the *pH* values of the baked loaves (without potassium bromate) are given.

TABLE VI
Influence of dry sour on pH

Dry sour added (%)	<i>pH</i> of bread
0	6.30
1	5.95
2	5.85
4	5.20
6	4.90

The results of baking tests enable us to draw the following conclusions which have been confirmed by experience gained in commercial bakeries during a period of several months:

1) Good brown bread may be obtained without difficulty from a flour blend containing up to 30 or even 40% damaged flour, provided a sour fermentation and optimum level of oxidizing improvers are employed. Under such conditions no deterioration of the bread quality will be observed by replacing the usual 30 to 40% of soft flour in our normal blend by the same quantity of damaged flour and even from 100% of damaged flour still bread of acceptable quality can be obtained.

2) A fair loaf of white bread may be baked from a blend containing up to 30% damaged flour with an addition of potassium bromate at the optimum level, provided

stiff doughs are prepared and the flour has been properly aged (3—4 weeks). Practically, however, the baker may meet difficulties in producing white bread of uniform quality owing to the poor dough handling properties which cannot be eliminated entirely without sour fermentation.

REFERENCES

1. NUORTEVA, P., 1953, *Luonnon Futkija*, **57**, 117.
2. KENT-JONES, D. W. AND AMOS, A. J., 1938, *Food*, **7**.
3. KRETOVITCH, L. L., 1944, *Cereal Chem.*, **21**, 1.
4. JONES, C. R. AND SIMPSON, A. G., 1938, British Patent No. 523,116.
5. LIMAN AND ZVILOV, in *Food Analysis* by N. Kozmin, W. Smirnov et al., 1949, *Gom, Torg and Izdetd Moscow* (in Russian).
6. ANKER, C. A. AND GEDDES, W. F., 1944, *Cereal Chem.*, **21**, 335.

LETTERS TO THE EDITOR

The Interaction Rubber—Sulphur—Brass

In a paper published recently¹, it was shown that the inclusion of brass powder in a compound, to which were added considerable amounts of sulphur, resulted in a severalfold increase of hardness and modulus and a decrease of tensile strength and of elongation as compared to equal loadings by volume of MPC black. It was postulated that this was due to a chemical reaction which bound the rubber to the brass through a sulphur bridge at fixed points on the brass particle.

At the time the paper was published, the writer was unaware of the existence of papers discussing the chemical nature of the bond between rubber and brass plating. Gurney² showed that the bond is sensitive to the type and proportion of accelerator in the rubber mix, in other words, to the rate of combination of the sulphur with the rubber. Buchan and Rae³ quote Satake's conclusion that copper is corroded by sulphur in a rubber mix to give a mixture of CuS and Cu_2S , in the ratio of 5 to 3, at an initial rate proportional to a power (presumably fractional) of the time of cure.

It is probable that if the rate of cure is so fast as to deplete the sulphur or to cause cross-linking at all the double bonds in the neighbourhood of the brass surface, no bonding will take place; or, in the case of a powdered brass filler, the brass will not stiffen the compound. It is equally probable that if the rate of cure proceeds so slowly as to permit the exhaustion of the sulphur in the formation of the sulphides of copper and zinc, then the formation of a rubber-sulphur-brass compound as postulated by Buchan and Rae will be effectively inhibited. The evidence presented by Gurney indicates that the rate constants governing ordinary cure and rubber-sulphur-copper formation are not affected by increased acceleration to the same extent.

Additional information has now been obtained to clarify the nature of the stiffening effect of brass powder in rubber. The following compounds were prepared and cured:

	766	766A	767	768	769
Smoked sheets	100	100	100	100	100
Zinc oxide	5	5	—	—	5
Stearic acid	1.5	1.5	—	—	1.5
PBN	1	1	1	1	1
MBT	1	3	—	—	1
DPG	—	1.5	—	—	—
Di-Cup 40 C (4)	—	—	4	4	—
Reichgold D8 brass powder (5)	180	180	180	—	—
Sulphur	36	36	—	—	36

These compounds were cured at 151°C for 20 and 40 minutes.

Certain difficulties in the curing of compounds 767 and 768 were encountered. If air is not absolutely excluded, the cured rubber is very soft and tacky, and because of the unavailability of suitable moulds, it was not possible to obtain flat sheets useful for more than the most elementary stress-strain testing. The hardness values obtained are, therefore, the only indications which can be used in reaching the following conclusions. However, these are considered valid.

	Hardness (ISO Degrees)				
	766	766A	767	768	769
20 minutes cure	73	57	30	30	51
40 minutes cure	—	—	30	34	—

Compound 796 shows the usual characteristics of rubber compounds with medium amounts of combined sulphur. The cured sheet has an obviously low tensile strength and a very low tear resistance. In contrast, compound 766 containing brass and sulphur is very tough. While this may be assumed to be due to the lower proportion of combined sulphur, part of the available sulphur having been used up in the formation of copper and zinc sulphide as shown by the substantial evolution of H_2S on treating compound 766 with HCl , the increased hardness of 766 is obviously due to the chemical effect of the brass. This follows from the facts that (a) the higher the proportion of combined sulphur, throughout the whole range, the higher the hardness, notwithstanding the deterioration of other mechanical properties over part of the range, and (b) the comparison of the hardness of compound 767 and 768 where the physical effect of the brass is shown not to increase the hardness⁶.

Comparison of compound 766A, which is accelerated with a very "lively" combination of accelerators, with 766 and 769 shows that, if the rubber is cured fast enough, the sulphur take-up by the rubber is such that little if any sulphur has time to react with the brass and form a bond. The colour of the cured 766A is only slightly darker than the gold colour of the brass, whereas that of 766 is a dark greenish gray.

Dicumyl peroxide appears to act as a curing agent through the formation of carbon-to-carbon cross-links, a mode of action which does not involve the brass. Hence the action of the brass in compound 767 is the purely physical one of an inert filler.

It is felt that the above observations show that, apart from the action of the sulphur involved in direct vulcanization, some interaction between rubber, sulphur and brass is responsible for the large increase in the hardness of the brass filled compound. They also lend support for the writer's visualisation¹ of inert, active and Rehner-type fillers in rubber.

The writer is grateful to the Hercules Powder Company and Eckart-Werke for experimental quantities of "Di-Cup 40C" and Reichgold D8" respectively.

Z. RIGBI
*Rubber Research Association,
 Haifa*

REFERENCES

1. RIGBI, Z., 1956, Etude du Renforcement: Emploi du Laiton comme charge renforçante, *Rev. gen. Caoutch.*, **33**, 243.
2. GURNEY, W. A., 1945, Adhesion of rubber to brass, *IRI Trans.*, **21**, 31.
3. BUCHAN, S. AND RAE, W. D., 1956, Chemical Nature of the Rubber-to-Brass Bond, *IRI Trans.*, **21**, 323.
4. Di-Cup 40C, dicumyl peroxide dispersed in calcium carbonate, manufactured by Hercules Powder Company, Wilmington, Del., U.S.A.
5. Fine brass powder, dispersed in di-2-ethyl hexyl phthalate, manufactured by Eckart Werke, Furth, Bavaria.
6. The lower hardness of the Di-Cup cured compound is possibly due to the degrading effect of brass in the absence of sulphur. This has been observed in rubber-brass masterbatches stored for long periods.

Preferential Removal of Bromides from Brines by Solvent Extraction

A preliminary investigation has been made of the possibility of preferential removal of bromides from brines originating from the Dead Sea by using an organic extracting solvent. An appreciable increase in the ratio Br^-/Cl^- was obtained in the extract, suggesting the feasibility of this approach and the possibility of developing the procedure for industrial application.

First, experiments were made with pure solutions of individual salts, CaCl_2 , MgCl_2 , CaBr_2 , using various solvents in a ratio of 1 part by volume of solvent to 5 parts by volume of aqueous solution, at a temperature of $30^\circ \pm 1$. Apparent partition coefficients were calculated in each case and are given in Table I.

TABLE I

Partition coefficients of pure halides between organic solvents and water

Starting solution Concentration eqs/litre	CaCl_2 9.86	MgCl_2 6.02	CaBr_2 9.55 4.75	$K_{\text{CaBr}_2}/K_{\text{CaCl}_2}$
Solvents	Distribution coefficient $K = \frac{\text{conc. g/l solvent phase}}{\text{conc. g/l aqueous phase}}$			
<i>n</i> -propanol	0.303			
<i>n</i> -butanol	0.144	0.053	0.387	2.7
<i>i</i> -amyl alcohol	0.032	0.010	0.236	7.4
benzyl alcohol	0.019	0.005	0.190	10.0
sec. butanol	0.016	0.015		3.1*
commercial mixture of pentanol, Sharples' "pentasol"	0.008	0.003		0.5*
methyl ethyl ketone	0.006	0.01		
methyl propyl ketone	zero	zero	0.0005	
carbon tetrachloride	zero	zero	zero	

* This comparison is not entirely rigorous since the equiv. concentration of the original CaBr_2 solution in these two cases was only approximately half that of the CaCl_2 solution.

The same procedure was then repeated using a Dead Sea brine and an "end brine" of compositions similar to the typical analyses given in Table II. The solvents used

TABLE II
Typical brine compositions

	Dead Sea brine (g/l)	End brine (g/l)
Cl ⁻	181	349
Br ⁻	4.5	12.2
Ca ⁺⁺	13.5	47.3
Mg ⁺⁺	36.1	90.4
K ⁺	6.0	0.66
Na ⁺	33.2	17 (by diff.)

were *i*-amyl alcohol and benzyl alcohol which, according to Table I, give the most favourable $K_{\text{CaBr}_2}/K_{\text{CaCl}_2}$ for the solvents examined. Results of the extraction of brines are given in Table III. These show that a noticeable increase in the ratio of bromides to chlorides was attained in the case of "end brine". In the case using *i*-amyl alcohol with Dead Sea brine this was also so, but the individual partition

TABLE III
Solvent extraction of halides from brines

		Halogen in orig. brine actual con- centration (g/l)	<i>i</i> -Amyl alcohol extraction			Benzyl alcohol extraction		
	Halogen		Halogen in alcohol layer (g/l)	$K = \frac{\text{g/l in alcohol}}{\text{g/l in aqueous}}$	$\frac{K_{\text{Br}}}{K_{\text{Cl}}}$	Halogen in alcohol layer (g/l)	$K = \frac{\text{g/l in alcohol}}{\text{g/l in aqueous}}$	$\frac{K_{\text{Br}}}{K_{\text{Cl}}}$
End brine	Cl ⁻	362	43.4	0.123	3.5	23.2	0.065	2.7
	Br ⁻	11.9	4.8	0.435		2.0	0.174	
Dead Sea brine	Cl ⁻	175	0.48	0.003	10.7	0.41	0.002	—
	Br ⁻	4.4	0.14	0.032		Not detectable	—	

coefficients are extremely low. The differences in partition coefficients for the same halogen in the case of pure solutions, "end brine" and Dead Sea brine, may be due to differences in concentrations as well as to the effect of the presence of other salts.

From this preliminary investigation it seems that primary alcohols are suitable extracting solvents but not secondary alcohols or ketones. Increase of length of carbon chain causes a decrease in halide solubility, but this is less marked in the case of bromides than of chlorides. Of the solvents examined *i*-amyl alcohol and benzyl alcohol are the most suitable.

By suitable selection of brine and organic solvent, significant extractions of bromide from the brine can be obtained and the ratio of bromide to chloride in the extract will be appreciably higher than in the aqueous brine. By a series of extractions of an "end

brine" type starting solution, back washing of chloride with a brine of suitable concentration and composition such as Dead Sea brine for example, final stripping of bromide from the alcohol solvent by a small quantity of dilute brine, it should be possible to manufacture a concentrated bromide brine containing of the order of 50—100 g bromide per litre and low in chloride.

The permission of the Directors of Israel Mining Industries to publish this material is duly acknowledged.

H. AHARON

A. BANIEL

R. BLUMBERG

*Israel Mining Industries,
Laboratories Haifa*

Received November 12, 1956.

On three layers in turbulent flow*

Laminar flow obeys the Navier-Stokes formulae which give the component of the acceleration (a) of a fluid particle as function of the external (gravity) and internal forces (pressure, viscosity).

In turbulent flow this is not true, but following Reynolds it is customary to assume the validity of the above formulae, only the instantaneous values of the velocity (u) and pressure are replaced by their averages (\bar{u}). It is necessary to add to the internal forces the imaginary Reynolds stresses, proportional to the correlation tensor of velocity fluctuations $u' = u - \bar{u}$ about their average, the components of which are $u'_i u'_k$ (u'_i is the i component of the fluctuation).

When water flows uniformly and steadily down a rectangular channel at a uniform slope I (direction x), there is only a longitudinal component \bar{u}_x , function only of the coordinate normal to the bottom (direction z). Experience shows that in the thin laminar layer (thickness d) near the bottom $\bar{u}_x = Cz$ and above it in the turbulent layer (thickness h) very approximately $\bar{u}_x = A \ln z + B$ (A, B, C , = constants). The components of the correlation tensor were measured as functions of z .

Introducing these experimental values into the Navier-Stokes equations, the average acceleration of a fluid particle may be computed. The results are surprising, as they show the existence of *three* layers of flow, instead of two only, namely:

1. The thin laminar layer (thickness d) without longitudinal acceleration: $\bar{a}_x = 0$.
2. The regular turbulent layer (thickness h), which comprises most of the fluid. The fluid particles fall on the average as if along an inclined frictionless plane: $\bar{a}_x = gI$.
3. The transition layer (thickness \sqrt{hd}) characterized by a very large negative acceleration which exceeds 30g: $\bar{a}_x = D/z^2$, where D is another constant. In the entire cross-section there is no acceleration on the average.

* Abstract of lecture held at the September 1955 Meeting of the Israel Society for Theoretical and Applied Mechanics, Haifa.

It is thus possible to define the average path of a turbulent fluid particle; to explain the rapidity of mixing phenomena of solutions and colours in such a flow; and the motion of bed load in rivers.

S. IRMAY

*Technion—Israel Institute of
Technology, Haifa*

Received January 25, 1957.

The Pantothenic acid content of mouldy wheat and flour

Results in this report are based on determinations of the pantothenic acid content of wheat and wheat flour as a function of progressive mouldiness. 1.5 kg samples of sound, soft wheat were stored in glass containers at 20–21°C. From an initial moisture of 11% the wheat was moistened to 23.5%. The pantothenic acid content was determined both in the wheat—after grinding on a Wiley mill (40 mesh sieve)—and in the milled flour. The flour was obtained from wheat, air dried to about 14% moisture, damped to 15.5% and cold-conditioned for 18 hours, prior to milling.

The wheat was milled on an experimental mill (Bühler) under uniform conditions (rate of feed, moisture of milled wheat, setting of rolls). Flour extraction was calculated as a percentage of all streams obtained. Pantothenic acid was determined by the microbiological method¹. Mould counts were made by the procedure of Christensen². The results are summarized in Table I.

TABLE I
Pantothenic acid content of mouldy wheat and flour

Length of storage (weeks)	Wheat		Wheat flour	
	Mould count of wheat meal (colonies/g)	Pantothenic acid ($\mu\text{g/g}$)	Extraction (%)	Pantothenic acid ($\mu\text{g/g}$)
—	1,000*	5.3	64.0	1.8
1	157,000	4.0	66.3	2.1
2	3,800,000	3.2	68.5	2.4

* All figures at 14% moisture

The results show that on progressive mouldiness there is a destruction of pantothenic acid in the wheat, whereas flours show a gradual increase.

This increase should be attributed to the higher flour extraction obtained from the mouldy wheat and release of aleurone layer into the mouldy flour.

The aleurone layer contains about the same amount of pantothenic acid as the endosperm, but the concentration of this nutrient was found³ to be about 12 times higher in the first layer than in the latter.

Y. POMERANZ

*Ministry of Trade and Industry,
Food Testing Laboratory, Haifa*

REFERENCES

1. BARTON-WRIGHT, E. C., 1945, *Analyst*, **70**, 283.
2. CHRISTENSEN, C. M., 1946, *Cereal Chem.*, **23**, 322.
3. HINTON, J. J. C., PEERS, F. G. AND SHAW, B., 1953, *Nature*, **172**, 993.

Received April 17, 1956

Determination of magnesium oxide in silicates

In the classical silicate analysis, the determination of magnesium oxide is one of the most time-consuming operations. The magnesium ammonium phosphate precipitate itself requires about twelve hours for completion, and after this a repetition of the precipitation is required. The titration with versenate on the other hand gives good results when the sum of calcium oxide and magnesium oxide is determined with eriochrome black T as indicator. The following titration of calcium oxide with murexide indicator, however, meets with difficulties, as the large amounts of ammonium chloride in the solution from the repeated precipitation of the sesquioxides acts as a buffer against the addition of sodium hydroxide solution, which is required to obtain the necessary pH . With some practice, the addition of sodium hydroxide solution can be carried out, using the colour of murexide as a guide, stopping when the colour turns into a distinct rose. This procedure needs experience and some may not recommend it for general use.

In order to avoid the titration with murexide, we tried to determine the magnesium oxide directly by taking an aliquot part of the solution, separating the calcium oxide as oxalate, and precipitating the magnesium oxide only once with ammonium phosphate. The magnesium ammonium phosphate was redissolved in dilute nitric acid, and the P_2O_5 in the solution was determined colorimetrically according to Kitson and Mellon¹ with vanadate-molybdate. The results obtained showed very good agreement with those deriving from the gravimetric determination of the twice precipitated phosphate salt. This may prove that the high results obtained gravimetrically when precipitating the $MgNH_4PO_4$ only once, are due mainly to the presence of $MgNaPO_4$, as the ratio between MgO and P_2O_5 remains the same in the $MgNH_4$ and $MgNa$ double salt.

As in most laboratories nowadays, phosphate is determined colorimetrically, the standards for phosphate estimation and solutions are usually ready for use.

TABLE I
*Results obtained gravimetrically and colorimetrically
MgO in percent*

Gravimetrically	11.30	2.14	3.13
Colorimetrically	11.40	2.19	3.21

W. BODENHEIMER

*Analytical Laboratory, Geological Survey,
Jerusalem*

REFERENCES

1. KITSON, R. E. AND MELLON, M. G., 1944, Colorimetric determinations of phosphorus as molybdi-vanadophosphoric acid, *Ind. Eng. Chem. Ann. Ed.*, **16**, 379—383.

Received February 16, 1957.

The titration of calcium with E.D.T.A. in the presence of limited amounts of fluoride

Fluoride in a high concentration is recommended as a masking agent for calcium in the titration of heavy metals with E.D.T.A.¹ Nevertheless, fluoride does not interfere in the titration of calcium with E.D.T.A. if the sample to be titrated does not contain more than about 10 mg of calcium and 20 mg of fluoride ions in a total volume of not less than 200 ml.

The following experimental results were obtained using as the titrant 0.01M E.D.T.A. which contains 0.01M zinc chelate. The titrations were carried out at pH 10 using ammonia-ammonium chloride buffer and Eriochrome Black T as indicator.

mg Ca ⁺⁺ taken	mg F ⁻ taken	Volume of solution during the titration in ml	mg Ca ⁺⁺ found	% error
2.004	2	200	1.99	— 0.7
2.004	10	200	1.99	— 0.5
2.004	10	200	1.98	— 1.2
2.004	2	50	1.99	— 0.5
2.004	10	50	1.96	— 2.2
4.008	4	200	4.020	+ 0.3
4.008	4	50	4.000	— 0.2
4.008	10	200	4.000	— 0.2
4.008	10	50	3.98	— 0.7
4.008*	20	50	2.53	—37
4.008	20	200	3.98	— 0.7
10.020	10	200	9.99	— 0.3
10.020*	10	50	9.55	— 6.5
10.020*	40	200	9.07	— 9.5
10.020	20	200	10.00	— 0.2
10.020	40	400	9.93	— 0.9
10.020*	40	200	9.30	— 7.2
10.020*	40	300	9.62	— 3.8

* Precipitation of calcium fluoride occurred during the titration. The blue colour of Eriochrome indicator slowly turned to red on standing. In all cases the titrations were carried out immediately, after the addition of buffer.

Standard E.D.T.A.: An amount of 0.8 g of zinc oxide was dissolved in 2 ml conc. hydrochloric acid (36%). To the solution thus obtained 7.5 g of the disodium salt of E.D.T.A. was added in a total volume of about 200 ml. Ammonia was added to bring the pH to about 8—9, followed by water up to one litre, before standardization with calcium or zinc solution as a primary standard.

Zinc is required since the end point for the titration of calcium with E.D.T.A. using Eriochrome black is not sharp without its presence. 0.8 g of zinc oxide added per litre of standard solution of titrant is equivalent to 0.01 M zinc. Therefore, 0.01 E.D.T.A. should be added to get all the zinc in the form of zinc chelate with E.D.T.A. This is equivalent to 3.7 g of E.D.T.A. per litre of solution. Another 3.7 g of E.D.T.A.

is added which will represent the amount of excess free E.D.T.A. necessary for the titration of calcium. The solution will now contain 0.01 M zinc E.D.T.A. ("neutral" towards Eriochrome Black T titration) plus 0.01 M free E.D.T.A. for titrating the calcium or any metal ion, say zinc, at pH 10. It is concluded, therefore, that the standard contains zinc chelate to give a sharp end point but does not contain zinc ions as such.

ACKNOWLEDGMENT

The authors wish to acknowledge the continued interest and helpful discussion of Dr. A. Alon, Chief Analyst, Israel Mining Industries.

The permission of the Directors of Israel Mining Industries to publish this material is duly acknowledged.

REFERENCE

1. PRIBIL, R., 1954, *Chem. Listy* **48**, 41; cf. *C.A.*, 1954, **48**, 5715.

J. MASHALL AND L. GEYER
Israel Mining Industries, Haifa

Received February 5, 1957.



SECOND ELECTRONICS CONVENTION IN ISRAEL

with the participation of the Israel Section of the Institute for Radio Engineers

and the Association of Engineers and Architects in Israel

held at the Weizmann Institute of Science, Rehovot June 16—17, 1957.

Some aspects of the design of a medium size general purpose analogue computer. S. MERHAV (LANDSBERG), *Scientific Department, Ministry of Defence*. In connection with the construction of a general purpose analogue computer at the Scientific Department, Ministry of Defence, some problems considering its optimum design are presented.

The problem of overall system design is explained with the aid of a simple example. Two different methods of approach (e.g. REAC and GEDA methods) are described, and the factors involved in their advantages and drawbacks are listed. In the light of this discussion the necessity of defining a criterion of optimization is stressed.

The system is presented in a generalized manner and consequently a figure of merit and an optimum design condition are obtained.

On the basis of this characterization, REAC and GEDA methods are discussed. Finally the computer now under construction is briefly described.

Error analysis of differential analysers. A. FUCHS, *Scientific Department, Ministry of Defence*. An error analysis of electronic analogue computers based on the matrix representation of linear equations is presented. The set-up problem is thereby considered from the general point of view of network synthesis (following Honnel and Horn).

In the particular case of the "integrator set-up" this error analysis is shown to yield results similar to those already obtained on another basis by MacNee.

The way to optimal set-ups is explained and as an illustration it is shown that one of the possible representations of the harmonic equation leads to half an error as compared with the usual techniques.

Packaged electronic digital computers. M. LEHMANN, *Scientific Department, Ministry of Defence*. After a discussion of the approach to circuit design for general purpose electronic digital computers the paper considers some of the advantages of packaged machines. As an illustration brief mention is made of two distinct sets of commercially available sets of

packages. The paper then considers proposals for a set of packages suitable for the control of a large and fast parallel machine together with an outline of the arithmetic unit for such a machine.

A numerical method for the simplification of truth functions. AVIEZRI FRAENKEL, *Electronic Computer Group, Weizmann Institute of Science, Rehovot*. A method is proposed for the evaluation of all the possible simplest normal disjunctive formulas Ψ_i , which are equivalent to a given truth function Φ with n Boolean variables. The prime implicants¹, i.e., all those conjunctive terms which are candidates of the Ψ_i 's are found by applying a mechanical numerical method to the table defining Φ .

Following Ledley², the n variables, their negations and all disjunctive and conjunctive terms which may be constructed thereof, are each represented by a sequence of 2^n binary digits, called designation numbers. However, unlike Ledley's method which necessitates scanning of an auxiliary chart containing all the 3^n-1 distinct conjunctive terms, which, in case of computer realization are composed of $2^n(3^n-1)$ bits, the proposed method produces the prime implicants directly under control of Φ , without having to consult charts. The prime implicants are then scanned similarly to Quine's method^{1,3}. A dual method holds for the establishment of the simplest conjunctive normal formulae.

Two standard subroutines have been programmed and run on WEIZAC, a high speed digital computer at the Weizmann Institute of Science. The subroutines are dual in the above sense. They simplify any given function out of the 2^{2^n} possible functions. As no charts are needed the method is applicable for larger values of n than has been feasible hitherto. An example of the manual evaluation of a seven variable function is presented.

REFERENCES

1. QUINE, W. V., 1952, The problem of simplifying truth functions. *Amer. Math. Monthly*, **59** (8).
2. LEDLEY, ROBERT S., 1954, Mathematical foundations and computational methods for a digital logic machine, *Journal of the*

Operations Research Society of America, 2(3).

3. QUINE, W. V., 1955, A way to simplify truth functions, *Amer. Math. Monthly*, 62(9).

Magnetic tapes for WEIZAC. Z. RIESEL and M. KRASNITZKI, *Electronic Computer Group, The Weizmann Institute of Science, Rehovot*. WEIZAC's high speed memory has a comparatively large capacity (4096 words). However, problems have been suggested requiring larger memory capacity. Magnetic tapes are an economic solution.

The tape transport system used is a Potter tape handler, Model 905. Tape speed is 70 inch/sec., number of channels 8.

The biggest problem is the presence of bad spots on the magnetic tape, i.e., spots where magnetic material is missing. The suggested solution is to write a synch track on one of the channels only in such places where there are no bad spots on the other channels. A character (consisting of 4 or 5 bits) will then be written or read only in such places where a synch is present. Since noise is picked up by the synch reading head while the other heads are writing, the synch reading amplifier must be disabled during writing, i.e. just after a synch pulse has been recognised.

Modes of communication between the tapes and the computer will be as follows:

- 1) Information on the tape will be written in blocks of words, 8 or 10 characters per word. The number of words per block is specified by the programmer. A block, including block start and end characters, will be written by means of a subroutine.

- 2) A read order will read an entire block into sequential addresses of the high speed memory.

- 3) An additional order will read a block into the computer but not the memory, with the aid of a subroutine. This is to be used for checking blocks.

- 4) There will be orders advancing and reversing the tape by one block.

Design of a relay servo for operation under external vibrations. ZE'EV BONENN, *Scientific Department, Ministry of Defence*. A system may be adapted for operation under vibrations in several ways. The simple approach is to use shock mounts or better components. Another approach is to design the system for satisfactory performance under these conditions. It is sometimes possible, by means of slight modifications

in design and without hampering normal operation, to considerably improve the performance under heavy vibrations.

Our example is a simple relay velocity servo. Experiment shows that its performance deteriorates under the influence of external vibrations. This cannot be improved by the use of a relay less sensitive to vibrations. Analysis of the mechanical and magnetic forces acting on the relay and their influence on its operation point the way for design improvement. Several changes involving arrangements of relays and contacts were tested and found to affect a considerable improvement in performance, almost without introducing any additional complication in equipment.

A new magnetic binary counter. DAVID TREVES, *Department of Electronics, The Weizmann Institute of Science, Rehovot*. A second harmonic type magnetic amplifier, loaded with a condenser, can become unstable, so that a current is induced in the output circuit with no input signal. The frequency of this current is a harmonic of the exciting current frequency.

The harmonic number is a function of the load. It was experimentally found, that with a certain load, there are two modes of oscillation, differing only by the phase between output and exciting currents.

This effect can be understood if one remembers that the inductance of the output circuit is a function of the absolute value of the exciting current, and if this is symmetrical, the output circuit cannot distinguish between positive and negative peaks of exciting current.

This duality leads to the above-mentioned two modes of oscillation. With suitable parameters, when the amplitude of exciting current is lowered and raised again, the oscillation changes mode regularly.

The magnetic amplifier operates then as a binary counter; the modulation pulse of the exciting current is the counted signal.

Such counters operating at the first harmonic can be cascaded to form a counter with several digits.

A magnetometer for measuring extremely small magnetic fields. A. A. WULKAN, *Scientific Department, Ministry of Defence*. A magnetometer in which saturable reactors and germanium diodes are used, is described. A brief description of the basic operation of saturable reactors is given, and is compared to a synchronous switch whose on-off periods are de-

terminated by a control field. The law of equal Ampere-Turns is proven. Two methods are given for increasing the A. T. Gain, namely — by positive magnetic feed-back and by blocked intrinsic feed-back. The principle of control by external magnetic fields is introduced requiring an open magnetic circuit — a rod. The internal field, the demagnetising factor and rod permeability are calculated. The final construction of the magnetometer is shown incorporating a slit rod to accommodate the AC and feed-back windings. Actual characteristics of two magnetometers are given.

The electrical constants of a nerve fibre. I. WEIZMANN, *The Hebrew University-Hadassah Medical School, Jerusalem*. The application of cable theory to the process of conduction of impulses along a nerve fibre is well known.

The line constants of a nerve fibre may be measured and the attenuation factor of the nerve line calculated.

In the light of the very high attenuation factor of this line, the observed progression of the nerve impulse without decrement may be explained by the amplifier-like behaviour of the nerve membrane. The nerve conducts the impulse as if amplifiers were continuously distributed along it.

The conclusion that devices, analogous to amplifiers, communication lines and oscillators are developed by the living cell, must be drawn by anyone investigating these phenomena. No satisfactory description of the structure of these devices has yet been given.

The living cell is built mostly of liquids and the charges are carried in it by ions. It seems that the living cell succeeded in developing a technique, based on the movement of ions in the liquid phase, which is analogous to the technique of electronics in the gaseous and solid state. The possibility of "electronics" or, let us call it "ionics" in the liquid phase might, perhaps, be profitably investigated.

Noise measurements in Radar receivers. JOSEF NAOB, *Israel Air Force*. Maintenance of high performance in microwave receivers demands periodic noise figure measurement. Two methods are in use in the Air force. The more accurate one employs a calibrated noise tube giving direct measurement to 0.1 db, but necessitates dismantling the waveguide and is used only for quarterly checks. More frequent measure-

ments are made by the single frequency method, using a signal generator connected via the directional coupler. This is accurate to about 1 db.

In both methods the noise output of the receiver connected to the signal source is measured with the latter unenergised. Sufficient power, noise or sinewave, is then injected to double the output noise. To avoid irregularities in the metering circuit, doubling is measured by insertion of a calibrated attenuator between the receiver to be measured and the measuring apparatus, and adjusting it for constant output power with or without signal. In the case of the noise tube, only the attenuator reading is observed, and a nomogram converts its reading to noise figure. For the signal generator, a 3 db attenuator is used and the remaining attenuation inserted at the signal generator — a simple calculation connecting the latter reading with the noise figure.

Application of dialling system to V. H. F. communications centre. URI MORDOVITZ, *Israel Air Force*. For an operator, a V. H. F. channel comprises facility for speech, reception and appropriate indicating lights. This necessitates about eight wires between the operator and communications.

If channel change is based on hand selectors, eight wires per channel are needed, and if more than one operator is connected, the complexity of the cabling increases.

On the other hand, for a dialling system, eight wires are needed per operator independent of the number of channels, apart from indicating lights. The Air Force system is based on Strowger selectors, but presents some novel features. Since our operators are accustomed to holding the microphone the whole time, a circuit was devised enabling a fresh number to be dialled without operating a cradle switch.

The selectors are in continual use so that modifications were introduced to deenergise all relays when a 'number' has been obtained. Provision is also made for a complete standby set of equipment to be switched on by the operator in the event of a suspected failure, with automatic alarm to the technician.

An overall sidetone circuit is incorporated by reducing receiver output on microphone operation and direct reception of the transmitted signal.

Yagi aeriels, J. O. SPECTOR, Scientific Department, Ministry of Defence. The radiation pattern of a Yagi aerial is usually calculated by the superposition of all the radiation fields due to currents in the aerial's elements. This calculation is too complicated for aeriels consisting of more than a few elements. It is suggested that the Yagi aerial be considered as a guide for surface waves, specifically the so-called Dipole Mode. Radiation occurs only from the plane perpendicular to the axis at the end of the aerial. From this aperture of infinite extent the radiation pattern may be calculated. Experimental values of the propagation constant of the surface wave have been used to predict the beam-width of long aeriels. There is good agreement with measured radiation patterns,

An improved UHF balun, EFRAIM WEISSBERG, Scientific Department, Ministry of Defence. The balun matches a 75 ohm shielded coaxial line to a 300 ohm balanced parallel wire line, over the frequency range of 470 — 890 mc/s. The design principles apply to other ranges of impedances and frequencies as well.

The improved design overcomes some of the difficulties inherent in baluns such as the half-wavelength-loop, the bazooka, etc. The balance efficiency of this balun is independent of frequency, and its remaining characteristics are symmetrical functions of frequency. The design is based on the principle of the series-parallel connection. Measured characteristics of production units chosen at random follow very closely theoretically computed values. This enables these units to be used as precision components in power, noise figure and impedance measuring setups, with no need for their individual calibration.

Conditions for the impedance and admittance matrices of n -ports without ideal transformers, I. CEDERBAUM, Scientific Department, Ministry of Defence. The matrices relating two adequate systems of simple network coordinates of the same network, e. g. node-pair voltages or loop currents are shown to have all their elements and subdeterminants equal to +1, -1 or 0. Any n -port may be looked upon as apart of an adequate system of independent node-pairs described on the network or loops inscribed into the network. In the former case the additional node-pairs, not included in the n -port ought to be considered as open-circuited and in the latter case the additional loops ought to be

looked on as short-circuited. The conditions for cut-set- and loop-incidence matrices are discussed and then the conditions for impedance and admittance matrices of n -ports without ideal transformers in terms of those incidence matrices are defined. The discussion of the conditions thus derived leads, among others, to a conclusion that matrices representing pure resistance n -ports are necessarily such that each principal minor of such a matrix is greater than the modulus of any minor built from the same rows (or columns).

Calculation of impedances and admittances using the modular determinant of the network matrix, S. LOUIS, Technion-Israel Institute of Technology, Haifa.

A. Calculation of impedances

The easiest way to calculate the amplification and the transfer in a lumped-parameters network, using loop analysis, is to choose one current only through each input and output loop. This choice implies a certain loop current configuration which is not necessarily the best for calculating the impedance seen from any branch towards the network.

The method here presented utilizes $\Delta(Z)$ — the determinant of the impedance matrix only, independently of the loop-current configuration;

If three currents i_1 , i_2 and i_3 pass through Z_y ; the impedance seen from Z_y towards the rest of the network is:

$$Z = \frac{\Delta(x)}{\Delta_{11} + \Delta_{22} + \Delta_{33} + \Delta_{23} + \Delta_{32} - \Delta_{13} - \Delta_{31} - \Delta_{12} - \Delta_{21}}; \quad (1)$$

the denominator of Eq. (1) equals the determinant of the same network with Z_y open circuited. Therefore:

$$\begin{aligned} \text{Denominator of Eq. (1)} &= \\ &= [\Delta(z)]_{Z_y \rightarrow \infty} = \Delta_{\text{open}}; \end{aligned} \quad (2)$$

$\Delta(Z)$ is invariant¹ to changes of the current configuration (except for a constant), its form being:

$$\begin{aligned} \Delta(Z) &= \text{Numerator of (1)} = \\ &= \Delta_{\text{short}} + Z_y \cdot \Delta_{\text{open}}; \end{aligned} \quad (3)$$

where Δ_{short} is the determinant of the network matrix with Z_y short circuited; $Z_y = 0$. Therefore:

$$Z = \frac{\Delta_{sh} + Z_v \Delta_{op}}{\Delta_{op}}; \quad (4)$$

and the corresponding theorem is:

The impedance seen from any branch Z_v , equals $\Delta(Z)$ divided by all the terms in $\Delta(Z)$ of which Z_v is a factor; If p currents are passing through Z_v , p^2 cofactors are needed to form Eq. (1), and their evaluation is quite cumbersome; Eq. (4) avoids this.

B. Driving point admittances (D.P.A.) calculated by means of nodal analysis

An analogue to the above mentioned method exists also for the calculation of D.P.A. in parallel with any branch Y_v ;

$$Y = \frac{\Delta_{open} + Y_v \cdot \Delta_{short}}{\Delta_{short}}; \quad (5)$$

We find again that the denominator of Eq. (5) is the factor of Y_v in the numerator of Eq. (5), and the latter is $\Delta(Y)$ itself which is invariant to changes of the reference point.

Equations (4) and (5) are valid both for active and passive networks.

REFERENCES

1. CEDERBAUM, I., 1956, *J. Math. Phys.*, **34**(4).
2. SHEKEL, J., 1954, *Proc. I.R.E.*, **42**, 1125.

The analysis of linear operational networks, AMOS NATHAN, *Faculty of Electrical Engineering, Technion-Israel Institute of Technology, Haifa*. A method of matrix analysis of linear networks containing transfer functions is presented, a transfer function characterizing an element of infinite input and zero output impedance. As an example, a network containing one operational (computing) amplifier is analyzed. The admittance matrix of the net-

work without the amplifier is first written down. The effect of the amplifier is then considered, noting that it can be represented by a suitable input current injected into the node into which the amplifier works. This current is finally eliminated from the network equations with the aid of the equation expressing the voltage constraint imposed by the amplifier.

The procedure is simple and straightforward and extends the techniques of matrix analysis to an important field. A fuller account will be published shortly.

The design of symmetrical linear-phase low filters with the aid of a potential analogue, J. NAVOT, *Technion-Israel Institute of Technology, Haifa*. To solve the approximation problem of synthesising a symmetrical linear-phase low-pass filter, use is made of a potential analogue in the complex frequency plane to represent the image transfer function of "m-derived" half sections (with Real. $m > 0$) connected in cascade. Conformal transformations are then introduced to map the potential analogue into related planes, and the importance is stressed of the loci of infinities of the image transfer function in either plane and the way in which they are distributed on these loci. A detailed examination is undertaken of some mappings, primarily chosen by virtue of their simple geometries in the transformed planes which lend themselves conveniently to the calculation of the corresponding filter characteristics. In particular, the "error" of the phase characteristics from linearity is expressed in a unified form which clearly shows their relative merits and shortcomings.

With the error linearity of the insertion phase conveniently expressed, including, if desired, the effect of uniform dissipation, an "improvement process" is developed which reduces it to a small tolerable quantity.

work without the amplifier is first written down. The effect of the amplifier is then considered, noting that it can be represented by a suitable input current injected into the node.

The procedure is simple and straightforward and extends the techniques of matrix analysis to an important field. A fuller account will be published shortly.

The design of symmetrical linear-phase low filters with the aid of a potential analogue, J. NAYLOR, Technion-Israel Institute of Technology, Haifa. To solve the approximation problem of synthesizing a symmetrical linear-phase low-pass filter, use is made of a potential analogue in the complex frequency plane to represent the image transfer function of "m-derived" half sections (with $\text{Re} s > 0$) connected in cascade. Conformal transformations are then introduced to map the potential analogue into related planes, and the importance is stressed of the loci of infinities of the image transfer function in either plane and the way in which they are distributed on these loci. A detailed examination is undertaken of some mappings, primarily chosen by virtue of their simple representation in the transformed planes which lend themselves conveniently to the calculation of

which clearly shows their relative merits and shortcomings. With the error linearity of the insertion phase conveniently expressed, including if desired, the effect of uniform dissipation, an "improved process" is developed which reduces it to a small tolerable quantity.

$$V_{in} + \sum V_{out} = \Delta_{op}$$

(4)

and the corresponding theorem is:

(1) Given V_{in} and V_{out} in terms of V_{in} and V_{out} is a factor, if V_{in} currents are passing through V_{in} and V_{out} currents are needed to form Ed. (1), and their evaluation is quite cumbersome; Ed. (4) avoids this.

(2) Driving point admittance (D.P.A.) calculated by means of node analysis.

An analogue to the above mentioned method exists also for the calculation of D.P.A. in parallel with any branch V_{in} .

$$V_{in} = \Delta_{open} + Y_{in} \Delta_{short}$$

(2)

We find again that the denominator of Ed. (2) is the factor of V_{in} in the numerator of Ed. (2), and the latter is $\Delta(Y)$ itself which is invariant to changes of the reference point. Equations (4) and (5) are valid both for active and passive networks.

REFERENCES

1. CERNIAK, I., 1956, J. Math. Phys., 34(4).
2. CERNIAK, I., 1957, J. Math. Phys., 35(4).

the, technion-Israel Institute of Technology, Haifa. A method of matrix analysis of linear networks containing transfer functions is presented, a transfer function characterizing an element of infinite input and zero output impedance. As an example, a network containing one operational (computing) amplifier is analysed. The admittance matrix of the net-

The 7th Annual Meeting of the
ISRAEL ASSOCIATION FOR THEORETICAL
AND APPLIED MECHANICS

The Seventh Annual Meeting of the Israel Association for Theoretical and Applied Mechanics was held at the Technion-Israel Institute of Technology, Haifa, on April 18-19, 1957. The guest lecture was delivered by Prof. Louis Rosenhead, University of Liverpool, on the subject *Comments on the History of Fluid Dynamics*. Twelve lectures were given in two morning sessions and one afternoon session. Their abstracts follow here.

A centripetal vacuum pump, M. REINER, Technion—Israel Institute of Technology, Haifa. An instrument was demonstrated in which a metal plate was brought into rotation around a vertical axis, relative to another stationary plate. Both plates are isolated from the external air by a cover made of glass. It was shown that the air enclosed inside the cover was slowly sucked out, the whole apparatus acting as a centripetal vacuum pump. At the same time the rotating plate was kept floating over the stationary plate, thus forming an air bearing device.

Reiner's effect and the Navier-Stokes equations, M. HANIN, Technion—Israel Institute of Technology, Haifa. The centripetal airpump effect, discovered recently by Prof. M. Reiner, apparently contradicts the Navier-Stokes equations. Solution of these equations shows that when a viscous fluid between two circular, parallel disks is set in motion by the rotation of one of the disks, the resulting fluid pressure at the centre should be lower than the external pressure. In Reiner's experiments, to the contrary, a positive excess pressure is produced at the centre, provided that the gap between the disks is sufficiently narrow.

In a recent paper, Sir Geoffrey Taylor presents an explanation of this contradiction. He assumes that the actual centripetal pump apparatus deviates from its idealized model in that (i) the disks are not perfectly parallel, (ii) the rotor oscillates in the direction of its axis. The effect of these imperfections on the pressure distribution is then evaluated by solving the Navier-Stokes equations under appropriate boundary conditions. To enable solution, the simplifying assumptions of the theory of lubrication are employed. For an incompressible fluid, these solutions indicate no pressure rise. When, however, compressibility is taken into account, the solutions predict a mean positive pressure excess between the disks, both in the case of the oscillations and of the angular imperfection. When reasonable values are assumed for the magnitude of the imperfections, the calculated pressure excess turns out to be of the same order of magnitude as in Reiner's experiments.

REFERENCES

1. REINER, M., 1956, Research on the Physics of Airviscosity, Technion Research Report.
2. TAYLOR, SIR G., 1956, Effects of Compressibility at Low Reynolds Numbers, *I.A.S.* preprint.

The Navier-Stokes equations do not describe gyroscopic effects, E. JABOTINSKY, Technion—Israel Institute of Technology, Haifa. Gyroscopic effects are defined as being those due to the accumulation of the moment of impulse throughout the volume occupied by moving matter. The N.-S. equations are obtained by applying the moment of impulse theorem to infinitesimal volumes only, describe only those inertial phenomena which are of a local nature. Thus they fail to describe the motion of solids as a limit of viscous flow for infinite viscosity, yielding for $\mu \rightarrow \infty$ only the fact that the "fluid" is indeformable. To determine the motion of solids an additional equation is needed: namely that obtained by applying the moment of impulse theorem to a finite volume.

Irrigation and water absorption rate, M. RAM, Water Utilisation Division, Ministry of Agriculture. Water absorption rate depends upon position of plot, conditions of cultivation, crop rotation, organic matter content of the soil, etc. Measurements have been made on water absorption rate, intensity and period of irrigation.

The direction cosines as two systems tensor in rectangular cartesian coordinates, Z. KARNI, Technion—Israel Institute of Technology, Haifa. The tensor character of physical quantities has been established, and these quantities were found to obey certain transformation formulae. For an absolute tensor of the second rank, for example, the transformation formula is

$$\bar{T}_{ij} = T_{\alpha\beta} \frac{\partial \bar{x}_i}{\partial x_\alpha} \frac{\partial \bar{x}_j}{\partial x_\beta}$$

where the partial derivatives denote the direction cosines. The question "do the direction cosines possess a tensorial character?" leads to a further distinction within cartesian tensors, as we now

have a two systems tensor of the second rank. The components of such a tensor relate simultaneously to two different coordinate systems belonging to the same point. The transformation formula for these components is

$$T_{ij} = T_{\alpha\beta} \frac{\partial x_i}{\partial \bar{x}_\alpha} \frac{\partial \bar{x}_j}{\partial x_\beta}$$

which includes the above transformation as a particular case. The geometrical interpretation of this transformation when applied to the direction cosines is a well known formula in trigonometry, and it is also shown that Kronecker Delta is another particular case of this interpretation.

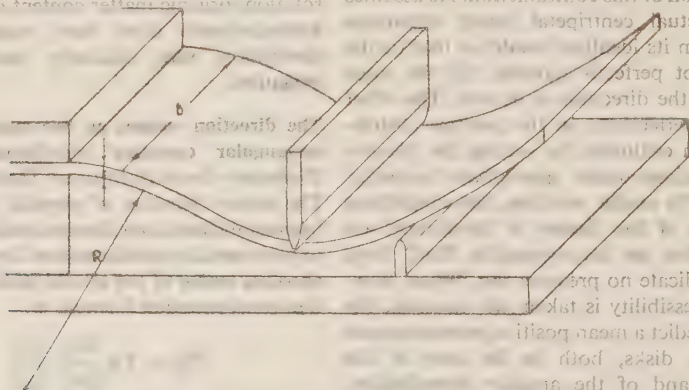
Vibrations around a differential, J. BOAS POPPER, Technion--Israel Institute of Technology, Haifa. The differential is an instrument that solves the equation

$$\sum_{i=1}^n a_i \ddot{x}_i = 0 \quad (1)$$

where a_i are the constant parameters of the mechanism, and x_i are the variable values which are introduced as rotational or linear movements.

The differential is an important accessory in many mechanical devices (e.g. vehicles, textile machines, automatic controls, computers etc.).

Antielastic bending of plates, A. KOGAN, Technion--Israel Institute of Technology, Haifa. In connection with a recent proposal to build de Laval nozzles for 2-dimensional wind tunnels by bending an elastic plate by a process that would ensure the profile accuracy in the longitudinal direction, the question came up whether it is permissible to neglect the anti-elastic deformations.



Yoder gave an approximate solution to the anti-elastic bending of plates by assuming a constant curvature in the longitudinal plane. This

Since one cannot often make a design satisfactorily, without the exact knowledge of the natural frequencies (ω) of the device, a procedure is described by means of which the frequencies and the relative amplitudes around the differential can be analyzed.

The calculation is based on the law of moments of the differential:

$$M_i \cdot \frac{1}{a_i} = M_j \cdot \frac{1}{a_j} \quad (2)$$

where M is the torque at any input or output shaft. The differential equations of the vibrations are expressed by

$$\frac{d^2 y_i}{dt^2} I_i + k_i (y_i - x_i) = 0 \quad (3)$$

where y_i denotes movement of the body y_i , which is connected to the differential by means of an elastic member k_i . Solving the equations 1, 2 and 3, a simple harmonic motion is obtained.

The principle is demonstrated on a differential with three shafts. The analysis of several special basic examples yields results which one cannot obtain by means of analogies to simple gear trains, a method which is generally adopted in literature.

Yoder's exact solution to the problem of anti-elastic bending of plates is a boundary value problem. It assumes an explanation of this contradiction. He assumes that the actual computed deviates from the theoretical disks are not periodic in the direction of these input and output shafts. This is the reason why solutions indicate no periodicity in the direction of these input and output shafts. This is the reason why solutions indicate no periodicity in the direction of these input and output shafts.

Yoder's exact solution to the problem of anti-elastic bending of plates is a boundary value problem. It assumes an explanation of this contradiction. He assumes that the actual computed deviates from the theoretical disks are not periodic in the direction of these input and output shafts. This is the reason why solutions indicate no periodicity in the direction of these input and output shafts. This is the reason why solutions indicate no periodicity in the direction of these input and output shafts.

Yoder's exact solution to the problem of anti-elastic bending of plates is a boundary value problem. It assumes an explanation of this contradiction. He assumes that the actual computed deviates from the theoretical disks are not periodic in the direction of these input and output shafts. This is the reason why solutions indicate no periodicity in the direction of these input and output shafts. This is the reason why solutions indicate no periodicity in the direction of these input and output shafts.

Yoder's exact solution to the problem of anti-elastic bending of plates is a boundary value problem. It assumes an explanation of this contradiction. He assumes that the actual computed deviates from the theoretical disks are not periodic in the direction of these input and output shafts. This is the reason why solutions indicate no periodicity in the direction of these input and output shafts. This is the reason why solutions indicate no periodicity in the direction of these input and output shafts.

Yoder's exact solution to the problem of anti-elastic bending of plates is a boundary value problem. It assumes an explanation of this contradiction. He assumes that the actual computed deviates from the theoretical disks are not periodic in the direction of these input and output shafts. This is the reason why solutions indicate no periodicity in the direction of these input and output shafts. This is the reason why solutions indicate no periodicity in the direction of these input and output shafts.

Yoder's exact solution to the problem of anti-elastic bending of plates is a boundary value problem. It assumes an explanation of this contradiction. He assumes that the actual computed deviates from the theoretical disks are not periodic in the direction of these input and output shafts. This is the reason why solutions indicate no periodicity in the direction of these input and output shafts. This is the reason why solutions indicate no periodicity in the direction of these input and output shafts.

Yoder's exact solution to the problem of anti-elastic bending of plates is a boundary value problem. It assumes an explanation of this contradiction. He assumes that the actual computed deviates from the theoretical disks are not periodic in the direction of these input and output shafts. This is the reason why solutions indicate no periodicity in the direction of these input and output shafts. This is the reason why solutions indicate no periodicity in the direction of these input and output shafts.

Yoder's exact solution to the problem of anti-elastic bending of plates is a boundary value problem. It assumes an explanation of this contradiction. He assumes that the actual computed deviates from the theoretical disks are not periodic in the direction of these input and output shafts. This is the reason why solutions indicate no periodicity in the direction of these input and output shafts. This is the reason why solutions indicate no periodicity in the direction of these input and output shafts.

Yoder's exact solution to the problem of anti-elastic bending of plates is a boundary value problem. It assumes an explanation of this contradiction. He assumes that the actual computed deviates from the theoretical disks are not periodic in the direction of these input and output shafts. This is the reason why solutions indicate no periodicity in the direction of these input and output shafts. This is the reason why solutions indicate no periodicity in the direction of these input and output shafts.

Yoder's exact solution to the problem of anti-elastic bending of plates is a boundary value problem. It assumes an explanation of this contradiction. He assumes that the actual computed deviates from the theoretical disks are not periodic in the direction of these input and output shafts. This is the reason why solutions indicate no periodicity in the direction of these input and output shafts. This is the reason why solutions indicate no periodicity in the direction of these input and output shafts.

Yoder's exact solution to the problem of anti-elastic bending of plates is a boundary value problem. It assumes an explanation of this contradiction. He assumes that the actual computed deviates from the theoretical disks are not periodic in the direction of these input and output shafts. This is the reason why solutions indicate no periodicity in the direction of these input and output shafts. This is the reason why solutions indicate no periodicity in the direction of these input and output shafts.

Yoder's exact solution to the problem of anti-elastic bending of plates is a boundary value problem. It assumes an explanation of this contradiction. He assumes that the actual computed deviates from the theoretical disks are not periodic in the direction of these input and output shafts. This is the reason why solutions indicate no periodicity in the direction of these input and output shafts. This is the reason why solutions indicate no periodicity in the direction of these input and output shafts.

Yoder's exact solution to the problem of anti-elastic bending of plates is a boundary value problem. It assumes an explanation of this contradiction. He assumes that the actual computed deviates from the theoretical disks are not periodic in the direction of these input and output shafts. This is the reason why solutions indicate no periodicity in the direction of these input and output shafts. This is the reason why solutions indicate no periodicity in the direction of these input and output shafts.

Yoder's exact solution to the problem of anti-elastic bending of plates is a boundary value problem. It assumes an explanation of this contradiction. He assumes that the actual computed deviates from the theoretical disks are not periodic in the direction of these input and output shafts. This is the reason why solutions indicate no periodicity in the direction of these input and output shafts. This is the reason why solutions indicate no periodicity in the direction of these input and output shafts.

Yoder's exact solution to the problem of anti-elastic bending of plates is a boundary value problem. It assumes an explanation of this contradiction. He assumes that the actual computed deviates from the theoretical disks are not periodic in the direction of these input and output shafts. This is the reason why solutions indicate no periodicity in the direction of these input and output shafts. This is the reason why solutions indicate no periodicity in the direction of these input and output shafts.

Yoder's exact solution to the problem of anti-elastic bending of plates is a boundary value problem. It assumes an explanation of this contradiction. He assumes that the actual computed deviates from the theoretical disks are not periodic in the direction of these input and output shafts. This is the reason why solutions indicate no periodicity in the direction of these input and output shafts. This is the reason why solutions indicate no periodicity in the direction of these input and output shafts.

Yoder's exact solution to the problem of anti-elastic bending of plates is a boundary value problem. It assumes an explanation of this contradiction. He assumes that the actual computed deviates from the theoretical disks are not periodic in the direction of these input and output shafts. This is the reason why solutions indicate no periodicity in the direction of these input and output shafts. This is the reason why solutions indicate no periodicity in the direction of these input and output shafts.

Yoder's exact solution to the problem of anti-elastic bending of plates is a boundary value problem. It assumes an explanation of this contradiction. He assumes that the actual computed deviates from the theoretical disks are not periodic in the direction of these input and output shafts. This is the reason why solutions indicate no periodicity in the direction of these input and output shafts. This is the reason why solutions indicate no periodicity in the direction of these input and output shafts.

Yoder's exact solution to the problem of anti-elastic bending of plates is a boundary value problem. It assumes an explanation of this contradiction. He assumes that the actual computed deviates from the theoretical disks are not periodic in the direction of these input and output shafts. This is the reason why solutions indicate no periodicity in the direction of these input and output shafts. This is the reason why solutions indicate no periodicity in the direction of these input and output shafts.

layer phenomenon, and the anti-elastic profile is independent of b/\sqrt{Rt} . For $b/\sqrt{Rt} < 4.03$, the deformation of the whole left hand side of the plate is influenced by stresses in the right hand side, and vice versa, and the profile depends strongly on b/\sqrt{Rt} . The region $4.03 < b/\sqrt{Rt} < 10.1$ is a transition range between these extremes.

The assumption of constant curvature is not justified in a de Laval nozzle. The preliminary results, of a series of measurements of anti-elastic profiles of plates bent to a strongly varying curvature indicated a marked influence of $b(d-Rt)/d(x/b)$ on the profile shape in the region $d/Rt > 10$. The total variation of anti-elastic deflection over the profile exceeds in certain cases twice the variation predicted by Yoler.

REFERENCE

1. YOLER, 1952, Aero. Eng. Thesis, C.I.T.

Safety factor in structures in non-proportional cases within the elastic range, A. ZASLAVSKY, *Technion—Israel Institute of Technology, Haifa*. There are cases of structures with the elastic range — Hooke's law being valid — when there is no proportionality between load and stress. Such well-known cases are structures where the change in the geometry of the structure due to deformation cannot be neglected in the application of equilibrium conditions, as for instance in buckling problems.

Other cases are: prestressed or partially prestressed structures; structures with induced or thermal stresses; foundations, columns, beams etc. reinforced to accommodate additional loads; composite steel and concrete structures (e.g. dead-load carrying steel beam combined with concrete slab for joint carrying of live load); structures with restraints becoming effective only after some initial deformation has taken place, structures under impact loads, etc.

In all cases mentioned above, the conventional method of design by admissible (working) stresses σ_{adm} does not lead to the correct factor of safety envisaged by this method. The design should be based on the load producing the critical, rather than the admissible stress. For instance, for a given reinforced steel beam, the critical load P_y would be the one producing the yield stress σ_y ; the admissible load P_{adm} then equals the critical load divided by the safety factor k :

$$P_{adm} = P_y/k$$

This admissible load is, of course, not identical with the directly calculated load producing the admissible stress $\sigma_{adm} = \sigma_y/k$. The difference is illustrated in a number of examples.

The paper deals with the elastic design method and not with the ultimate load method by which a structure is designed to support a certain failure load in the plastic range.

Cracking of houses built on heavy soil, S. ROSENHAUT, *Technion—Israel Institute of Technology, Haifa*. About 200 houses were built in the years 1953—1955 as part of a large housing scheme. The first cracks appeared in the interior partitions, then spread to the walls, and finally in the reinforced concrete structure.

The aims of the investigation were: a) to find the causes of cracking, b) to propose means for repairing, c) to devise an improved building method for the same region which would avoid the appearance of cracks.

The investigation consisted in: a) exploration of the existing foundations and soil tests, b) investigation of the structural design and standard of execution, c) measurements of the changes in crack-width (using demountable strain-gauges), d) testing of wall models (scale 1:2) to differential settlements.

It was found that the causes were differential settlements of the foundations and horizontal thrusts of the soil on the foundation.

The repairing consisted in keeping constant soil humidity increasing the stiffness of the existing buildings.

Improved building methods were proposed and are now tested in the 1:2 scale models.

- * The investigation was carried out at the Technion by the Structures Department of the Building Research Station in collaboration with the Soil Testing Laboratory.

Phenomena of static fatigue, J. GLUCKLICH, *Technion—Israel Institute of Technology, Haifa*. Various investigators observed phenomena of static fatigue in brittle materials such as glass, porcelain and synthetic resins. The author noticed this in neat cement. In view of the general rheological behaviour of this material, an explanation is attempted here which is based on the delayed elasticity effect. It is shown that the solid phase of the material, which can be considered as a gel, received the full amount of the externally applied load only at infinite time. It is also shown that the deviatoric energy content of such a material, when loaded by a constant load, increases with time. Both these

changes of stress and energy are exponential functions of time, which is in agreement with observations of various investigators with regards to strength of various materials. Another agreement between the proposed theory and observations is the sensitivity of the static fatigue to moisture. It is explained here that the presence of moisture in the gel pores of the cement stone is very similar in its damping effect to the presence of moisture on the surface of a material such as glass, the cracking being initiated in the first case inside the material and in the second case on the surface.

Flow of rubber in a plastometer, Z. RIGBI, *Rubber Research Association*. The condition of the parallel plates (friction, etc.) of a Williams Plastometer may influence considerably by end effects the value of the "Plastic Number" of a rubber specimen investigated in this apparatus. The flow of rubber in the apparatus was observed by making use of two-coloured samples and showed that influence.

On the mean acceleration of fluid particles in turbulent flow (second note), S. IRMAY, *Technion—Israel Institute of Technology, Haifa*. The three components of the mean acceleration \bar{a} of fluid

particles, may be expressed by the Reynolds form of the Navier-Stokes equations for incompressible channel flow in terms of the mean velocity \bar{u} or the correlations $\bar{u}'\bar{w}'$, $\bar{w}'\bar{w}'$, measured by Laufer as functions of distance from wall z .

In the direction of flow \bar{a}_1 vanishes at wall and near the wall ($z = e = \sqrt{dh}$; h = half channel width; $d = 3\nu/u_*$ = thickness of sub-laminar boundary layer); very small for $z < d$; positive and almost constant ($= gJ$, J = hydraulic gradient) in most of turbulent zone; strongly negative up to $100g$ ($g = 981 \text{ cm/sec}^2$) for $d < z < e$. The areas of positive and negative \bar{a}_1 are equal.

Normally to wall \bar{a}_3 vanishes at wall, on channel axis, and near the wall. It is strongly positive near wall, and mildly negative elsewhere. $\bar{a}_3 = 0$ everywhere.

The physical meaning of large \bar{a} is strong curvature e of mean turbulent path.

This may explain the rapidity of mixing phenomena, the mechanism of sediment transportation, define mean turbulent paths. It justifies Prandtl's momentum transfer theory versus Taylor's vorticity transfer and Karman's similarity theory.

Similar results are obtained in circular pipe flow.

BOOK REVIEWS

Rubber Chemicals. J. VAN ALPHEN. Elsevier Publishing Company, 1956.

According to the author, this volume was written to meet the want of a guide to the rapidly expanding list of rubber chemicals, particularly of accelerators, antioxidants and other products for use in dry rubber and latex compounds. A first glance through the book shows that the field is well and truly surveyed, and contains all that is promised in the preface. However, closer study will emphasize serious shortcomings of the particular layout selected by Mr. van Alphen.

Thus, although the products are classified into broad groups, and these subdivided into smaller classes, it is almost impossible to see the relation between individual products in these classes without reference to the table of contents. The table given by Mr. Buist as an appendix to his book "The Ageing and Weathering of Rubber", although not as complete, gives a far better picture of the antioxidants in present use than is obtained from the volume under review. Some additional information on the compounds described would have been welcome, such as physical form, solubility, etc. For example, the stark description of Nonox B (amongst other similar condensation products) as "antioxidant" does not distinguish its somewhat discolouring nature from Nonox NSN described in the same way.

In spite of these shortcomings, the book will prove extremely valuable to rubber manufacturers and others, who are often called upon to switch from one source of supply to another, and to compounders who have to select a new type of ingredient for a specific purpose, and it is highly recommended to them. Although other lists have been published in various forms, the reviewer knows of none so complete and embracing.

The suggestion is made that it may prove possible for the publishers to offer the contents of this volume in the form of a card index; this may then be brought up to date by additional cards, prepared either by the user or issued by the publishers.

Z. RIGBI

*Rubber Research Association,
Haifa*

Preparation and Technology of Fluorine and Organic Fluoro Compounds. Edited by CHARLES SLESSER AND STUART R. SCHRAM. McGraw-Hill Book Company Inc., New York, 1951. XXIII + 868pp., \$11.50.

In 1886 Moissan discovered the electrolytic production of fluorine, but until World War II, fluorine and its organic compounds had found only limited applications. The diffusion process for the separation of uranium isotopes in the form of uranium hexafluoride required the development of methods for producing many tons of

fluorine, while previously only grams had been prepared. Another problem was to find nonmetallic materials that could be used safely in contact with uranium hexafluoride. Completely fluorinated hydrocarbons were found to fulfill this need.

This book is one of the many volumes of the National Nuclear Energy Series. It is a record of the immense effort carried out by many chemists and engineers of the Manhattan Project and the United States Atomic Energy Project in transforming fluorine from a scarce and dangerous laboratory chemical into a material produced on a large scale, and in bringing its hazards under fair control.

Part I describes the generation of elementary fluorine by the electrolysis of potassium biferfluoride, and traces the development from laboratory studies up to large 2000 ampere cells. In the course of this work it was discovered that polarization, which had been the main obstacle in the commercial operation of carbon anode cells could be eliminated by the addition of lithium fluoride. In five chapters various types of cells are described in detail. They are invaluable to anyone planning to construct fluorine generators.

Part II deals with the problems of the industrial handling of fluorine, such as methods of purification and compression, and of disposal of waste fluorine. It contains useful data on safety precautions, on the physiological effects of fluorine and on first aid measures.

Parts III to IV deal with fluorination of hydrocarbons and give a wealth of detail on fluorination with hydrogen fluoride, antimony pentafluoride, silver difluoride, cobalt trifluoride, and elementary fluorine. There is no mention of the application of alkali fluorides and some organic fluorinating agents. Among the more important compounds which became available as a result of this research, perfluoroheptane, perfluoro (dimethylcyclohexane), polychlorotrifluoroethylene and polytetrafluoroethylene should be mentioned.

The whole book is profusely illustrated with photographs and drawings of apparatus, and with tables and diagrams of experimental results. Many questions concerning the mechanism of action of elementary fluorine and of the various catalysts still await solution.

Being a collection of reports by different groups, there is considerable repetition and duplication, which makes reading rather laborious. The main use of the book is therefore to the chemical technologist who can find in it many important details on how to produce, handle and apply fluorine.

M. HALMANN
The Weizmann Institute of Science
Rehovot

The Metallurgy of Zirconium. Edited by B. Lustman and F. Kerze Jr., McGraw-Hill, New York, National Nuclear Energy Series, Div. VII, 1955, \$ 10.00.

The foremost experts in zirconium research have cooperated to write this book. Among these scientists and technologists are theoreticians on the solid state such as R. Smoluchowski, an expert on the metallurgy of powders such as H. H. Hausner, the thermodynamicist K. K. Kelly, and many other noted scientists. The fact that the name Kroll is missing is not to the credit of the editors since his name is closely connected with the development of methods of zirconium extraction.

The great interest which scientists have taken in zirconium since its importance has been revealed for atomic reactors, stimulated the serious and ramified research the results of which are publications presented in this book. However, as in the case of other publications of secret research, this book leaves the reader with a feeling of uncertainty — not due to inaccuracy in presentation, but due to material which is missing.

The two factors which motivated the writing of the book were: 1) The necessity to publish collectively the results of scientific research which has appeared only in secret reports till now, and 2) the desire to encourage investigation of further uses of zirconium.

Indeed, in connection with the first aim the editors succeeded to collect in one book extensive and valuable material which will undoubtedly serve as the handbook for zirconium for many years. And as for their second aim, the book is encouraging, although only the future will show whether new uses can be found for zirconium.

The book is divided into the following chapters:

1. Zirconium and its application to nuclear reactors.
2. Application of zirconium for other uses.
3. Occurrence of zirconium.
4. Zirconium production methods.
5. Iodide decomposition process for production.
6. Melting and shaping of zirconium and its alloys.
7. Forming and finishing of zirconium.
8. Physical metallurgy of zirconium and its alloys.
9. Zirconium alloy systems.
10. Mechanical properties of zirconium and its alloys.
11. Corrosion of zirconium and its alloys.
12. Analytical Chemistry of zirconium.

Appendix A Metallography of zirconium.

Appendix B Industrial Hygiene and Safety.

and other few addenda. At the end there is a detailed subject-author index.

The book opens with a discussion on the role of zirconium in atomic reactors and the second chapter describes at length the limited numbers of uses known today.

A justified emphasis has been placed on the chapters on the development of new methods for melting. The longest and most extensive chapter, however, deals with corrosion (123 pp.) since most uses of zirconium projected for the future are based on its properties of resistance to corrosion. Chemists and chemical engineers dealing with corrosive solutions will do well to read this chapter and look into the possibility of using zirconium. Of most interest is its resistance to hydrochloric acid.

It is most unexpected that the chapter "Metallography" is placed among the appendices. It seems to me that metallography is an inseparable part of metallurgy, and it would be more fitting that an independent chapter be devoted to it. On the other hand, the chapter on analytical chemistry is beyond the scope of the book, and if it belongs anywhere, it should be placed among the appendices.

This book has been written for metallurgists and chemists — but not for beginners. Metallurgists will find great interest in the methods of working and dealing with zirconium, and chemists — in the new methods for extraction of metals, and in the qualities of resistance to corrosion of zirconium.

Of the three books available today dealing with the metallurgy of zirconium (The other two are G. L. Miller: *zirconium* and A. S. M. Symposium: *zirconium and zirconium alloys*) I would recommend the book reviewed here, as being superior to the other two, both in scope and in standard. It is, furthermore, the latest publication, and its price is relatively low.

A. BERMAN

Israel Atomic Energy Commission
Chief Metallurgist

Ultimate Load Design of Steel and Reinforced Concrete Structures (in Hebrew), by A. Zaslavsky.

Published under the auspices of the Postgraduate Extension Courses for Engineers and Architects of the Technion, the Association of Engineers and Architects, and the Technion Graduates' Association. Second enlarged edition, Haifa, 1957, pp. 116 + 16 + VIII, IL.4.500.

Ultimate Load Design (or Limit Design) permits a closer estimation of the true strength of a structure, as well as determination of a uniform safety factor for both statically determinate and indeterminate systems. It represents, in fact, a point of view which is rapidly gaining ground in all technologically advanced countries. (For example, it has now been included in the revised U.S. and British Codes of Practice).

The present volume is, as far as known, the first comprehensive handbook on this subject dealing with both steel and reinforced concrete structures. The second edition has been considerably enlarged, with chapters added, inter alia, on the design of frames, on rectangular reinforced concrete sections in torsion and on sections under combined skew bending and axial compression. By way of illustration, about 60

problems are worked out in detail, including comparisons with the conventional elastic design method. Tables and references to the various Codes of Practice are also included.

A thorough grasp and clarification of the basic concepts in the analysis of structural stability and strength are essential in modern engineering. As a means to that end, this timely contribution is to be recommended without reservation for the Israeli engineer's library. Let us also reiterate the author's hope that this attempt will expedite the introduction of a suitable Israeli Code of Practice.

D. ITZHAKI

*Technion—Israel Institute
of Technology, Haifa*

Manual on document reproduction and selection. Part II. Selection, by U. N. Educational, Scientific and Cultural Organization International Federation for Documentation, The Hague, 1957. 100.— Dutch guilders, forwarding expenses extra. (Part I–II).

The International Federation for Documentation has published, with the financial help of Unesco, the second section of this practical international guide to methods of document reproduction and selection. Part II which completes the *Manual* lists the various selection methods currently available. It can serve as a basis for choosing the best means of meeting particular document selection problems.

Introductory section of each chapter are in English and French. There are chapters on classification and adaption for mechanical punched cards and photo-electric and electronic methods in documentation. Full page illustrations of equipment and specifications have been supplied by some manufacturers.

NOTICE TO CONTRIBUTORS

Contributors to the *Bulletin of the Research Council of Israel* should conform to the following recommendations of the editors of this journal in preparing manuscripts for the press.

Contributions must be original and should not have been published previously. When a paper has been accepted for publication, the author(s) may not publish it elsewhere unless permission is received from the Editor of this journal.

Papers may be submitted in English, French and Russian.

MANUSCRIPT

General

Papers should be written as concisely as possible. MSS should be typewritten on one side only and double-spaced, with side margins not less than 2.5 cm wide. Pages, including those containing illustrations, references or tables, should be numbered.

The Editor reserves the right to return a MS to the author for retyping or any alterations. Authors should retain copies of their MS.

Spelling

Spelling should be based on the Oxford Dictionary and should be consistent throughout the paper. Geographic and proper names in particular should be checked for approved forms of spelling or transliteration.

Indications

Greek letters should be indicated in a legend preceding the MS, as well as by a pencil note in the margin on first appearance in the text.

When there is any room for confusion of symbols, they should be carefully differentiated, e.g. the letter "l" and the figure "1"; "O" and "0".

Abbreviations

Titles of journals should be abbreviated according to the *World List of Scientific Periodicals*.

Abstract

Every paper must be accompanied by a brief but comprehensive abstract. Although the length of the abstract is left to the discretion of the author, 3% of the total length of the paper is suggested.

References

In Sections A and C, and in Letters to the Editor in all Sections, references are to be cited in the text by number, e.g., ... Taylor³ ... and are to be arranged in the order of appearance.

In Sections B, D and E, the references are to be cited in the text by the author's name and date of publication in parenthesis, e.g., ... (Taylor 1932).... If the author's name is already mentioned in the text, then the year only appears in the parenthesis, e.g., ... found by Taylor (1932).... The references in these Sections are to be arranged in alphabetical order.

The following form should be used:

3. TAYLOR, G. I., 1932, *Proc. roy. Soc.*, A138, 41.

Book references should be prepared according to the following form:

4. JACKSON, F., 1930, *Thermodynamics*, 4th ed., Wiley, New York.

TYPOGRAPHY

In all matters of typography the form adopted in this issue should be followed. Particular attention should be given to position (of symbols, headings, etc.) and type specification.

ILLUSTRATIONS

Illustrations should be sent in a state suitable for direct photographic reproduction. Line drawings should be drawn in large scale with India ink on white drawing paper, bristol board, tracing paper, blue linen, or blue-lined graph paper. If the lettering cannot be drawn neatly by the author, he should indicate it in pencil for the guidance of the draftsman. Possible photographic reduction should be carefully considered when lettering and in other details.

Half tone photographs should be on glossy contrast paper.

Illustrations should be mounted on separate sheets of paper on which the caption and figure number is typed. Each drawing and photograph should be identified on the back with the author's name and figure number.

The place in which the figure is to appear should be indicated in the margin of the MS

PROOFS

Authors making revisions in proofs will be required to bear the costs thereof. Proofs should be returned to the Editor within 24 hours, otherwise no responsibility is assumed for the corrections of the author.

REPRINTS

Reprints may be ordered at the time the first proof is returned. A table designating the cost of reprints may be obtained on request.

Orders in America should be addressed to Interscience Publishers Inc., New York, N. Y., and in England and Europe to Wm. Dawson & Sons, Ltd., Cannon House, Macklin Street, London, W. C. 2, directly or through booksellers.

Annual subscription per section (four issues): IL.4.000 (\$5.50, £ 2)
Single copy IL.1.000 (\$1.50, 12 s.)

Printed in Israel
R. C. Cohen's Press Ltd., Jerusalem